A SOLAR WATER PURIFICATION SYSTEM FOR RURAL AREAS

PAULINE JOELLA KOURA MBADINGA

2015

Cape Peninsula
University of Technology

A SOLAR WATER PURIFICATION SYSTEM FOR RURAL AREAS

by

PAULINE JOELLA KOURA MBADINGA

Thesis submitted in fulfilment of the requirements for the degree

Master of Technology: Mechanical Engineering

in the Faculty of Engineering at the

Cape Peninsula University of Technology

Supervisor: Prof J. Gryzagoridis
Co-supervisor: Mr K.E Kanyarusoke

Bellville Campus
Septembre 2015

DECLARATION

I, **PAULINE JOELLA KOURA MBADINGA**, declare that the contents of this thesis represent my own unaided work, and that the thesis has not previously been submitted for academic examination towards any qualification. Furthermore, it represents my own opinions and not necessarily those of the Cape Peninsula University of Technology.

15/10/15

Signed **Date**

ABSTRACT

Access to adequate quantities of clean drinking water has become a serious issue on the worldwide level. This is particularly true in arid and rural areas where for the majority of people water is a limited and a vulnerable resource. These water sources which are often highly contaminated are potentially the cause for several diseases (waterborne diseases) and ultimately death especially in infants. Due to poverty and sometimes to the remote conditions of their regions, the population is unable to afford adequate water purification technologies, since they are relatively expensive and energy intensive. It is therefore vital to investigate appropriate water purification technology that people can afford or construct, operate and maintain themselves.

A promising technology is solar distillation for the supply of drinking water on a small-scale level. It has proved to be a unique purification method as it can purify almost any type of water by using the high solar energy potential of the affected regions. The most basic form of solar distillation is the use of a single basin single slope solar still. However the downside of this technology is that it presents a low efficiency and productivity. To try to tackle this problem, many studies have been carried out to enhance productivity, effectiveness and efficiency of single-basin solar stills.

In this present study, a solar distillation unit was designed, fabricated and experimentally tested. Its performance in terms of distillate output and energy efficiency was analysed under Cape Town conditions and compared to similar stills that have been reported in the literature. The main configuration of the solar still is a double glazed single basin solar still coupled to an external condenser.

The study indicated that the performance of the solar still unit can be enhanced by increasing the evaporation rate which is a combined effect of solar radiation, ambient temperature, and the system components temperature. It was concluded that the applied techniques such as the external condenser, double glazing, good insulation and low level of water are effective. The unit was found to have an efficiency ranging between 21 and 29% over the test period and a mean distillate yield of about 2.5 litres per square meter was achieved per day.

ACKNOWLEDGEMENTS

I wish to thank and express my gratitude to:

- **Prof Jasson Gryzagoridis** and **Mr K.E Kanyarusoke** for the supervision of this research work. Their support, advice, guidance and constructive criticism made the completion of this thesis possible.

- The CPUT University Research fund committee for funding this project.

- The Mechanical Engineering Workshop staff and students for their practical assistance.

DEDICATION

I would like to dedicate this thesis to my family and friends.

TABLE OF CONTENTS

LIST OF FIGURES

LIST OF TABLES

NOMENCLATURE

Symbols	Description	Unit
A	Area	m^2
ab	Beam air mass exponents	-
ad	Diffuse air mass exponents	-
C_p	Specific heat	$\frac{kJ}{kg.K}$
E	Estimated solar radiation	W/m^2
H	Altitude	m
hfg	Latent heat of evaporation	kJ/kg
I	Solar radiation intensity	W/m^2
I_{SC}	Solar constant	W/m^2
K	Thermal conductivity	W/mK
L	Latitude	$degrees$
m	Mass, mass of air	kg
n	Day of year	-
P	Pressure, vapour pressure	Kpa
Q	Heat energy	kJ
R_b	Ratio of beam radiation on inclined plane to horizontal	-
R_d	Ratio of diffuse radiation on inclined plate to horizontal	-
t	time	$hours$
T	Temperature	℃

Subscript

a	Air/ambient
b	Beam
ba	Basin
co	Condenser
d	Diffuse
gi	Inner transparent cover
go	Outer transparent cover
refl	Reflected
v	Vapour
w	Water

Greek symbols	**Description**	**Unit**
β	Solar still cover inclination	Degrees
η	Efficiency of the solar still	%
θ_i	Incident angle	Degrees
θ_z	Zenith angle	Degrees
τ	Pseudo optical depth	-
ω	Hour angle	Degrees

CHAPTER 1 INTRODUCTION

1.1 MOTIVATION AND BACKGROUND TO THE RESEARCH PROBLEM

1.1.1 THE WATER CRISIS

It is a necessity for humans to have access to water in adequate quantity and quality. Water is the source of life and development on earth. It makes up more than half of the human body and an average adult consumes about 2.5 litres of water per day. In terms of direct drinking water, 1litre a day can be sufficient since the balance bodily requirements can be consumed in fruits and cooked food. However, in many parts of the world and especially in rural and arid areas, water is a limited and vulnerable resource in terms of quantity and quality. In 2012, it was reported that roughly about 780 million people around the world do not have access to clean and safe drinking water (UNICEF & WHO: 2012).

Although water is the most spread substance on earth since it covers more than 70% of its surface with an approximate value of 1400 million km^3, freshwater resources represent only about 2.5% (35 million km^3) of the total water volume (Bundschuh and Hoinkis: 2012).

These freshwater resources are in crisis, and water shortage is becoming a global issue because of contamination by humans and industrial activities, increasing population, economic growth, climate change, lifestyle, urbanisation, misuse and over exploitation (Sampathkumar 2010, Kumar *et al.*: 2013). There is as much as 20% of the world population that lacks access to safe, clean drinking water. This situation contributes to the death of approximately 1.5 million children worldwide every year caused by water-borne diseases as a result of improper water and sanitation facilities (Tiwari: 2006).

In order to overcome this crisis, numerous methods of providing clean water have been studied and are being implemented in many regions of the world. These water treatment methods require energy. Since water and energy are interdependent to each other, many regions in the world which are deficient in freshwater sources also experience lack of energy.

Seawater and brackish water desalination is usually performed to overcome the issue of water shortage since the sea is by far the greatest source and store of water (97.5% of earth's water) (Blanco *et al.*: 2009). However, desalination is energy intensive and quite an expensive process since it is mostly using energy supplied from fossil fuels and it usually requires specific and expensive infrastructure and maintenance (Pillai *et al.*: 2013).

Currently the interest on desalination is focused on conducting studies to develop cost-effective ways of producing suitable water for desired-end use by considering available options with adaptations and improvement and by exploring existing technology. The use of non-conventional methods and resources must also be considered to resolve the global water crisis.

1.1.2 THE ENERGY CRISIS

Water and energy which are prominent as top international issues have been found to be "intensely inter-related" (Von-Uexkull: 2004), and are "essential commodities for sustaining human life on earth" (Gude et al.: 2010).

Ever since the days of the industrial revolution, the world energy system largely relies on fossil fuel and nuclear energy sources to maintain economic growth and social development (EIA: 2013). However, economically and safely exploitable conventional energy resources are found to be relatively limited while energy demand is increasing and will continue to increase in the next decades (Huth et al.: 2012). For instance, the International Energy Outlook 2013 (IEO: 2013) estimated that the world energy consumption will grow by 56% between 2010 and 2040. This is about 524 quadrillion BTU (154 trillion kWh) energy used in 2010 to 820 quadrillion BTU (241 trillion kWh) expected to be used in 2040. This demand is escalating mainly for the same causes cited for the water demand increase. That is to say: increasing population growth and rapid industrialization.

1.1.3 WATER PURIFICATION METHODS

Water treatment/purification technologies have been studied, used and improved over the past centuries to remove contaminants (pathogens and chemicals) to produce suitable drinking water for human consumption. These technologies are often adapted to particular demand; they can have application to personal, individual households and municipal water treatment. Some widely used purification methods consist of chlorination, flocculation, filtration, desalination and distillation. However, with the sea being by far the greatest source and store of water, water desalination is usually performed to overcome the issue of water shortage. Water desalination processes refer to the removal of salts, and minerals from sea or brackish water, in order to produce freshwater. More than 15000 desalination plants are in operation or under construction worldwide, thus providing some relief on the issue of potable water in some countries (Mohammedi *et al.*: 2013). Conventional desalination methods include processes such as Reverse Osmosis and Electrodialysis (membrane processes) and Multi-Stage Flash, Multi-Effect Distillation, Vapour Compression and Solar Distillation (Thermal processes).

- Multi-Stage Flash (MSF)

Multi-Stage Flash distillation is the most commonly used distillation process in the world. It accounts for around 60% of all desalinated water in the world. In the MSF process, seawater is heated in a closed vessel and then flows into a stage (another vessel) where the water will be heated rapidly to its boiling temperature due to the reduced pressure inside the vessel. The quick introduction of heated water in the vessel causes it to boil fast and it flashes into steam The MSF unit uses a series of stages set at gradually lower pressures (Kalogirou: 2005). The water which passes from one stage to another is boiled repeatedly. No more heat is necessary. Multi-Stage Flash distillation is an effective water purification process. The steam produced by flashing is condensed by heat exchanges through each stage and is converted to fresh water. However, it is complex (in terms of mathematical design and equipment installation) and has high energy consumption (thermal energy for heating the seawater and mechanical energy for driving the various pumps in the system). The unit cost of MSF was estimated by Ettouney et al. (2002) to be in the range of us$0.77 to $1.84 per cubic meters.

- Multi-Effect Distillation (MED)

Similar to MSF, a multi-stage process takes place in a series of vessels. In this process, vapour from each stage is condensed and vapourised again in the next vessel at a lower pressure. The latent energy exhausted during the process evaporates some of the unclean water as it goes through a first evaporator. The feed goes through multiple boiling without any heat being added after the first effect.
The unit cost of MSF is estimated to be in the range of us$0.84 to $1.95 per cubic meters (Ettouney et al.: 2002).

- Vapour Compression (VC)

Vapour compression distillation is a thermal process in which compression is the source of heat for water evaporation This process generally uses the principle of reducing the boiling point temperature by reducing the ambient pressure (Bundschuch ND Hoinkis: 2012). Vapour is usually condensed using two methods: Mechanical Vapour Compression (MVC) (generally electrically driven) and Thermal Vapour Compression (TVC) using a steam jet thermo-compressor (Kalogirou: 2005). In MVC (the most used method), the compression of vapour is utilised as a source of heat for evaporating the feed water. The cost of MVC varies between us$0.46 and $2.48 per cubic meters for systems producing more than 750 cubic meters per day (Ettouney et al.: 2002).

Distillation is the oldest and most commonly used method of desalination. It proved to be a unique purification method in the sense that it can produce water of high quality and almost any type of water can be purified by means of this process. However, because of its expensive processes, this water treatment method is very often impractical in rural areas as the people are financially unable to afford devices like those used in urban and industrialised areas. This is the reason why in some rural communities, when required, drinking water is usually heated or boiled before consumption. This is very often performed by burning fuels such as wood, coal or charcoal. However, in the case where there is no scarcity of resources, the burning of wood or charcoal is not environmentally friendly as it creates considerable air pollution which has a negative effect on both the health of people and the environment.

With regards to the challenges encountered in the conventional water purification methods, it is apparent that the implementation of a technology which uses a sustainable source of energy, preferably green, to purify water would be beneficial to all.

The use of solar radiation as the source of heat for water purification is an attractive proposition. As a matter of fact, with the majority of rural and arid areas situated in regions with high solar radiation levels, the problem of solar distillation in these areas is not so much of technical feasibility as of socio-economic viability.

1.1.4 PROBLEM STATEMENT

Many regions of the world lack access to a proper source of clean drinking water. As a matter of fact, most of the water found in, lakes, streams, rivers, wells and seas carries germs or diseases, or is simply not suitable for consumption and therefore has a negative effect on health. Populations who lack access to safe drinking water are most of the time poor and thus do not have the necessary infrastructure to make and support large scale water purification plants. There is therefore a need for an effective, sustainable, small scale and relatively low cost system that can provide clean drinking water for individuals, families and other small users.

1.1.5 SOLAR DISTILLATION TECHNOLOGY

Solar distillation is a process in which solar radiation is the source of heat for water evaporation. It is based on a phase change process: the heated water is evaporated thus separated from dissolved salts and microorganisms and is condensed as pure water. Solar distillation is performed using the direct distiller or Solar Still (SS) which is the most basic technique. It reproduces the natural water purification sequence (i.e. evaporation of water, condensation and precipitation) based on passive solar heating in an airtight basin with transparent cover. Solar radiation passes through the transparent cover causing the water to heat up and evaporate, leaving contaminants in the basin. The vapour condenses on the undersides of the transparent cover and is collected as freshwater. Solar distillation produces high quality water and the concentration of the feed water is not a limiting factor unlike physical separation desalination processes (reverse osmosis, electrodialysis) (Bundschuch and Hoinkis: 2012). Moreover, it does not require the use of expensive equipment and energy sources, since it can be made from readily available materials and uses the energy of the sun.

Therefore, solar distillation which is a promising and attractive technology because of its simplicity will be the focus of this study.

1.1.5.1 THE SUN AND SOLAR ENERGY

The sun is a sphere with a blackbody temperature of approximately 6000 ^{o}C (Kane: 2005) which emits radiation. Solar energy travels from the sun to the earth in the form of electromagnetic radiation. The total amount of solar radiation on a surface which is above the atmosphere, at a right angle to the direction of propagation of solar energy, is practically constant throughout the year and is defined as the solar constant I_{sc} which has a value of 1367 W/m^2 (Gueymard: 2004). Most of the solar radiation emitted includes infrared radiation (~37%), visible light (~43%) and UV light (~7%).

Outside the earth atmosphere, only beam solar radiation can be found. However, once the solar radiation passes through the atmosphere, some of it enters undisturbed directly from the sun to a receiver surface while the rest of it (diffuse radiation), is scattered, absorbed, transmitted or reflected (Sharma and Pal: 1965). Hence, the global solar radiation reaching a receiver on the Earth's surface can be classified into two components: beam radiation and diffuse radiation (Yang et al.: 2001). The average daily global solar radiation (direct + diffuse) is one of the most important parameters affecting solar energy utilisation.

1.1.5.2 HISTORICAL BACKGROUND

Back in late Antiquity, the Greek philosopher and scientist Aristotle (384-322 BCE) described in his treatise "*Meteorologica*", the hydrological cycle in nature and observed that water evaporates from sea and condenses as sweet water to return to Earth: it was a clear description of the seawater desalination process by distillation. The first known use of solar distillation dates to medieval times when Arab alchemists are believed to have used solar stills to desalinate seawater (Delyannis: 2003). In the same period of time, Della Porta, in his book "*Magiae Naturalis*" (1589) mentions and describes a solar distillation unit to produce freshwater from brackish water (Delyannis: 2003).

However, no experimental applications of solar distillation are known of until 1870 when Wheeler and Evans (1870) studied and described the basic principles of operations of the solar stills as currently understood. They investigated and discussed theories such as the greenhouse effect, the condensation and evaporation processes, the dark surface absorption as well as sun tracking. Two years later in 1872, the first known installation of a large-scale solar still was designed and built at Las Salinas in a mining community on the Northern deserts of Chile by Swedish engineer Carlos Wilson (Delyannis: 2003). The plant was made out of 64 wood bays blackened at the bottom to absorb sun radiation and covered with a single sheet of glass. The unit, which had a total surface area of 4450 m^2 was used to treat brackish water and supply freshwater to the community (Figure 1-1). On a typical summer day, it produced 23000 litres of freshwater per day. This plant operated for 40 years until the mine work ceased.

Following these experiments, almost all solar stills studied and built have been based on the same principles. And yet, it was not until the Second World War that research on solar distillation was intensified. The primary purpose was to supply freshwater to troops located in areas lacking safe drinking water. Consequently, in the second half of the 20^{th} century, many designs of solar stills were developed. However, the most used design is the conventional solar still which is the single basin, single slope solar still.

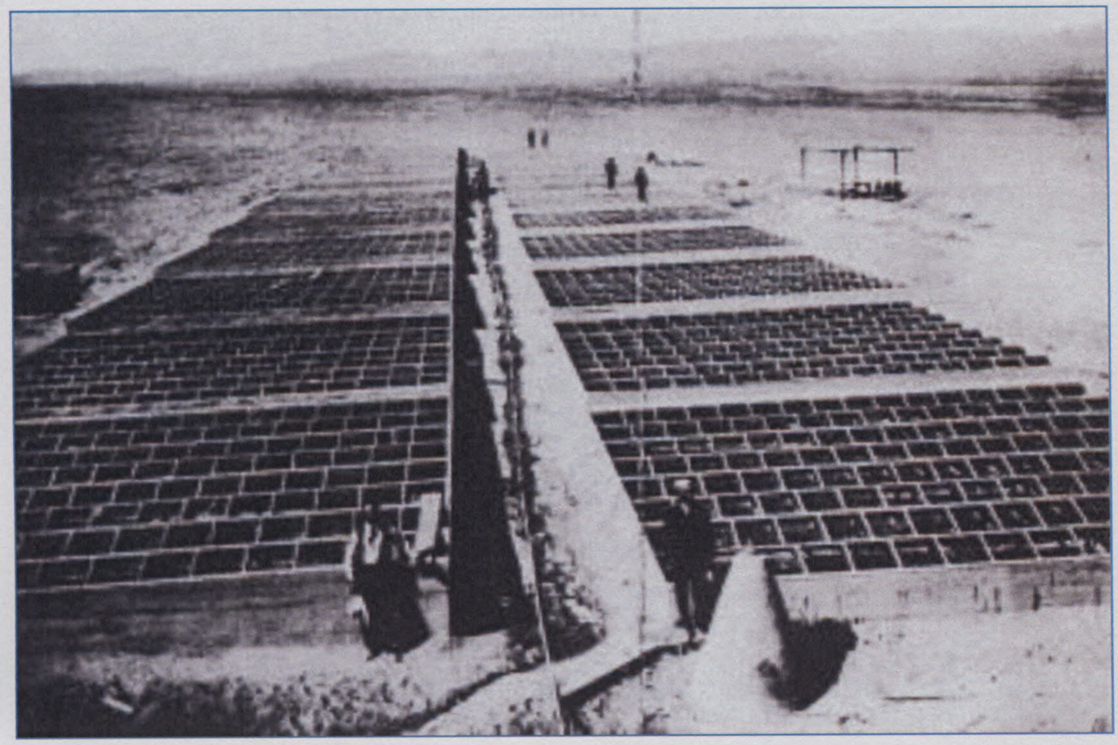

Figure 1-1: The first solar distillation plant at Las Salinas

Chile Telkes 1956b (in Delyannis: 2003)

1.1.5.3 THE CONVENTIONAL SOLAR STILL

The conventional basin type solar still (Figure 1-2) consists of an airtight blackened basin containing the contaminated water and enclosed by a transparent cover through which solar radiation is transmitted. Solar radiation is absorbed by the basin plate and heat is transferred to the water increasing its temperature to the evaporation temperature. Evaporation occurs, and water vapour rises upward to the cooler inner surface of the transparent cover and condenses as pure water which runs down along the slopped cover due to gravity and is collected in a collection trough at the lower edge of the cover (Gnanadason et al.: 2011). The cover is at sufficient slope so that surface tension of water will cause it to run down to the trough without falling back into the basin.

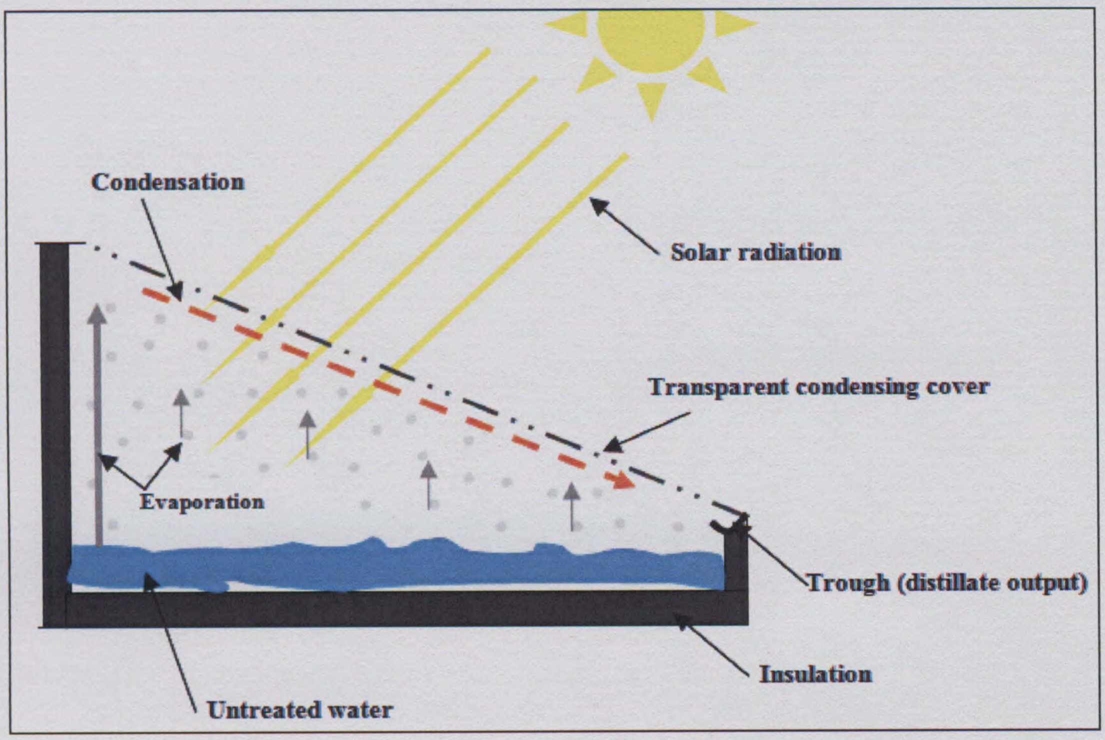

Figure 1-2: Conceptual diagram of a conventional single basin solar still

1.1.5.4 ENERGY FLOW IN SOLAR STILL

The main energy flows and mechanisms within a single basin-single slope solar still are illustrated in Figure 1-3. The incoming solar radiation composed of direct and diffuse radiation enters the still through the glass cover after a small fraction of it has been reflected and absorbed by the glass itself. Once in the evaporation chamber, the radiation is further reflected, transmitted and absorbed by the water until it reaches the black basin which fully absorbs it. The basin then begins to heat up, and a large part of the absorbed energy (heat) is transferred from the basin base surface to the water, while a small fraction of it is lost to the ground (or insulation) by conduction or convection through the basin (bottom and sides). The sensible heat absorbed by the water makes its temperature and vapour pressure to rise, thus causing partial vaporisation to occur. The heat is transferred to the transparent cover (generally cooler than the brine) by the vapour that condenses while other parts of it are transferred to the cover by convection and by radiation.

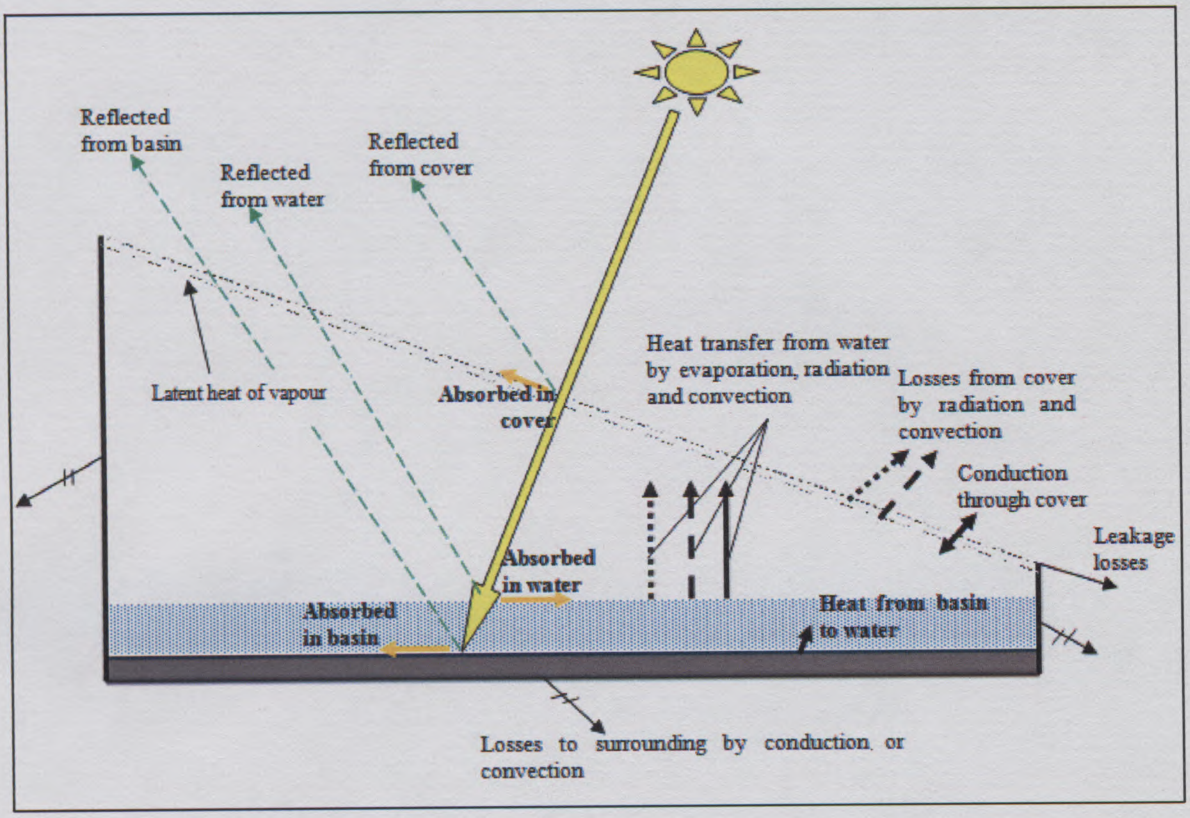

Figure 1-3: Energy flow diagram in solar still

Because of the low temperature of the glass cover which is generally lower than the dew point temperature (temperature at which water saturates), the vapour starts to condense on the bottom surface of the glass cover and forms droplets. These will grow and accumulate until they become large enough to be forced by gravity to run down to the lower edge of the glass where the condensate will be collected.

The heat received by the inner surface of the glass cover from the condensed film of water, and by radiation from the brine surface is conducted to the external surface of the cover and is further transferred to the atmosphere by convection and radiation. However, some heat is accumulated in the still in the form of sensible heat of the system while some of heat may be lost to atmosphere due to leakage of water vapour and water from the still.

1.1.5.5 SOLAR STILLS EFFECTIVENESS

As the state-of-the-art of solar stills became clearly understood in terms of thermodynamics and geometry, the productivity and efficiency of the solar still proved to be low. For that reason, the demand existing on freshwater and energy sources brought about research in the late 20th and early 21th centuries that focussed on new designs to improve the effectiveness of these devices. The main objectives of these improvements are to absorb the maximum solar radiation into the basin and to increase the evaporation rate of the water by increasing the temperature difference between the evaporating and the condensing surfaces. Depending on the methods of improvement, solar distillation systems can be classified into two categories: passive solar stills and active solar stills.

In the passive mode, distillation does not use additional heat but takes place by direct sun light under operating temperatures below 60^0C (Gupta *et al.*:2013). The two most used passive solar stills are the conventional single slope solar still and the conventional double slope solar still (see Figure 1-4 for classification of solar distillation systems) in which the improvements made usually consist of some simple modification and/or material addition inside the still which enhance the effectiveness of the unit. For instance, Tanaka & Nakatake (2006) improved the distillate output by adding internal and external reflectors to the still. Sponge cubes placed in the basin to improve the evaporation area (Abu-Hijleh& Rababa'h: 2003) and energy absorbing material such as rubber and gravel to increase the heat capacity of the still (Nafey et al.:2001) were reported to improve the productivity of the solar unit. The simplicity of the design as well as the low manufacturing and installation cost and the simple maintenance of the passive solar still make it a suitable technology for water purification in remote areas.

On the other hand, in active solar stills, additional devices such as flat plate collectors (Bacha et al. 2007), sun tracking systems (Abdallah & Badran, 2008) or fans (Ali, 1991) are used to increase the evaporation rate. This category of stills would be most appropriate for commercial production of distilled water (Bhattacharyya: 2013). Active solar distillation may be further classified into high temperature distillation and nocturnal distillation (Figure 1-4).

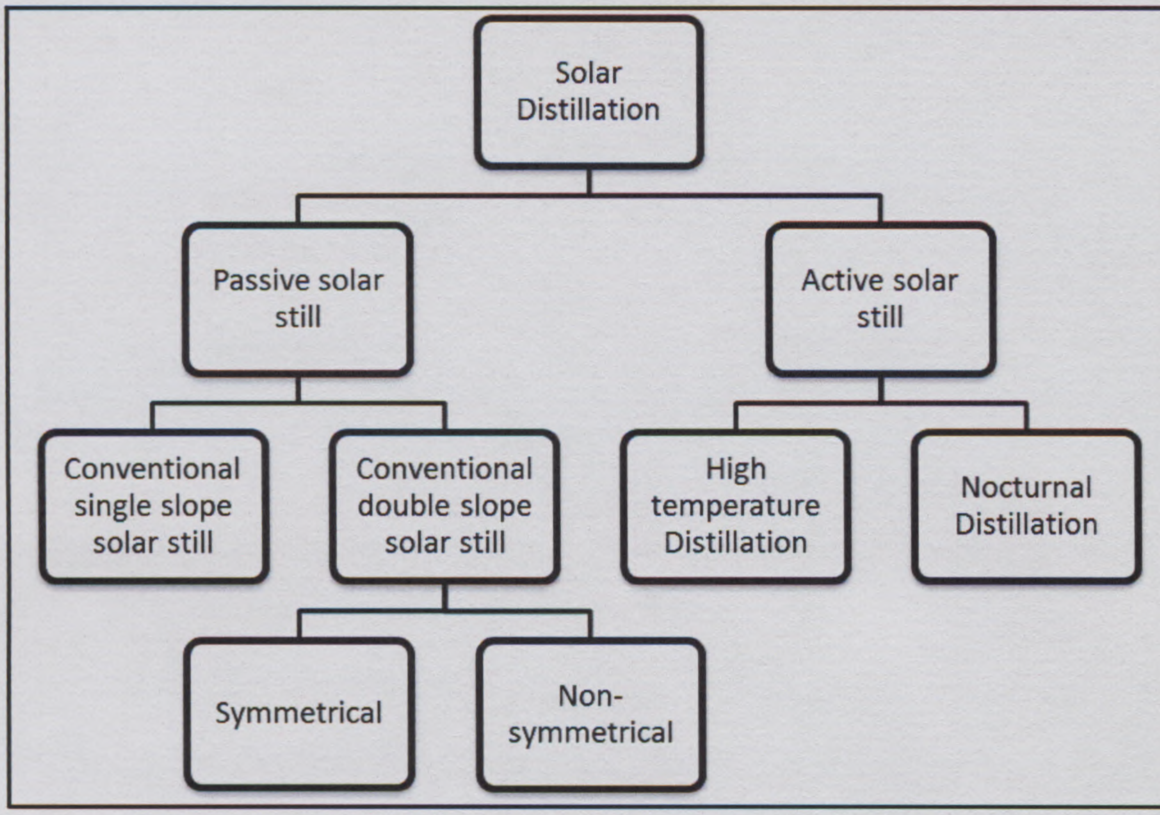

Figure 1-4: Classification of solar stills

(Adapted from Tiwari: 2006)

1.1.6 BASIC PRINCIPLES OF SOLAR DISTILLATION PROCESSES

Distillation is the combination of two processes which are *Evaporation* and *Condensation.* It always takes place in a closed system so that heat losses may be prevented.

1.1.6.1 EVAPORATION

Evaporation is a phenomenon which takes place at the surface of a layer of fluid. During this endothermic process, molecules increase their kinetic energy and escape the surface tension of the liquid and change their state from liquid to gas (vapour). The kinetic energy of a molecule being proportional to its temperature, the higher the fluid temperature, the faster evaporation occurs. Evaporation happens below the boiling point temperature of the liquid. In order to increase the process efficiency, the fluid to be distilled generally has to be raised to a certain temperature level. Evaporation is also influenced amongst others by the following factors:

-Pressure: Evaporation happens faster at lower pressure

-Surface area: The larger the surface area of the substance, the faster evaporation happens.

1.1.6.2 HEATING ENERGY

During distillation processes, working temperature usually range between 30 °C and 90 °C. The energy required for heating the substance to a necessary temperature is calculated as follow:

$$Q_H = mC_p\Delta T \tag{1-1}$$

where Q_H is the required heating energy (kJ)

m is the mass of the fluid (kg)

C_p is the specific heat capacity of the fluid (KJ/kg.K)

ΔT is the difference between the necessary temperature and the initial fluid temperature (K).

1.1.6.3 ENERGY OF VAPOURISATION

The energy of vapourisation is the quantity of heat necessary to convert water molecules from the liquid to vapour. The total energy required by the process for evaporation is calculated as follow:

$$Q_{evap} = m\Delta h_{evap} \tag{1-2}$$

where Q_{evap} is the required vaporization energy (kJ)

Δh_{evap} is the enthalpy difference of latent heat of vapourisation of the fluid at specific temperature and corresponding saturation pressure (KJ/kg).

The total energy necessary for a fluid to be evaporated is the sum of the energy required for heating and the energy needed for evaporation:

$$Q_{T_{evap}} = Q_H + Q_{evap} \tag{1-3}$$

Thus,

$$Q_{T_{evap}} = m(C_p.\Delta T + \Delta h_{evap}) \tag{1-4}$$

1.1.6.4 CONDENSATION

Condensation is the reverse process of evaporation and is the change of the physical state of a substance from gaseous phase to liquid phase. Vapour commonly condenses when it reaches its dew point while being in contact with a surface having a lower temperature than itself, or when it is compressed to its saturation limit. Condensation is an exothermic process: the vapour releases the heat acquired by evaporation, cools down and is then converted into liquid.

1.1.6.5 ENERGY OF CONDENSATION

If it is assumed that the losses in the system are negligible, the energy released by condensation is equal to the energy of evaporation. The energy release occurs during the temperature loss of the vapour at the condensing surface and is expressed as:

$$Q_{re} = m.C_p.(T_w - T_{co}) \tag{1-5}$$

where Q_{re} is the energy released during cooling of vapour to saturation temperature,

T_w is the temperature of vapour,

T_{co} is the saturation temperature at a specific pressure of the condensing surface

The total energy required for a fluid to condense is the sum of the energy required for evaporation and the energy require for cooling of the vapour.

$$Q_{cond} = Q_{evap} + Q_{re} \tag{1-6}$$

where Q_{cond} is the total energy required for the process.

1.1.7 PARAMETERS AFFECTING THE PRODUCTIVITY OF SOLAR STILLS

In order to improve the yield of the solar still, several authors studied the effect of various parameters affecting the productivity of solar stills. It was found that solar still productivity and efficiency depend on parameters such as location, solar radiation intensity, ambient temperature, wind velocity, basin water depth, glazing cover material, thickness and inclination and heat capacity of the still (basin and insulation). These parameters are classified into two categories: climatic parameters and design parameters (Tiwari and Tiwari: 2008).

1.1.7.1 CLIMATIC PARAMETERS

- Solar radiation

Solar radiation intensity (which depends on the latitude of the location), is one of the most important parameters affecting the performance of solar stills because of its great effect on the rate of evaporation in the still (Sampathkumar: 2010). As described by Talbert et al. (1970), the yield of usual basin-type solar stills increases exponentially with solar radiation since the overall operating efficiency increases as the temperature of the saline water and the components increase. This is supported by many other authors who demonstrated that the still productivity is proportional to the solar radiation intensity (Malik et al.: 1982, Mowla et al.: 1995. Pillai et al.; 2013).

The productivity of solar stills in literature is usually plotted as a function of the total solar radiation received on the surface. It should be noted that the solar radiation data used in the studies refers to the average hourly solar radiation composed of direct and diffuse radiation.

- Ambient temperature

In various studies, the effects of ambient temperature on the still productivity were evaluated. Talbert *et al.* (1970) observes an increase of productivity of about 40% as the ambient temperature rises from 15.5 °C to 27 °C. Likewise, in a parametric study of different variables, Nafey et al. (2001)'s numerical results show that there is a slight increase of 3% in the solar still productivity by increasing the ambient temperature by 5 °C. Rajvanshi (1981), El-Sebaii (2004), Badran (2007) and Wassouf et al (2011) agree in their conclusions that the solar still productivity is directly proportional to the ambient temperature. However, an average increase in the yield was indicated to be ~ 5% for an increase of 5 °C in ambient temperature (Zaragoza et al. in Budschuch and Hoinkis: 2012).

- Wind velocity

Several studies on the effect of wind speed on the productivity of solar stills have been conducted, and it was understood that as the wind speed increases over a solar still, a heat loss from the cover occurs by convection. This implies a drop of temperature of the cover (condenser) which increases the rate of condensation inside the still, hence the productivity of the still. On the other hand, as the cover temperature decreases, the rate of heat transfer by radiation and evaporation from water to cover increases, thus decreasing the brine temperature until a thermal balance is reached at lower temperatures. The evaporation rate exponentially decreases with the brine's temperature, thus causing a decrease in productivity (Talbert *et al.*:

1970). These facts may explain the contradictions identified in literature about the effect of wind speed on productivity of solar stills. Authors such as Soliman (1972), Malik and Tran (1973), Dimri et al. (2008), Ismail (2009), Tiwari et al. (2009) reported that an increase of wind speed causes an increase in the still productivity. On the contrary, Hollands (1963), Eibling et al. (1971), Yeh and Chen (1985), (1986), Kaushal and Varun (2010) found that an increase in wind speed causes a decrease in productivity. Morse and Read (1968) conversely claimed that the wind speed presents no significant effect on productivity. However, El-Sebaii (2004), (2010) reported and explained that for active solar stills, the productivity increases with increasing wind speed until a typical value of wind speed, beyond which it becomes insignificant. Whereas, for passive solar stills there is a critical depth of water in the basin beyond which the productivity increases with increasing wind velocity until a typical value of this velocity. For lesser water depth, the productivity decreases with increasing velocity until a typical value of the speed, beyond which it also becomes less dependent on the wind velocity.

Nevertheless, once a location is chosen, these variables cannot generally be controlled and adapted to the needs. Instead, the solar still productivity may easily be influenced by some design parameters that can be varied and adapted to the use.

1.1.7.2 DESIGN PARAMETERS

The following design parameters proved to affect the performance of solar stills.

- Basin water depth

Basin water depth is agreed upon by several researchers to be the design parameters with the greatest influence on the overall productivity of solar stills. Experiments revealed that the shallower the layer of brine in a basin-type solar still, the higher the total productivity. This result may be explained by the fact that shallow layers of water reach higher temperatures than deeper bodies. The rate of evaporation increases exponentially with an increase in brine temperature, therefore causing a great percentage of the available solar energy to be used for evaporation and a lesser percentage to be lost from the basin (Talbert *et al.*:1970, Tiwari and Tiwari: 2008).

Khalifa and Hamood (2009) reviewed a large number of studies on the effect of water depth on the performance of basin solar still and developed a correlation from the data reported by each study and then developed a concluding correlation from all the investigations. The study verified the inverse proportionality of the still productivity to the water depth in the basin throughout the day and revealed that the brine depth could influence the still productivity by up to 48%.

Furthermore, the same study reviewed the effect of water depth during nocturnal operations. It was observed that the still presented a greater nocturnal production with higher brine depth. This is a result of the large volume of water that absorbs solar radiation and stores the heat during the day to drive evaporation at night.

Given these points it is therefore evident that water depth affects the performance of solar stills. Shallow water depth increase the still productivity during the day while thicker layers of water increase the productivity during nocturnal hours (See Figure 1-5 for daily and nocturnal output for different brine depths).

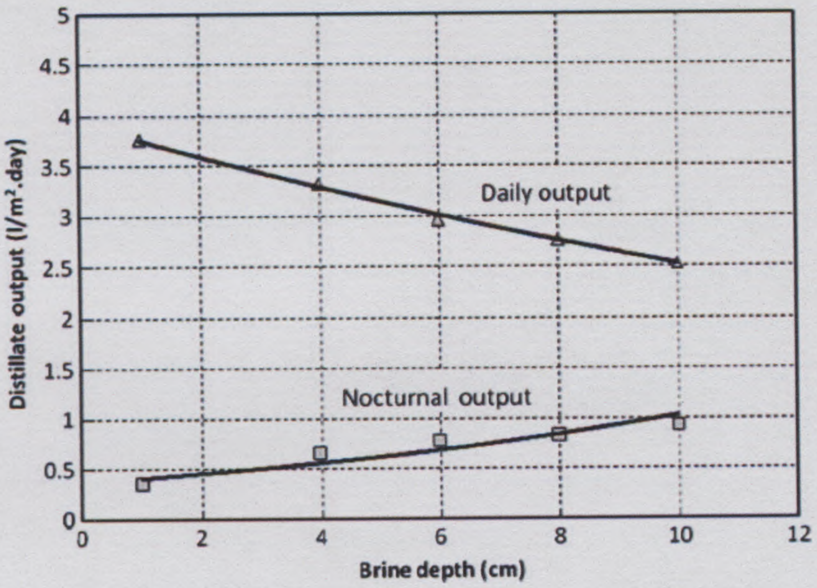

Figure 1-5: Daily and nocturnal output for different water depth.

(Khalifa and Hamood: 2009), Copyright (2009) with permission from Elsevier

- Glazing

The effect of cover designs on the productivity of solar stills has been largely studied and reported in literature. The cover thickness, material and inclination have been reported to influence the yield and efficiency of basin-type solar stills. These will be discussed in subsection 2.3.2.

- Basin material

The structural materials generally used for basin are reported by Phadatare *et al.* (2007) as wood, galvanized iron, aluminium, asbestos cement, masonry bricks and concrete. The literature pertaining to the theoretical or experimental comparison of different basin materials' effect on the solar still productivity is not prominent.

In order to minimise reflectance loss, the basin should be made out of black or black coated materials to enhance its ability to capture solar radiation. For optimal use and productivity of the still the basin material is recommended to have the following properties (Kalidasa Murugavel: 2008, Badran: 2007, Talbert *et al.*: 1970):

- Heat resistant
- Resistant to corrosion
- High absorbance to solar radiation
- Good resistance to accidental puncturing
- High water tightness
- Insulation

- Insulation

Insulation of the basin plays an important role in the overall productivity of solar stills. As a matter of fact, in order to achieve high efficiency of the system, heat losses from the sides and base of the solar still should be minimised. This helps secure the storage of the absorbed thermal energy in the basin. The insulation material should have a good thermal resistance as well as adequate strength to resist under the weight of the basin water. Abu-Arabi *et al.* (2002) performed a theoretical study of a conventional solar still in which a perfect insulation was assumed. The results show that there is a maximum water temperature increase of 67% in the basin. He therefore concluded that the performance of the still depends on the amount of insulation used. Subsequently, in an experimental investigation on the effect of variable insulation thickness on the productivity of single slope stills, Khalifa and Hamood (2009b) found that increasing the insulation thickness increases the solar still productivity by up to 80% which is partly due to the increase in the operating temperatures of the still.

1.2 PROJECT OBJECTIVES

In this study, a solar water purification system is based on distillation principle where the evaporation and condensation chambers are separate.

The aim of this study is to design, develop and construct this solar water purification system with improved productivity which is to be used in rural/remote areas. The objectives are as follow:

- To investigate specific features, possible construction materials and parameters affecting the productivity of the solar still.
- To design and model the solar still:
- To build the physical solar still.
- To test of the prototype:
    - Collection and measurement of relevant data necessary
    - Performance analysis for solar still

1.3 SIGNIFICANCE OF THE STUDY

The general purpose of this study is to contribute to the technical knowledge of solar distillation as an alternative water purification method for small scale use. It will make a contribution by providing supplementary experimental results and performance of a solar purifier system operated as distiller. It may as well give additional insight in the use a separate condenser for the productivity enhancement of solar water purifiers.

1.4 DELIMITATIONS

The present study aims at analysing the performance of the designed and constructed solar still unit. The social and economic impact of the implementation of this unit in rural areas will not be developed and discussed.

1.5 DISSERTATION ORGANISATION

Chapter One provides the motivation for the present study as well as general background information on the water crisis, the existing water purification methods and solar distillation.

Basic principles of solar distillation and some parameters affecting the performance of this process are also presented.

Chapter Two describes the design considerations and choices of the studied solar distillation units. It presents illustrations and the description of different components of the solar purification system.

Chapter Three describes the experimental set up, the materials and methods for testing the solar still units. Determination of derived data is also described.

Chapter Four reviews and discusses the results of the solar still units.

Finally the main conclusions will be drawn from this investigation and recommendations for future work will be made in Chapter Five.

CHAPTER 2 DESIGN AND CONSTRUCTION OF THE SOLAR DISTILLATION UNIT

2.1 INTRODUCTION

As stated in the previous chapter, the performance of a solar distillation system depends on the location climatic parameters but as importantly on the design parameters. With the general solar distillation units presenting a low efficiency, it is a necessity to consider various techniques to minimise energy losses, maximise energy absorption and increase evaporation and condensation rates in the unit, thus consequently maximising distillate production. Though it can be rather costly to manufacture a solar still that is both effective and long lasting, it can produce clean water at a relatively low cost if it is built, used, and maintained correctly. This section describes and explains the considerations and choices made for the design of the solar distillation unit.

2.2 DESIGN OF THE STILL COMPONENTS

2.2.1 BASIN DESIGN

The basin which contains the solar still is a major component to design for a good performance of the solar still. Important aspects to consider are the material used, the thickness, geometry and strength. These will be described in the next paragraphs.

2.2.1.1 MATERIAL SELECTION

Several materials were considered for use as the basin material such as aluminium, stainless steel and galvanized steel.

Aluminium was first considered because of its resistance to corrosion, light weight, long life and because it is easy to clean. Also, it is easier to be used for sheet bending. With a higher strength to weight ratio than steel, aluminium seemed to be the right material for the basin. However, because of its high cost per kg, a solar still made out of aluminium would be relatively expensive to build.

Wood which is generally readily available in rural areas was also considered. However, it gets damaged with time and ambient conditions and therefore was not retained as a basin material.

Stainless steel is by nature corrosion resistant and contains chromium which provides the stainless and corrosion resisting properties. It has a high impact and shock resistance. Its hygienic surface due to the smooth and minimally porous surface and it's easy to clean ability are perfect for drinking water treatment processes, since high hygiene is required. However, because of its high cost, stainless steel would make the still unsuitable (not affordable) for use in rural areas.

Galvanised steel is steel that has undergone chemical processing called "continuous hot-dip" in which it is coated with layers of zinc oxide in order to make it corrosion resistant. It does not require any additional or secondary painting or coating to protect it from corroding. With its high strength, easy to clean surface due to the coating and relatively low cost, galvanised steel would be one of the most both economical and technically viable materials to be used for solar still basin. Galvanised steel was used for this project.

Since the basin temperature should be able to rise as much and fast as possible by the absorbed solar radiation, it is therefore important to coat or paint it with a black material or black colour. This coating and paint should be able to withstand high temperatures, constant contact with water, and be clinically and biologically compatible with drinking water.

2.2.1.2 GEOMETRY

The basin consists of sheets of galvanized steel bent and welded together (Figure 2-1). It possesses 4 walls with the dimensions seen in Table 2-1. A rectangular slot of dimension 1000x150mm was cut on the top part of the back wall to allow steam to flow from the evaporation chamber to an external condenser (section 2.2.3). The technical drawings and dimensions of the basin are found in APPENDIX A.

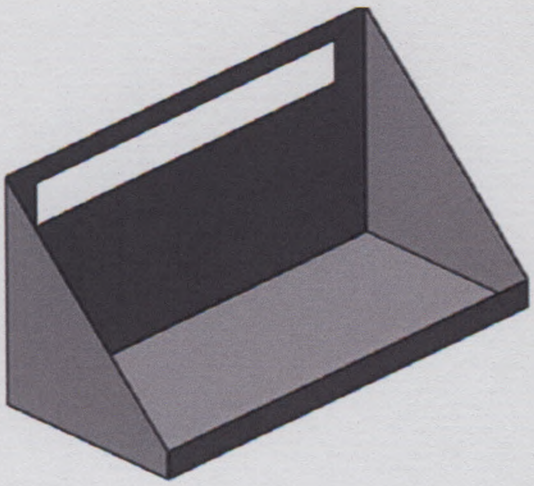

Figure 2-1: Basin geometry

Table 2-1: Basin geometric specifications

Wall	Height (m)	Length (m)	Width (m)
Front	0.1	1.2	.
Back	0.8	1.2	.
Bottom	.	1.2	0.54
Side (x2)	0.8	.	0.54

2.2.2 Glazing design

2.2.2.1 Material selection

The most widely used material for solar still cover is glass. It is reported to provide good transmission of solar radiation as well as little absorption and reflection and has a long life expectancy. However, its fragility makes it delicate to handle and work with. Glass has a poor thermal efficiency and is relatively expensive.

Polycarbonate which is more affordable than glass is naturally transparent with the ability to transmit light close to that of glass. It has an excellent impact strength and toughness and has good heat resistant properties. Although polycarbonate is reported to change colour over time, it can stay functional for several years.

Polycarbonate is the material chosen for the glazing of this solar still.

2.2.2.2 NUMBER OF COVERS

Benhammoud and Draoui (2013) studied the effect of double glazing on a solar still with external condenser. They observed that the yield of condensation on the simple glazing was higher than that on a double glazing. Moreover, the temperatures of the still components increased appreciably in the case of double glazing, the external condenser performed better and more overall distillate yield was obtained (5% more).

Double glazing is the method of covering the still with two layers of transparent covers with a space between them designed to reduce heat loss from the top of the still (Figure 2-2: Double glazing). Through the air gap, heat loss by convection is considerably reduced. The air gap between the covers acts as an insulation and intensifies the greenhouse effect inside the solar still. It will then result in a significant increase of the temperature of all the components inside the still.

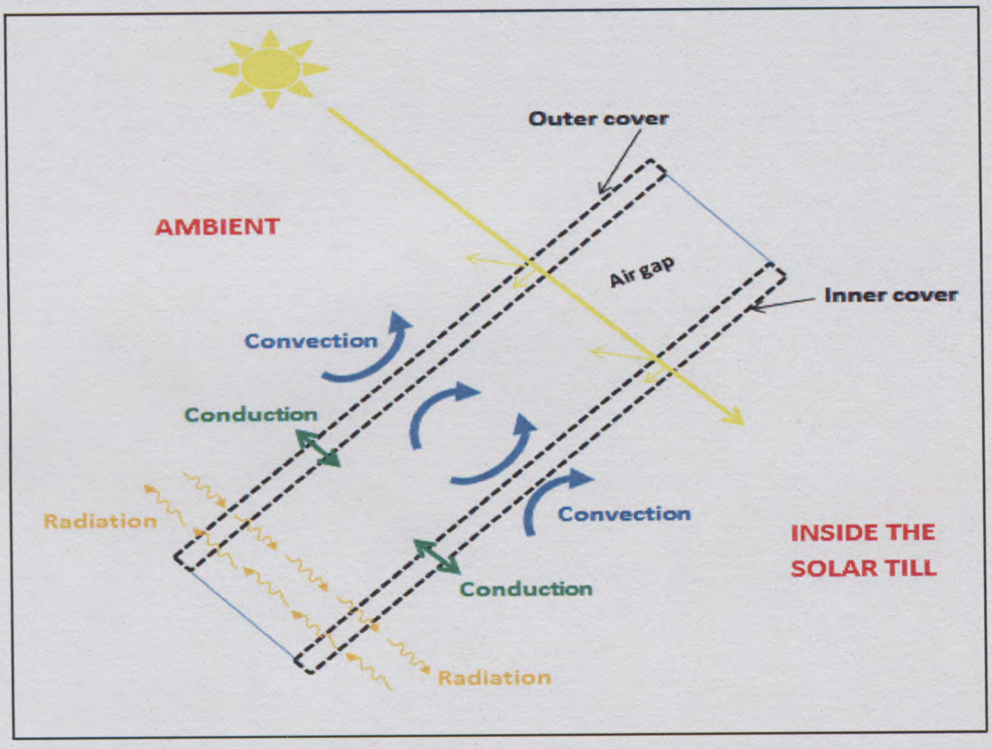

Figure 2-2: Double glazing

2.2.2.3 THICKNESS

Two sheets of polycarbonate were used for the solar still glazing. Their thicknesses were chosen to be 5mm each. This thickness helps improve the thermal performance of the solar still as well as well as is more resistant to buckling under its own weight due to its large area.

2.2.2.4 INCLINATION

According to Tanaka (2010) who studied the monthly optimum inclination of glass cover on solar still at location 30° N latitude, the optimum glass cover inclination is about 10° in summer and 50° in other seasons. This is taken as a base in the choice and calculation of the inclination in the present study. Moreover, Kanyarusoke et al. (2012) proposed the best inclination angle on a given day to be:

$$\beta^{\circ} = |L^{\circ} - \delta^{\circ}| \quad \textbf{(2-1)}$$

with L = Latitude of the place and δ = Sun declination angle (calculated using equation (3-6).

From the present study, the optimal angle for the solar still transparent cover in winter would be equal to: $|-33.93 - 23.45| = 57.4^{\circ}$ from the horizontal. However, considering some geometrical constraints of the unit such as the height to base ratio which would make the still to be too high, an angle of 53° from the horizontal was chosen. This angle will be tested in winter and spring with respectively a scaled model solar still and a prototype solar still which differ by their sizes and a few features such as the number of glazing covers and the insulation

.

2.2.3 CONDENSER DESIGN

During the distillation process, condensation droplets on the transparent cover usually causes absorption and reflection of the incident solar radiation on the solar still. This causes a reduction on the total incident solar radiation inside the basin, thus a decrease of the distillate output of the still. There is therefore a need to eliminate or at least reduce that condensation on the cover. In order to do so, a separate condenser was incorporated to the still unit.

Several researches have suggested the use of separated condensers to improve the performance of solar stills. For instance, Fath & Elsherbiny (1993) and El-Bahi & Inan (1999) coupled the single-slope single basin solar still with an external condenser located in the shadow zone of the still, and obtained an increase in the still performance compared to a solar still with no external condenser.

The external condenser consists of galvanized sheets of metal welded together as seen in Figure 2-3. Metallic condensing chamber is chosen for its low heat capacity. The condenser is formed as a transformation duct, going from a rectangular shape and size of the slot provided on the back wall of the basin, to a small square shape. It has an inclination of 60° to the vertical to allow the flow of the condensed water into a collecting jar. This condenser makes up a total condensing surface of 0.70 m^2 (inside walls). The technical drawings with dimensions of the external condenser are found in APPENDIX A.

With the intensified greenhouse effect in the solar still, the temperature of the inner transparent cover will be raised. The temperature difference between the water surface and the cover will be reduced, which will slow down the condensation process. An large quantity of steam will therefore diffuse through the rectangular slot on the back wall of the basin, into the condenser at a much lower temperature.

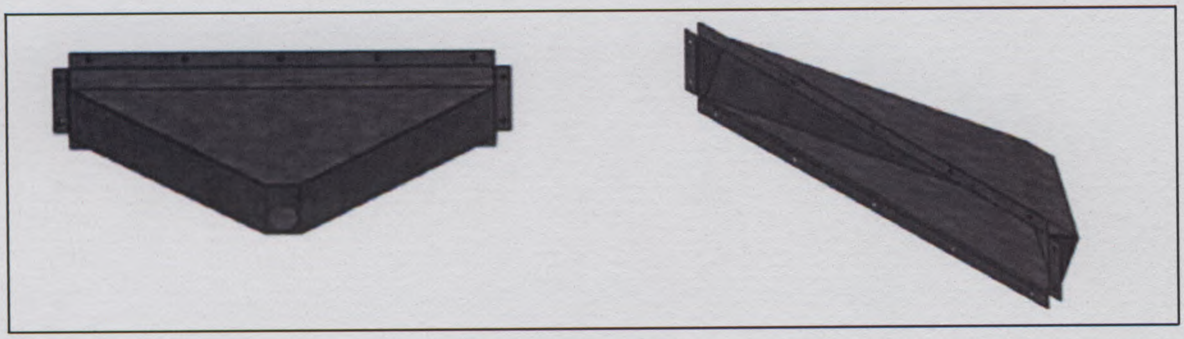

Figure 2-3: External condenser drawing

There is a need to shield the external condenser since if not shielded, it would be exposed to solar radiation and its temperature would rise significantly during the day time. This would cause a reduction of the performance of the still.

2.2.4 INSULATION

Considering the material (steel) and the thickness (2.5 mm) of the basin, there is a necessity to insulate the solar still to assure a high operating temperature of the system, and keep the temperature of the evaporation chamber as high as possible throughout the day. Insulation on the walls and bottom of the still contributes to minimize the energy losses of the unit.

Polystyrene is reported to be a good insulator with a thermal conductivity of 0.03 W/MK. Its robustness makes it a good material to use for solar still, as it can withstand the weight of the system. Moreover, this material which is relatively low in price, does not degrade easily especially at temperature below 70 °C. For an effective insulation, a thickness of a least 2 cm is necessary.

2.2.5 COLLECTIVE CONTAINER AND EVAPORATIVE COOLING

Evaporative cooling is another technique that can be used to increase the distillate output of the still. It consists in placing the solar still collecting container into a meshing basket with a porous material stuffed between the two. Figure 2-4 shows an illustration of the concept of evaporation cooling. The porous material has to be constantly wetted. Due to the slow evaporation of the water from the porous material, the glass container is cooled down. Aimiuwu (2008) reported that the glass container can be cooled down to 15 °C below the ambient temperature and under favourable conditions. Since the external condenser and the collecting jar are being connected together through fittings, the difference between the higher condenser and lower container temperature will drive some of the uncondensed steam in the condenser to flow from the condenser to the container where it will condense.

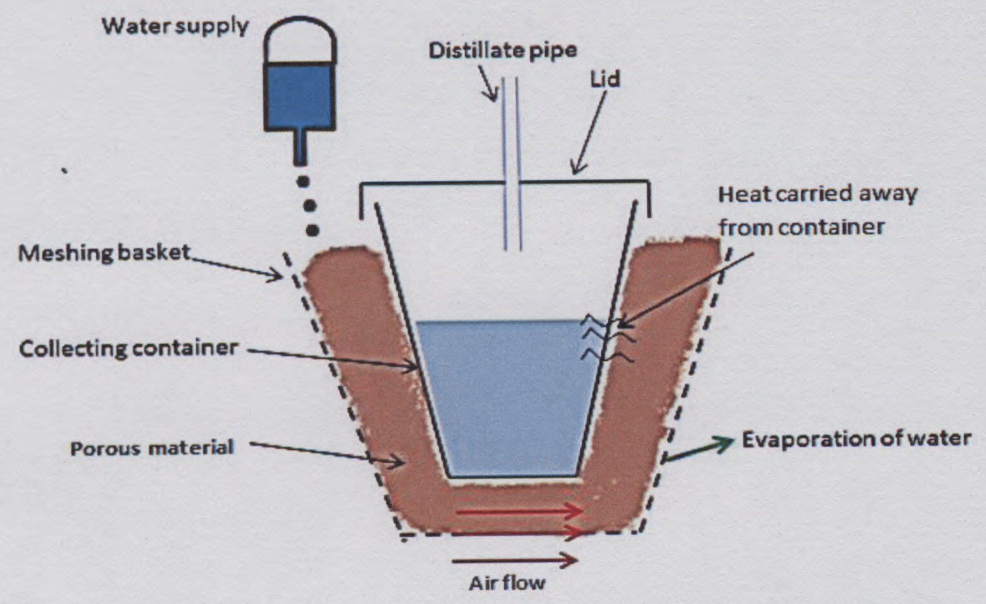

Figure 2-4: Evaporation cooling

2.3 FABRICATION OF THE STILL

The solar still prototype was fabricated in the workshop of the mechanical engineering department of the Cape Peninsula University of Technology. The basin which is made out of 2.5mm thick mild steel sheets has an evaporating area of 1.056 square meters for a basin length and width of 1.2 m and 0.54 m. The sheets were cut, bent and welded together before being sent for galvanising in a local company. The welded corners of the basin were sealed with a high temperature and waterproof silicone sealant to prevent leakage. It was then painted in black with a high heat resistant, waterproof and food safe paint (Figure 2-5).

Next, steel flat and angle bars have created a continuous support on the inner glass cover edges. They were welded together to the basin to create a frame support for the inner transparent cover. Sealant was again applied on the welded joints and self-adhesive sponge rubber strips were placed on the frame.

The external condenser was made out of four cut pieces of mild steel (1.6mm) welded together as seen in Figure 2-6. The welded corners were sealed and painted in a white waterproof and weather resistant paint to reduce solar radiation absorption. A 15mm hole was drilled on the inferior side of the condenser to provide room for pipe fittings to connect it to the collecting jar. It was then attached to the basin by fixing it on the rectangular slot provided on the back wall of the basin. The two were welded together and the welded joints were sealed to prevent leakage.

Regarding the solar still glazing, a trough made out of 20 mm pipe cut lengthwise was attached to the lower edge of the inner transparent cover. It was fixed at a slight slope along the plane of the cover to allow the water condensed on this cover to run down to the lower side of the cover through a 22 mm hole in the right side of the basin and into a plastic flexible pipe down to a 1 Litre collecting container. The PVC pipe was shaded using aluminium tape to prevent solar radiation from heating the condensed water inside the cut pipe, so that it does not evaporate a second time (See Figure 2-7).

Once the trough was attached, the inner cover was bolted to the basin frame. Clear silicone sealant was then spread uniformly along the edges of the cover by means of a spatula. The outer cover was then placed on the top edges of the basin and supported on its edges by the insulation sheets.

A 25mm hole was drilled on the right side of the still to attach the inlet pipe coupled to a valve. A funnel was placed on the vertical pipe to facilitate water feed inside the still.

Polystyrene sheets 25mm thick were used on the sides, bottom and back of the solar still to insulate it (Figure 2-8). It was all covered up using 0.2mm thick sheets of aluminium to protect it from weather aggression. The edges of the aluminium sheets were bent for safety and duct tape was used to cover them.

The external condenser was attached to a 2 litres container with the use of appropriate fittings and a clear flexible plastic pipe. A car shade was fixed above the condenser and held stretched by strings attached to the weather station pole (Figure 2-9).

For the evaporative cooling, the collecting container was placed inside a meshing basket with wood shavings stuffed between the two (Figure 2-10). In order to allow the wood shavings to be constantly wetted, a plastic container was placed higher than the glass container. A plastic flexible pipe with small holes drilled along its length and connected to the tap of the plastic container is placed all around the meshing basket on top of the wood shavings to allow water to drip into it.

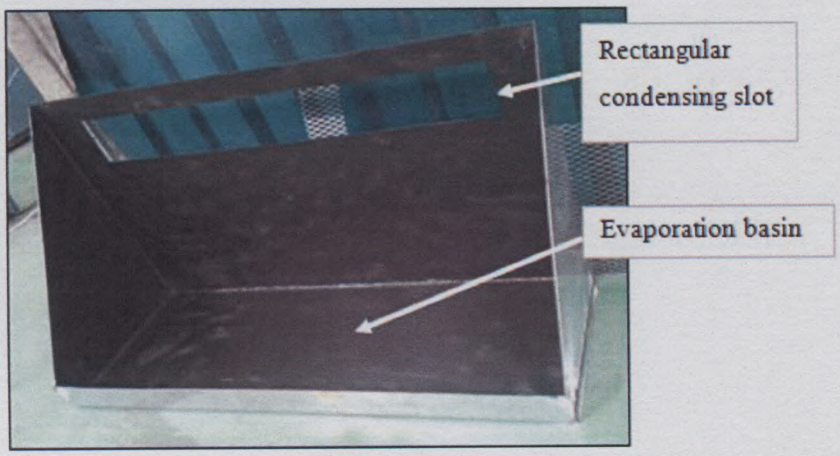

Figure 2-5: Black painted evaporation basin

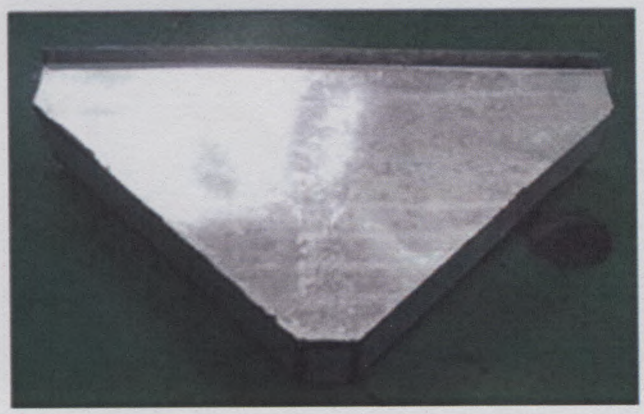

Figure 2-6: External condenser

Figure 2-7: Front cover collecting system

Figure 2-8: Condenser attached to basin

Figure 2-9: Side view of the still

Figure 2-10: Evaporative cooling system

The still was installed on clay bricks instead of being laid directly on the surface of the roof. This permitted to slope the unit when necessary since the height of the blocks could be easily adjusted using small pieces of wood. The materials used in the construction of the unit as well their cost are shown in Table A- 1 (APPENDIX A).

2.3.1 MODEL SOLAR STILL

For the purpose of experimentations, a model solar still was fabricated. Some material had to be changed for cost purpose.

The model solar still unit was constructed in the workshop of the Mechanical Engineering department of Cape Peninsula University of Technology, Bellville Campus. The still consists of a single basin-single slope unit with evaporator area 0.163 m^2 (600 mm x 270 mm) and thickness 1.6 mm made out of black painted galvanised steel containing saline water. The high-side wall depth is 400 mm and the low-side wall height is 50 mm (Figure 2-11). It was fabricated by sheet metal work by bending and cutting. The bottom and sides of the still were painted black to increase absorption of sun radiation by the basin and thus increasing the evaporation rate. An external condenser is attached to the back of the unit through a slot of size 500x75 mm. This condenser, mounted as a transformation duct at an angle of 60 degrees is made out of plastic 1.6mm thick welded together. A collecting container is attached to the narrow and lower part of the transformation duct by means of a pipe 40 mm in diameter and a bend of 120^{o}.

A glazing cover made of 600x450x3mm ($0.27\ m^2$) clear Perspex sheet to allow and trap sunlight in the still was mounted at an angle of 53^{o} to allow maximum solar radiation to enter the evaporator. This particular angle was selected for its optimality during the test (June month – winter in the Cape).

Figure 2-11: Solar still model

2.4 WORKING OF THE SOLAR STILL

The operation of the solar still studied is illustrated in Figure 2-12.

After being reflected, absorbed and transmitted from the double transparent cover, solar radiation enters the evaporation chamber of the unit. This transmitted radiation is further reflected and absorbed by the layer of water, after which it reaches the black painted evaporation basin where it is absorbed. After absorption of the solar radiation by the basin, most of the thermal energy is transferred to the water, while the rest is lost to the ground. This heat loss is however reduced with the use of the polystyrene insulation. Because of the double polycarbonate glazing, heat loss from the top is reduced which results in the temperature of the inner cover to increase significantly, thus reducing the overall temperature difference between the water and the inner cover.

The pressure in the condenser is therefore relatively low as compared to the evaporation chamber and the difference of pressure between the two chambers causes the vapour to be transferred from the evaporation chamber to the condensing chamber through the rectangular slot provided.

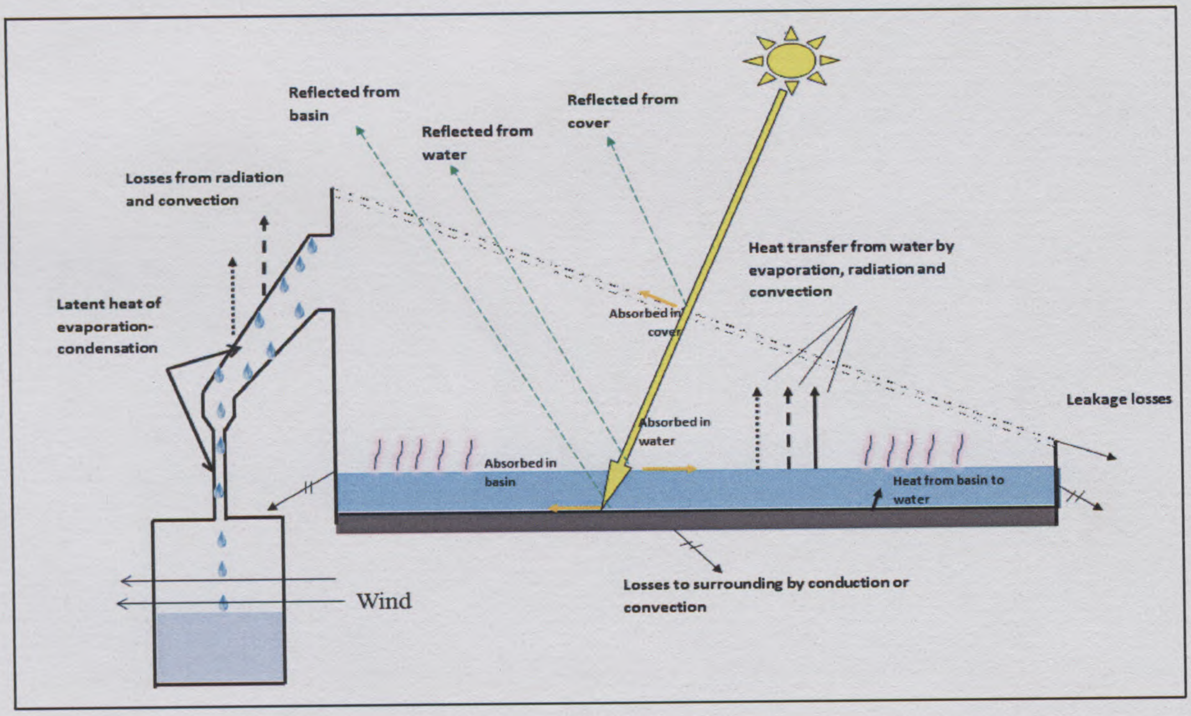

Figure 2-12: Solar still working

The transferred vapour is condensed on the internal walls of the condenser which are tilted so that the condensate is collected in the back collecting jar. Moreover, the temperature difference between the water surface and the inner transparent cover causes some condensation on the cover. The solar still distillate output is the sum of the output from both condensers (cover + external condenser).

2.5 SUMMARY

The summary of the design parameters of the stills is shown in Table 2-2.

Table 2-2: Design parameters of the solar still

Parameter	Model	Prototype
Basin material	Galvanised steel	Galvanised steel
Basin thickness	1.6 mm	2.5 mm
Height of back wall	400 mm	800 mm
Height of front wall	50 mm	100 mm
Width of basin	270 mm	540 mm
Area of condensing slot	0.035 m^2	0.15 m^2
Area of evaporative surface	0.163 m^2	0.65 m^2
Transparent cover material	Clear Perspex	Clear polycarbonate
Number of covers	1	2
Thickness of cover	3 mm	5 mm
Tilt angle of cover	53°	53°
Area of collecting surface	0.27 m^2	1.056 m^2
External condenser material	Plastic	Galvanised steel
Area of external condensing surface	0.35 m^2	0.70 m^2
Insulation material	.	Polystyrene
Insulation thickness	.	25 mm
Shading of external condenser	No	Yes
Evaporative cooling	No	Yes

CHAPTER 3 EXPERIMENTAL SETUP AND METHODOLOGY

The study of the systems described in CHAPTER 2 was performed in June 2014 for a period of 21 days on the scaled model of the solar distillation unit and in November 2014 for a period of 8 days on the actual unit. The experiments were run in the climatic conditions of Bellville, Cape Town Zone. This chapter presents and analyses the data from the test period. Section 3.1 presents the test zone general climatic conditions. Section 3.2 describes the instrumentation and testing procedure and section 3.3 deals with derived and calculated data necessary to study the performance of the solar distillation unit.

3.1 BELLVILLE CAPE TOWN ZONE CONDITIONS

- Latitude and longitude: 33.93°S and 18.42°E, respectively.
- Average ambient temperature during winter and summer seasons: 18.5 °C and 24.3 °C, respectively.
- Average wind velocity: 6.9 m/s
- Average daily sunshine hours in June and November: 6h and 10h respectively.
- Average humidity in June and November: 80% and 70% respectively.

3.2 EXPERIMENTAL SETUP AND INSTRUMENTATION

3.2.1 MODEL TESTING

3.2.1.1 TESTING PROCEDURE

The experiments were carried out under atmospheric conditions in Bellville, Cape Town. Measurements were recorded during the day, from 9:00 to 18:00 for a period of 21 days during the month of June 2014.

3.2.1.2 TEST RIG

The test rig located in the compound of the Mechanical Engineering building consisted of the model solar still and the measuring instruments as shown in Figure 3-1. The weather station was located on a roof close to the test rig. Each part will be separately described in detail in the following sections.

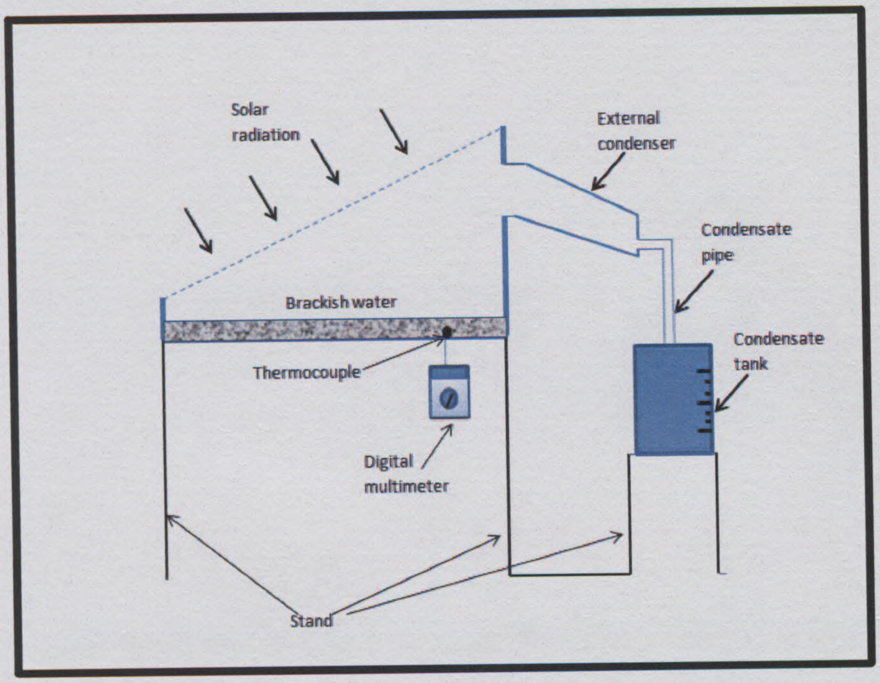

Figure 3-1: Schematic diagram of the model solar still test rig

3.2.1.3 MEASURED DATA AND INSTRUMENTATION

For the whole test period, solar radiation intensity, wind speed and ambient temperature were collected from the Campbell Scientific weather station at the mechanical engineering department. This weather station (Figure 3-2) is composed of one pyranometer to measure total hemispherical solar radiation (beam and diffuse), a pyranometer with shading ring to measure diffuse radiation and a cup anemometer to measure wind velocity. These are all connected to a Data logger.

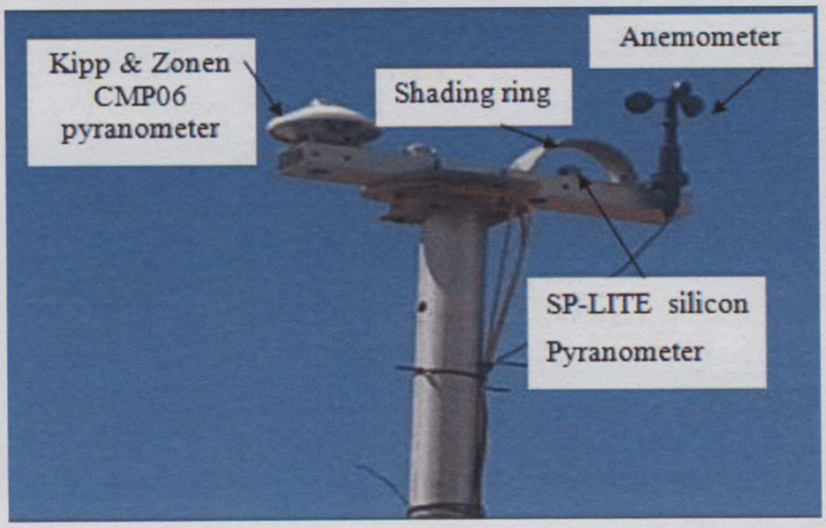

Figure 3-2: Weather station

- Solar radiation measurement

For the purpose of this study, global solar radiation (direct + diffuse) and diffuse solar radiation were measured throughout the days of test.

Total solar radiation intensity was measured using a Kipp & Zonen CMP06 type pyranometer. It consists of a series of 64 thermocouples junctions connected in series of sensing element and has a high quality blackened thermopile (detector) protected by a double glass dome (Figure 3-3). Its flat spectral sensitivity, from 285 to 2800 nm, makes it ideal for measuring natural sunlight and it is most usually used to measure solar radiation being received on the horizontal plane. This pyranometer produces a millivolt signal that is measured directly by a Campbell Scientific control data logger. See APPENDIX B-1 for technical specifications of the pyranometer.

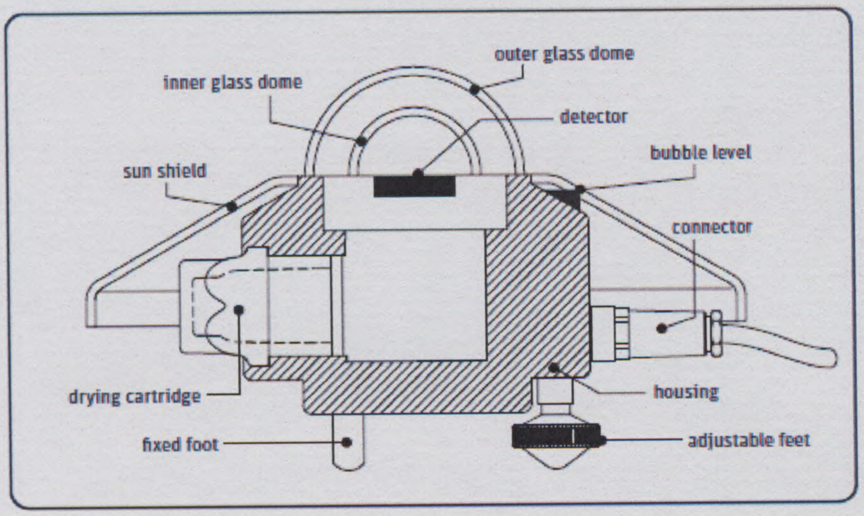

Figure 3-3: Schematic diagram of the Kipp & Zonen CMP06 Pyranometer

http://www.ames.si/files/attachments/KippZonen_Brochure_Pyranometers.pdf

Diffuse solar radiation was measured using a Kipp & Zonen SP-LITE silicon Pyranometer (Figure 3-4) integrated with a shading ring to shade the instrument from beam radiation. It consists of a photodiode complete with housing and cable. The circuit includes a shunt resistor for the photodiode in order to generate a voltage output. The SP-LITE has a spectral range of 400 to 1100 nm. See APPENDIX B-2 for technical specification of the pyranometer.

Figure 3-4: Kipp & Zonen SP-LITE silicon pyranometer

http://s.campbellsci.com/documents/us/manuals/sp-lite.pdf

The semi-circular shading ring as shown in Figure 3-2 is fixed in such a way that it shades the thermopile element and the double glass dome at all time from direct sunlight. It then results in the pyranometer measuring only the diffuse radiation received from the sky. The shading ring is made out of aluminium with a width of 10 cm.

- Wind speed measurement

Wind speed was measured using a 03101 R.M Young three cup anemometer (Figure 3-5). The rotation of the cup wheel produces an AC sine wave voltage with a frequency proportional to wind speed. The anemometer is directly connected to a data logger, which measures the anemometer's pulse signal and converts the signal to meters/second (m/s). It works in a range of 0- 50 m/s. See APPENDIX B-3 for technical specifications of 03101 R.M Young three cup anemometer.

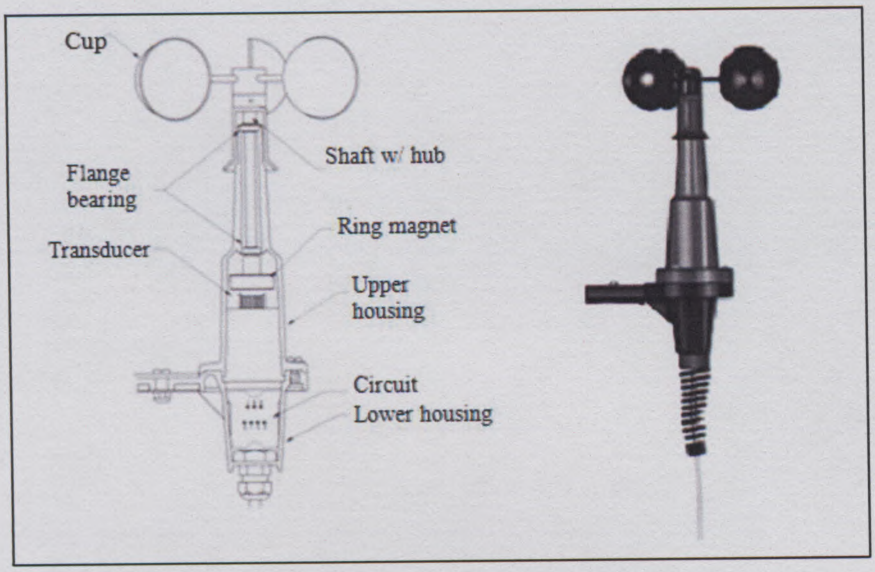

Figure 3-5: 03101 R.M Young Anemometer

https://s.campbellsci.com/documents/af/manuals/03002.pdf

TP02A K-Type thermocouples were used to measure the ambient temperature and the water temperature in the still. As part of the solar station, a shielded thermocouple connected to the data logger measured the ambient temperature of the location at an interval of 10 minutes. The thermocouple used to measure the water temperature was connected to a Multi-meter from which the temperatures were read hourly.

- Data recording instruments

The Multi-meter used to measure the water temperature was a UNI-T UT53 model. Measurements were taken every hour for the whole period of test in the month of June.

The data logger used to process the sensor measurements was a Campbell scientific Inc. CR1000 model (See Figure 3-6). Measurement were taken and stored every 10 minutes in order to get accurate graphs for the test period.

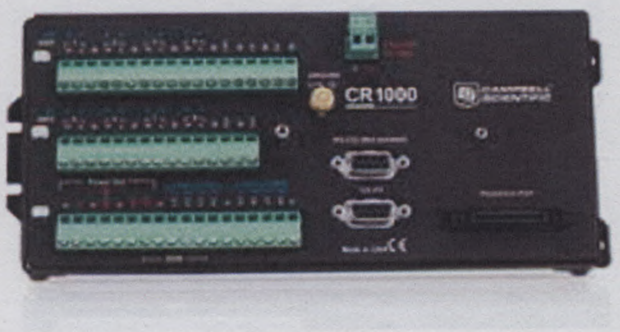

Figure 3-6: Data logger

3.2.1.3.1 DISTILLATE YIELD

The distillate yield was measured using a graduated measuring cylinder. The level of water was read hourly from 9:00 to 17:00 during the test period.

3.2.2 PROTOTYPE SOLAR STILL TESTING

3.2.2.1 TESTING PROCEDURES

The experiments were carried out under atmospheric conditions in Bellville, Cape Town. Measurements were recorded during the day, from 7:00 to 18:00 for a period of 8 days during the month of November 2014.

The solar still was batch-fed early each morning. The outer transparent cover was cleaned of the accumulated dust during the previous day and night in order to avoid a reduction of solar radiation entering the system. During seven test days, tap water was used, while water from the lake at the CPUT was only used on the first day of test. Lake water was not used throughout the testing period as deposits from water would cumulate inside the basin and proved to be difficult to remove since proper drainage system was not designed for. Since the effect of these deposits on the performance of the still was not known, and since this study mainly concerns the productivity of the designed solar still, tap water was used for the rest of the tests.

3.2.2.2 TEST RIG

The test rig erected on the rooftop of the mechanical engineering building at CPUT consisted of the solar distillation unit, the weather station, and other measuring system instruments (Figure 3-7). The weather station was erected at two meters above the surface of the roof to prevent any shading and other disturbance o the sensors (Figure 3-8). Each component will be described in detail in the following sections.

Figure 3-7: Perspective view of the test rig on roof top

Figure 3-8: Upper view of the test rig

3.2.2.3 MEASURED DATA AND INSTRUMENTATION

During the test period, solar radiation intensity, wind speed, ambient temperature, different system components temperature and distillate collection were measured.

- Solar radiation intensity and wind speed

Global and diffuse solar radiation and wind speed were measured using the same instrumentation used during the model testing. The measured data were recorded every 15 minutes for the full day, while only data recorded from 7:00 to 16:00 (during sunshine) were used and analysed.

- Temperature measurements

K-type thermocouples Figure 3-9 were used to measure different system component's temperature. Seven thermocouples were used in the system to measure the following temperatures distributed as shown in Figure 3-10.

- 1. Outer transparent cover (T_{go}),
- 2. Inner transparent cover (T_{gi}),
- 3. Vapour temperature (T_v),
- 4. Water temperature (T_w),
- 5. Basin temperature (T_{ba}),
- 6. Condenser temperature (T_{co}),
- 7. Ambient temperature (T_a).

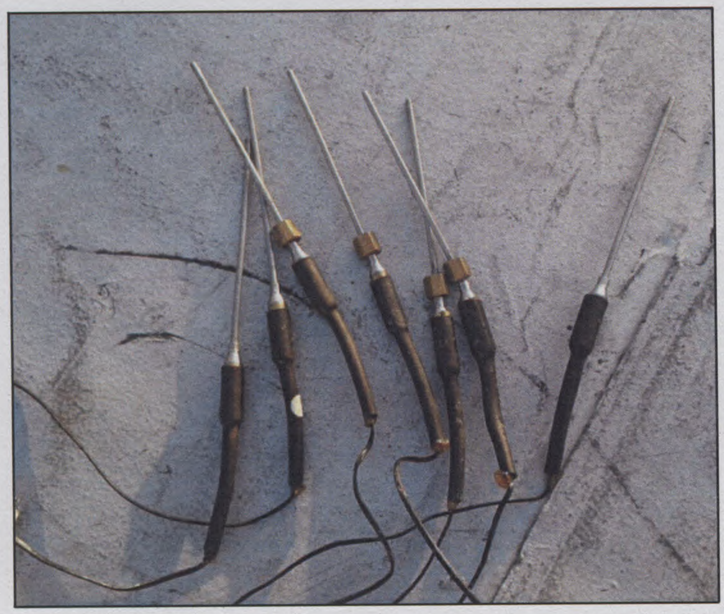

Figure 3-9: K-type thermocouples

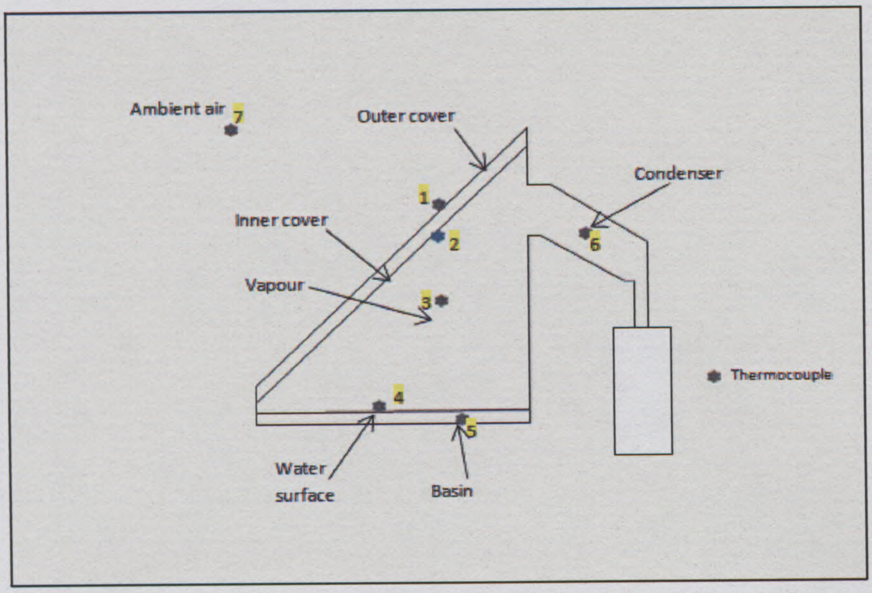

Figure 3-10: Thermocouples distribution in the still

Considering the relatively small areas and volume of the still and the availability of thermocouples, one thermocouple was placed on each component in the best possible location and the temperature of the point of contact is assumed to represent the temperature of the component measured. These thermocouples were distributed as shown in Figure 3-10.

- One thermocouple was fixed on the outer transparent cover while a second was fixed on the inner side of the inner transparent cover. The covers are considered thin enough so that the temperature gradient through the thickness of the cover is negligible. In order to get good thermal contact between thermocouples and the polycarbonate covers, two small scratches were made on the emplacement of the thermocouples, then a thermal conductive paste was applied for fixing. A small piece of aluminium tape was stuck on the cover to shade the tip of the probe from direct sunlight, so as not to alter the sensor's readings.

- Two thermocouples were placed inside the still in the basin. One measured the basin temperature while the other measured the water temperature. The basin thermocouple was fixed directly on the basin with the thermal conductive paste and covered with aluminium tape. The water thermocouple was fixed on the inner black wall of the solar stills in such a way that the tip of the thermocouple is dipped into the water.

- Another thermocouple was used to measure the temperature of the vapour inside the basin. The thermocouple wire was fixed to the transparent cover and the probe was left hanging inside the still.

- The condenser thermocouple was fixed vertically inverted on top of the condenser through a drilled hole and the probe was measuring the vapour inside the condenser

- A thermocouple was used as part of the weather station to measure the ambient temperature. This thermocouple was shaded so that the solar radiation would not alter the readings of the sensor.

The temperature measurements were recorded every 15 minutes and they were stored in the data logger.

- Distillate output

The distillate output from the solar still unit was read and recorded hourly from two graduated jars. One of the jars collected the condensate from the back condenser while a second smaller jar collected the condensate from the trough fixed to the inner transparent cover.

3.3 DATA REDUCTION

From the data collected during the experiment, the following parameters were determined:

- Solar radiation incident on glazing (entering in the solar still),
- Productivity of the solar still,
- Performance of the system.

3.3.1 DETERMINATION OF SOLAR RADIATION INCIDENT ON GLAZING

In this subsection, the method of calculation of the incident radiation on the sloped glazing of the solar still was developed. This method was used based on the solar radiation on a horizontal surface which was measured from the data collected at the weather station. Unless stated otherwise, the equations presented in this section are taken from Duffie & Beckman (2013).

The incident solar radiation is the sum of the beam radiation, diffuse radiation and radiation reflected from the ground and the surrounding and is expressed as follow:

$$I_T = I_{T_b} + I_{T_d} + I_{T_{refl}} \quad \textbf{(3-1)}$$

Different models have been proposed to determine radiation incident on an inclined plane. These mathematical models can be classified into two types namely the isotropic and anisotropic models. Isotropic sky diffuse models were developed by assuming that some of the diffuse radiation from the sky as well as the ground reflected radiation are constant across the sky dome (Hottel and Woertz: 1942, Liu and Jordan: 1960). This type of model is conservative as it tends to underestimate I_T. On the other hand, anisotropic sky diffuse models are improved models which consider the circumsolar diffuse and horizon brightening components of solar radiation on an inclined surface.

For the analysis of this solar still unit, the hourly global irradiation on a tilted surface was calculated using the anisotropic solar radiation diffuse model based on Perez et al. (1990). This model, which is a detailed analysis and provides more accurate prediction compared to other models takes into account all the components of solar radiation as shown schematically in Figure 3-11.

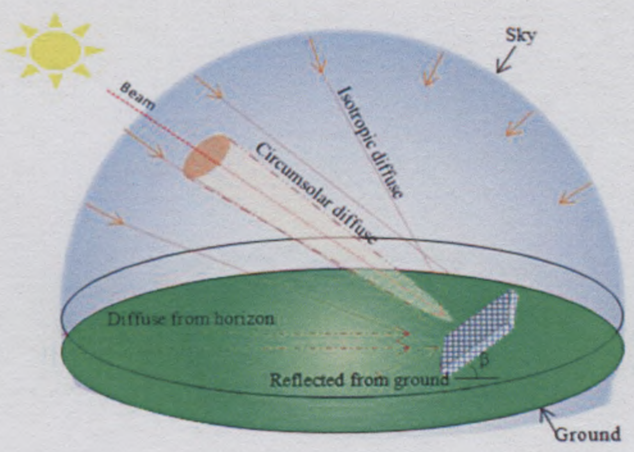

Figure 3-11: Components of solar radiation on a tilted surface

3.3.1.1 BEAM RADIATION

Beam radiation on a tilted surface at an angle β from the horizontal was determined by multiplying the direct horizontal radiation I_b by a geometric factor R_b. R_b is the ratio of beam radiation incident on an inclined surface to the beam radiation on a horizontal surface at a given time.

$$I_{T_b} = I_b R_b \quad \textbf{(3-2)}$$

$$R_b = \frac{I_{b'}}{I_b} = \frac{I_N cos\theta_i}{I_N cos\theta_z} = \frac{cos\theta_i}{cos\theta_z} \quad (3\text{-}3)$$

Where:

I_b is the flux of beam radiation incident on a horizontal surface,

$I_{b'}$ is the flux of beam radiation incident on a tilted surface,

I_N is the intensity of beam radiation,

θ_z is the zenith angle which is defined as the angle between the vertical and the line of the sun

θ_i is the incident angle of beam radiation.

$cos\theta_i$ and $cos\theta_z$ are respectively determined using the following equations:

$$cos\theta_i = cos(L+\beta)cos\delta cos\omega + sin(L+\beta)sin\delta \quad (3\text{-}4)$$

$$cos\theta_z = cosLcos\delta cos\omega + sinLsin\delta \quad (3\text{-}5)$$

Where δ is the declination angle of the sun was calculated from the approximate equation of Cooper (1969):

$$\delta = 23.45\, sin(360\frac{284+n}{365}) \quad (3\text{-}6)$$

with n being the day of the year which can be obtained with the help of Table C-1 in APPENDIX C.

L is the latitude of the location, with north positive.

β is the tilt angle,

ω is the hour angle which is equal to

$$\omega = 15(t - t_{noon}) \quad (3\text{-}7)$$

with t is the local time and t_{noon} is solar noon . ω is negative before noon and positive after noon.

Solar noon is determined as:

$$t_{noon} = 720 + 4 * longitude - (equation\ on\ time) \quad (3\text{-}8)$$

Equation of time is expressed as:

$$Equation\ on\ time = 9.87\sin 2B - 7.53\cos B - 1.5\sin B \quad (3\text{-}9)$$

Where:

$$B = (n - 81)(\frac{360}{365}) \quad \textbf{(3-10)}$$

Therefore the geometric factor obtained from equations (3-2) and (3-3) is expressed as:

$$R_b = \frac{cos(L + \beta)cos\delta cos\omega + sin(L + \beta)sin\delta}{cosLcos\delta cos\omega + sinLsin\delta} \quad \textbf{(3-11)}$$

3.3.1.2 DIFFUSE RADIATION

Diffuse radiation is the fraction of solar radiation which is received by the earth's surface after is it propagated in many different directons by the atmosphere (Kondratev: 1969). Diffuse radiation which is generally umpredictable is a set of three components:

Isotropic diffuse radiation: Intensity of solar radiation received from the entire sky.

Circumsolar diffuse radiation: Fraction of solar radiation received from further scattering and located in the region of the sky close to the sun.

Horizon brithening: Part of the solar radiation concentrated near the sky line which is mostly observed on cloud free skies.

According to Perez et al. (1990), the total diffuse radiation on a tilted surface is given by:

$$I_{T_d} = I_d\left[(1 - F_1)\left(\frac{1 + cos\beta}{2}\right) + F_1\frac{a}{b} + F_2 sin\beta\right] \quad \textbf{(3-12)}$$

Where F_1 and F_2 are circumsolar and horizon brightness

coefficients a and b are values that account for the angles of incidence of the sun on the sloped and horizontal surfaces. a and b are expressed as follow:

$$a = max(0, cos\theta) \quad \textbf{(3-13)}$$

$$b = max(cos85, cos\theta_z) \quad \textbf{(3-14)}$$

F_1 and F_2 depend the zenith ange θ_z (°C), a clearness parameter ε and a brightness parameter Δ.

The clearness parameter is given by

$$\varepsilon = \frac{\frac{I_d+I_{b,n}}{I_d} + 5.535 \times 10^{-6}{\theta_z}^3}{1 + 5.535 \times 10^{-6}{\theta_z}^3} \tag{3-15}$$

where $I_{b,n}$ is the normal incidence beam radiation given by

$$I_{b,n} = \frac{I_b}{cos\theta_z} \tag{3-16}$$

The brightness parameter Δ is

$$\Delta = m\frac{I_d}{I_{on}} \tag{3-17}$$

where m is the air mass calculated from:

$$m = \frac{1}{cos\theta_z} \tag{3-18}$$

m [kg], $cos\theta_z$ [-].

and I_{on} is the extraterrestrial normal-incidence radiation at any point in time determined by

$$I_{on} = I_{sc}\left(1 + 0.33cos\frac{360n}{365}\right) \times cos\theta_z \tag{3-19}$$

with the solar constant I_{sc} **= 1367 W/m^2.**

The brighteness coefficients F_1 and F_2 are given by:

$$F_1 = max\left[0, \left(f_{11} + f_{12}\Delta + \frac{\pi\theta_z}{180}f_{13}\right)\right] \tag{3-20}$$

$$F_2 = \left(f_{21} + f_{22}\Delta + \frac{\pi\theta_z}{180}f_{23}\right) \tag{3-21}$$

The coefficients $f_{11}, f_{12}, f_{13}, f_{21}, f_{22}, f_{23}$ are statistically derived for ranges of values of the clearness parameter ε. These brightness coefficients for Perez Anisotropic Sky can be obtained from Table C-2 in APPENDIX C.

3.3.1.3 REFLECTED RADIATION

The ground reflected radiation incident on a horizontal surface depends on the global radiation on the horizontal surface I_h, the ground reflectance ρ_g, and the angle of tilt β as:

$$I_{T_{refl}} = I_h \rho_g \left(\frac{1 - cos\beta}{2}\right) \tag{3-22}$$

Where $\rho_g = 0.2$ for non-snow cover.

3.3.1.4 TOTAL SOLAR RADIATION INCIDENT ON A TILTED SURFACE

From equations (3-2), (3-12) and (3-22), the total solar radiation on a surface tilted β is expressed as:

$$I_T = I_b R_b + I_d \left[\left(1 - f_1\right)\left(\frac{1 + cos\beta}{2}\right) + F_1 \frac{a}{b} + F_2 sin\beta\right] + I_h \rho_g \left(\frac{1 - cos\beta}{2}\right) \tag{3-23}$$

Sample calculations of the solar radiation incident on the transparent cover are shown in APPENDIX D.1.

3.3.2 ESTIMATION OF CLEAR SKY SOLAR RADIATION USING THE ASHRAE MODEL

Clear sky solar radiation is assumed to be the maximum solar radiation incident on a horizontal surface when all shadowing and scattering agents have been neglected (sky turbidity, cloudiness, ambient humidity…). It depends on the position of the sun at a particular location, day of the year and position of the sun in the sky. Various models have been developed in order to estimate the direct and diffuse components of the clear sky solar radiations for specific locations.

Here, the ASHRAE model (ASHRAE: 2009) was used to estimate the maximum solar radiation for clear sky conditions on the days on tests. The obtained results will be used for comparison purposes with the measured solar radiation incident on a horizontal surface.

The global clear sky solar radiation on a horizontal surface is expressed as:

$$E = E_b + E_d \tag{3-24}$$

where E_b is the beam radiation component

E_d is the diffuse radiation component.

The beam radiation component is expressed as:

$$E_b = I_{on} exp\left[-\tau_b m^{ab}\right] \tag{3-25}$$

and the diffuse radiation component is expressed as:

$$E_d = I_{on} exp[-\tau_d m^{ad}] \quad \textbf{(3-26)}$$

where I_{on} is calculated from equation (3-19),

m is calculated from equation (3-8),

τ_b and τ_d are the beam and diffuse pseudo optical depths,

ab and ad are the beam and diffuse air mass exponents .

These values depend on the location of the place, the local atmospheric conditions and the time of the year. Thevenard (2009) in an ASHRAE research project tabulated these values for the 21st day of each month for several locations worldwide, amongst which Cape Town. Daily values throughout the year are found by interpolation. Kanyarusoke et al. (2012) interpolated the daily values of beam and diffuse pseudo optical depths and air mass exponents for Cape Town which can be found in Table C-3 in Appendix C.

See sample calculation of ASHRAE solar radiation estimation in Appendix D.2

3.3.3 PRODUCTIVITY OF THE SOLAR STILL

The productivity of the solar still unit was estimated by collecting the distilled water from the condensing chamber to a graduated jar at the back of the still and from a collecting trough to a smaller graduated jar on the side of the still to arrive at the total quantity of distilled water during a chosen period.

The daily productivity of the solar still is defined as the total volume of distillate collected during the day per unit of solar radiation collecting area.

$$P_d = \frac{V_T}{A} \ (\frac{L}{m^2}) \quad \textbf{(3-27)}$$

Where,

P_d is the daily productivity of the solar still (litres/m^2)

V_T is the total daily distillate production which is equal to the sum of the instantaneous production $V_T = \sum V_i$, (litres) ; subscript i indicates hourly collection of distillate.

A is the collecting area (area of the transparent cover) m^2

See sample calculations of Pd in Appendix D.3.

3.3.4 PERFORMANCE- EFFICIENCY

The performance or efficiency of the solar still depends on the amount of solar energy used for vapourising the raw water inside the solar still. It is expressed as follow:

$$\text{Efficiency of solar still} = \frac{\text{Energy used in vapourising water}}{\text{Amount of solar energy incident on transparent cover}} \quad \textbf{(3-28)}$$

$$\eta = \frac{m \times h_{fg}}{A \times \int I\, dt} \quad \textbf{(3-29)}$$

where, m is the daily distillate output in kg. The density of the distilled water is taken to be 1000 kg/m^3. h_{fg} is the latent heat of vapourisation of water, A is the transparent cover area and I is the intensity of incident solar radiation.

For this study, h_{fg} was calculated using the latent heat of evaporation dependant of vapour from Tiwari and Tripathi (2003):

$$h_{fg} = 3.1615 \times 10^{6} \times [1 - (7.616 \times 10^{4} T)]\, for\ T > 70°\text{C} \quad \textbf{(3-30)}$$

$$h_{fg} = 2.4935 \times 10^{6} \times [1 - 9.4779 \times 10^{-4} T + 1.3132 \times 10^{-7} T^{2} - 4.7979 \times 10^{-9} T^{3}]\, for\ T < 70°\text{C}$$

where T is the vapour temperature inside the basin.

See sample calculations of h_{fg} and η in Appendix D.4.

CHAPTER 4 RESULTS AND DISCUSSION

4.1 INTRODUCTION

This section reports the results of the studies on the scaled model of the solar still as well as the actual solar still prototype and treats on the meteorological condition of the testing location on the testing period, the temperature of the system components, the distillate output and the efficiency of the solar still units. It is found that the performance of the actual solar still is satisfactory. Other results are discussed in details.

4.2 SOLAR STILL MODEL PERFORMANCE

The solar still model was tested during the month of June, from June 2 to June 30. Tests were performed during 21 days. On the 7, 8, 14, 15, 22, 23, 28 and 29 June (weekend days) no data were recorded.

4.2.1 WEATHER CONDITION

The variation of weather at time intervals of 10 minutes on a sample day of experiments (21 June 2014) is shown in Figure 4-1. It is observed that the solar radiation incident on a surface inclined at 53° from the horizontal was higher than solar radiation on a horizontal surface during the entire day (Figure 4-1(a)). This is in agreement with findings from Kanyarusoke et al. (2012) as discussed in section 2.2.2.4.

Solar radiation recorded levels showed to be satisfactory for a site at relatively high latitude in the southern hemisphere during the month of June. The solar radiation reaches a maximum value of 970.73 W/m^2 between 11:00 and 13:00.

The air ambient temperature was relatively fair for a winter day, varying between 10 and 23°C during the test period (Figure 4-1 (b)). The wind speed was intermittent and varied between 0 and 2.8 m/s (Figure 4-1(c)).

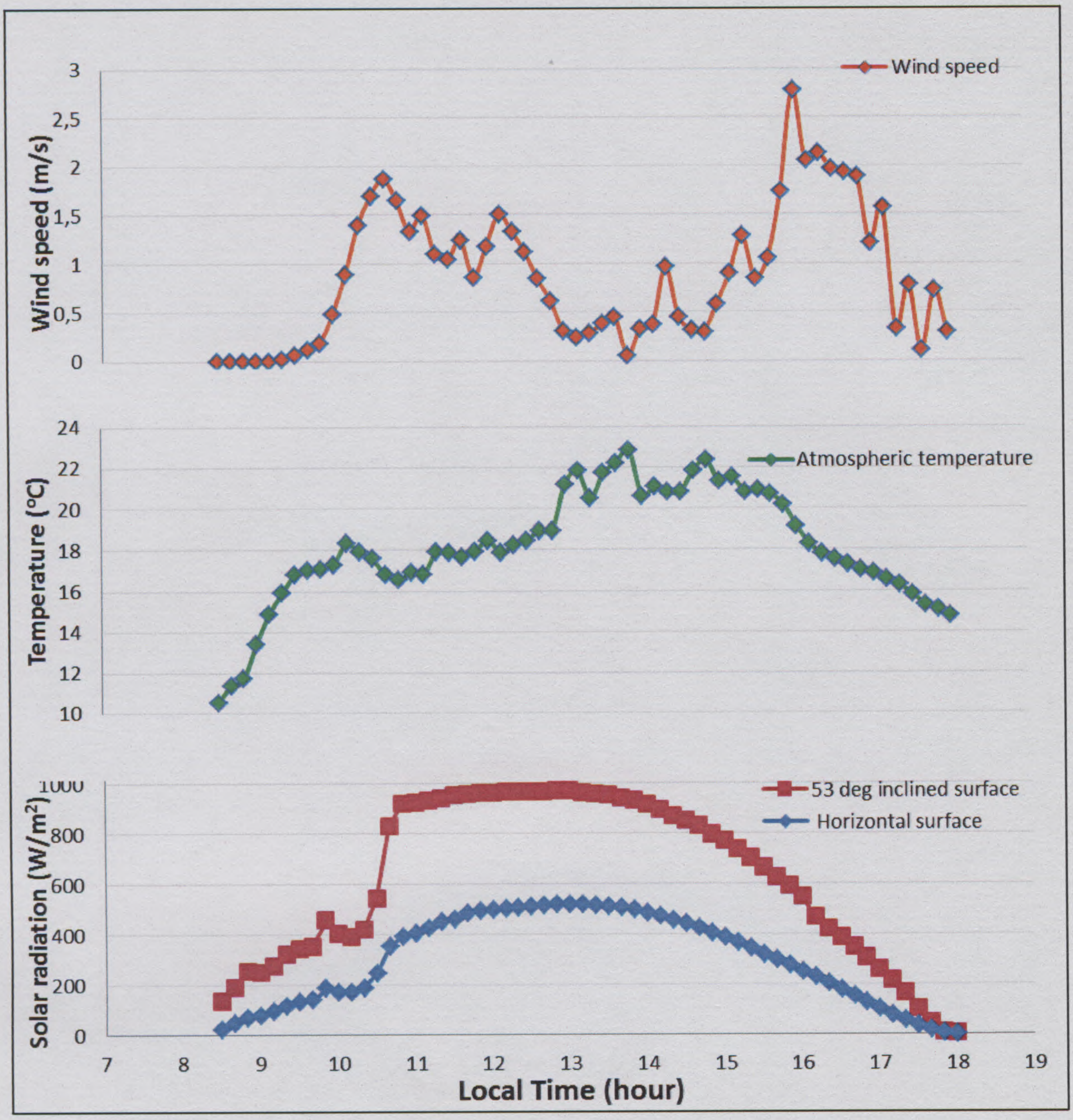

Figure 4-1: Variation of a) solar radiation on horizontal surface and 53° inclined surface, b) ambient air temperature and c) wind speed with local time on 21 June 2014 at Cape Peninsula University of Technology.

Figure 4-2 compares the global solar radiation estimated using the ASHRAE model with the measured global solar radiation using the Kipp & Zonen CMP06 Pyranometer. It is found that for the month of June, the computed and the measured global solar radiation present a reasonably good agreement. The difference is due to the atmospheric conditions variation from the ASHRAE standard definition of "clear sky "in Cape Town on that day.

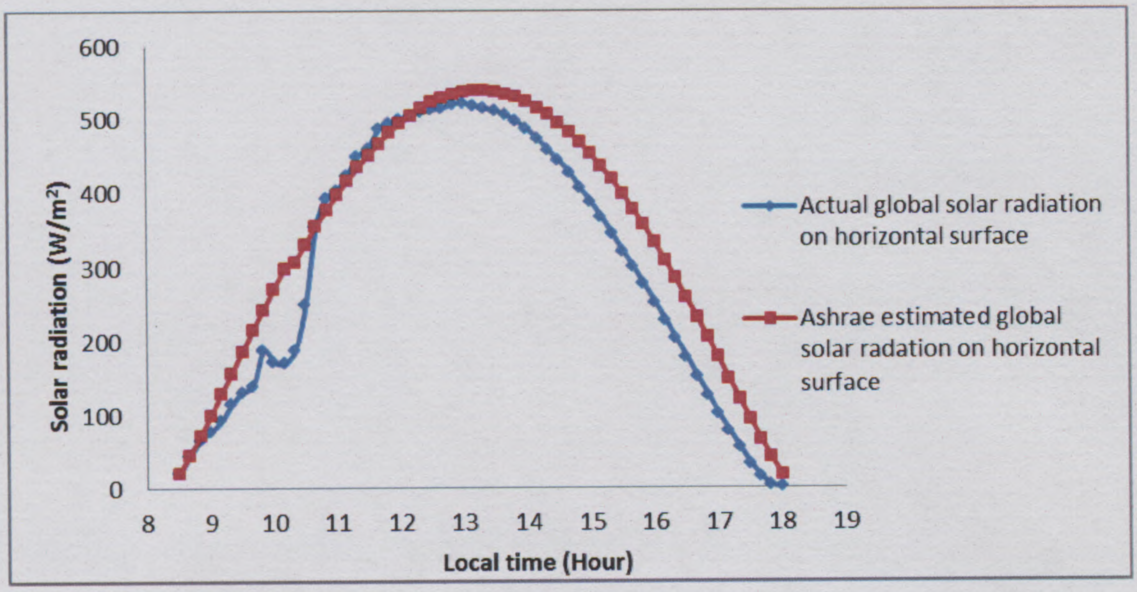

Figure 4-2: Comparison between estimated ASHRAE global solar radiation and measured global solar radiation on the 21 June 2014 (Day 16)

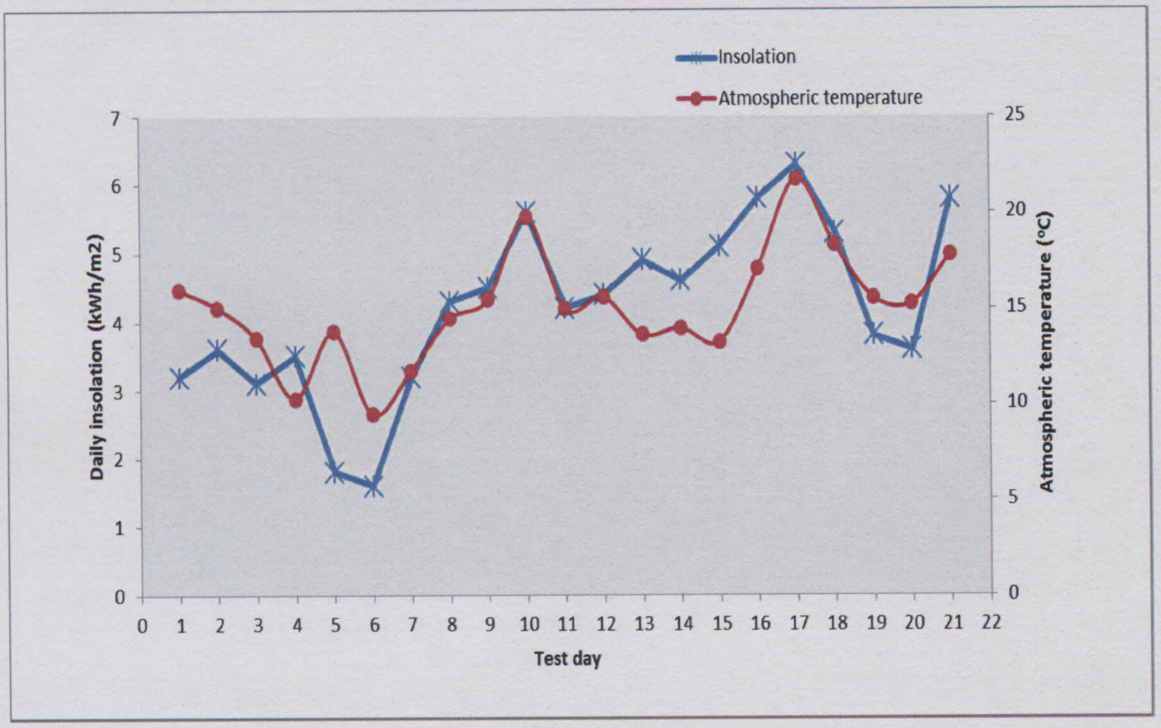

Figure 4-3: Variation of daily insolation and average atmospheric temperature over the test period (from June 2 to June 30)

Figure 4-3 shows the variation of the daily insolation (1.6 -6.3 kWh/m^2) and average atmospheric temperature (9.48 – 21.72 ^{o}C) over the test period.

4.2.2 WATER TEMPERATURE AND DISTILLATE OUTPUT

When solar radiation enters the still through the transparent cover, the water temperature rises and some water evaporates. Figure 4-4 shows the response of the solar still to the solar energy. As solar radiation increases, the water temperature in the basin also increases, reaching a maximum of 52°C at 13:00 hours.

The hourly distillate output is seen to peak around noon (12:00) with 82 ml of water produced. It rises and decreases with solar radiation and water temperature. The total distillate output on the 16th day (21 June 2014) was 0.502 litres of water or 1.86 kg/m^2.

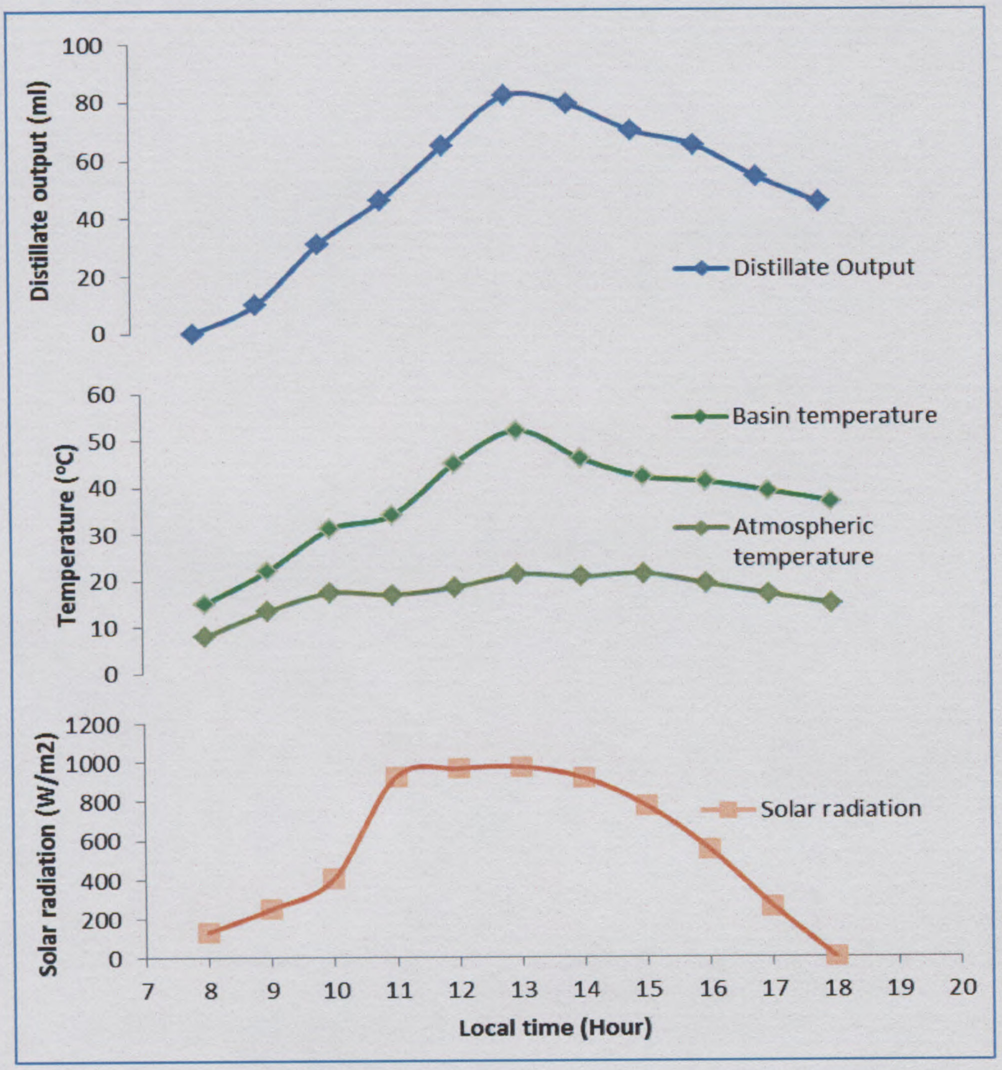

Figure 4-4: Hourly solar radiation, temperature and distillate yield on 21 June 2014 (Test day 16)

Figure 4-5 shows the daily distillate yield over the test period. The yield ranges from 0.074 kg/m^2 to 1.98 kg/m^2. Low yields on the 5th and 6th day of test are a results of very low solar radiation as shown in Figure 4-3.Figure 4-6 shows the variation of daily distillate productivity with daily insolation at the Cape Peninsula University of Technology. It is seen that the productivity linearly increases with solar radiation with a correlation R^2=0.9027 between the two variables Y (productivity) and X (insolation).

The effect of wind speed and ambient temperature on the solar still productivity was studied. From the very low correlation (R^2=0.1588) between the daily average wind speed and the daily production (Figure 4-7), it can be concluded that wind speed does not significantly affect the solar still productivity, thus agreeing with past works from Morse and Read (1968). However, El-Sebaii (2004) found that for water masses less than 45kg/m^2, the distillate yield decreases with increasing wind speed. An attempt to draw a regression line for this case of 10 kg/m^2 yielded a small negative slope through the scatter (Figure 4-7 (a)).

Figure 4-7(b) presents the positive moderate correlation between ambient temperature and distillate yield. It can be concluded that although the ambient temperature does not seem to have a major effect on the solar still productivity, it still influences it. As the ambient temperature rises, the condensing cover temperature rises as well, thus reducing the heat transfer between the evaporation chamber and the ambient. The greenhouse effect becomes therefore more effective, which causes a higher evaporation rate. However, the intermittent variation of temperature during the days of test may have increased the error range.

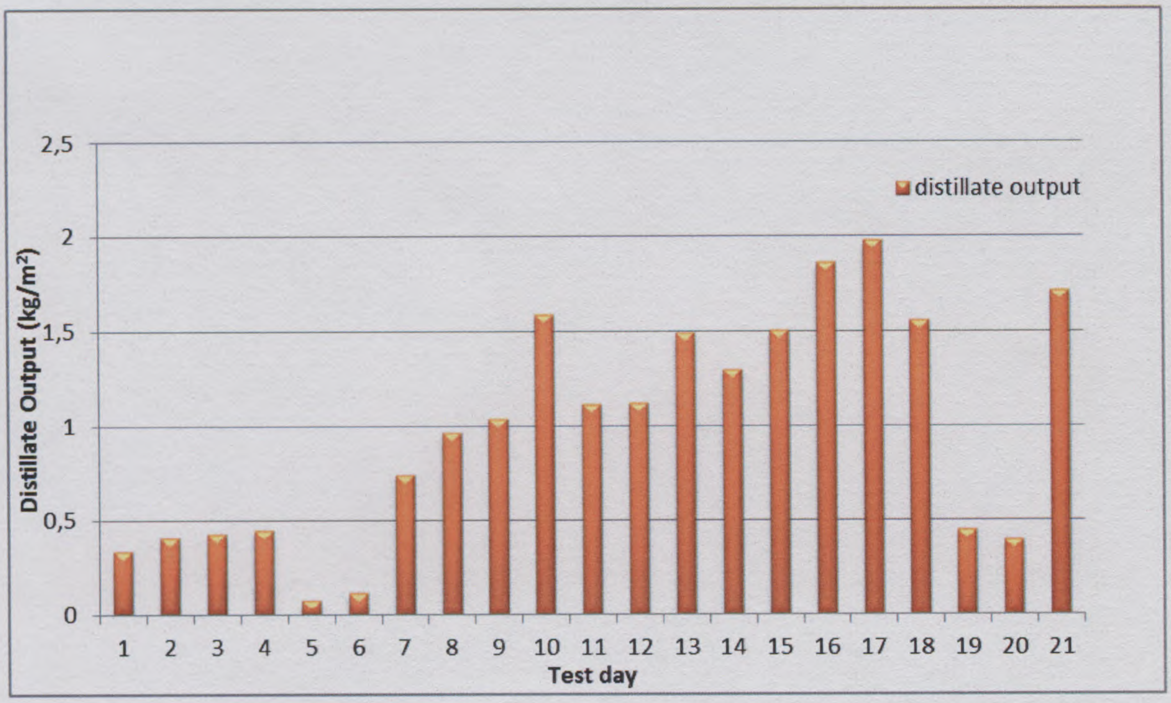

Figure 4-5: Daily distillate yield on days of test (June 2 to June 30)

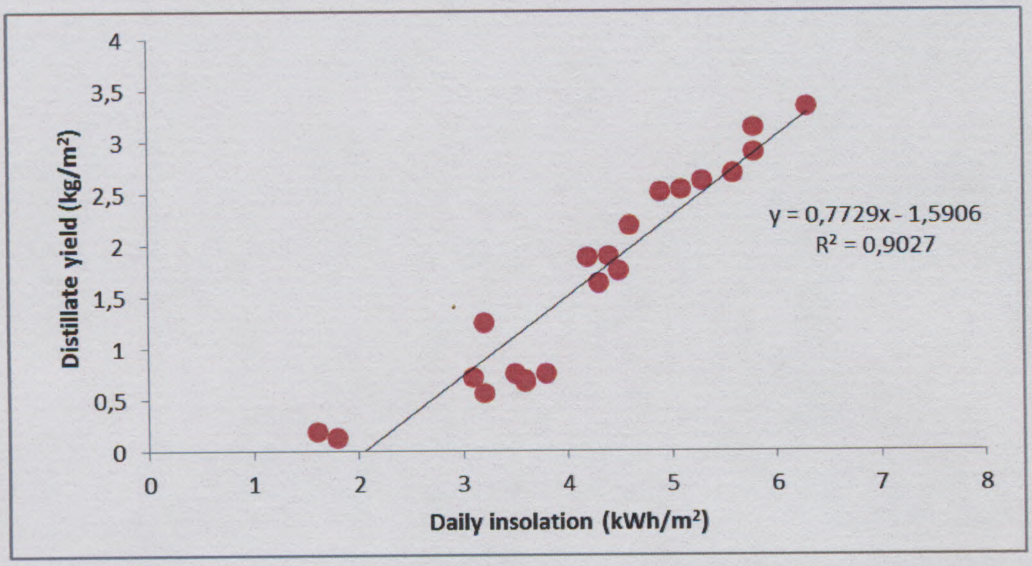

Figure 4-6: Variation of the distillate yield with insolation

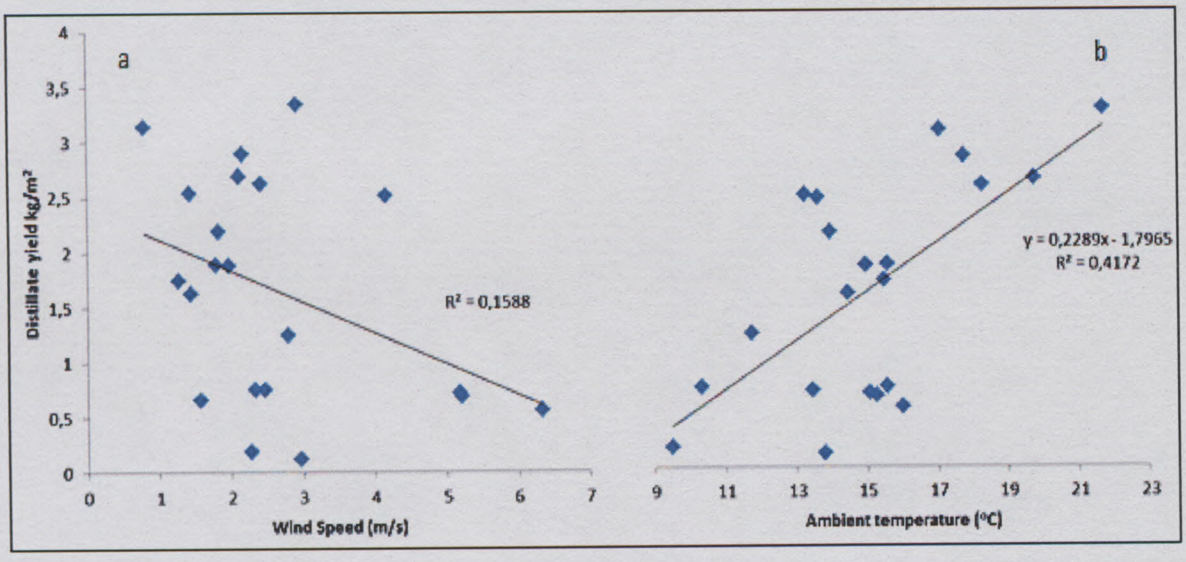

Figure 4-7: Variation of the distillate yield with a) wind speed and b) ambient temperature.

4.2.3 EFFICIENCY

The efficiency of the solar still is based on the amount of useful solar energy that the still converts as a function of incident solar radiation. The variation of the efficiency of the solar still which was calculated using equation (3-29) with atmospheric temperature and daily solar insolation is shown in Figure 4-8. However, it is to be noted that solar radiation has got more effect on the efficiency of the still than ambient temperature, taking into account the fact that ambient temperature also depends on solar radiation.

Daily efficiencies varied between 3.5% and 21% with an average value of 14%. These efficiencies are low compared to solar stills worldwide (in the vicinity of 25%) and this is mainly due to high heat losses from walls and bottom in the basin resulting from absence of insulation on the model.

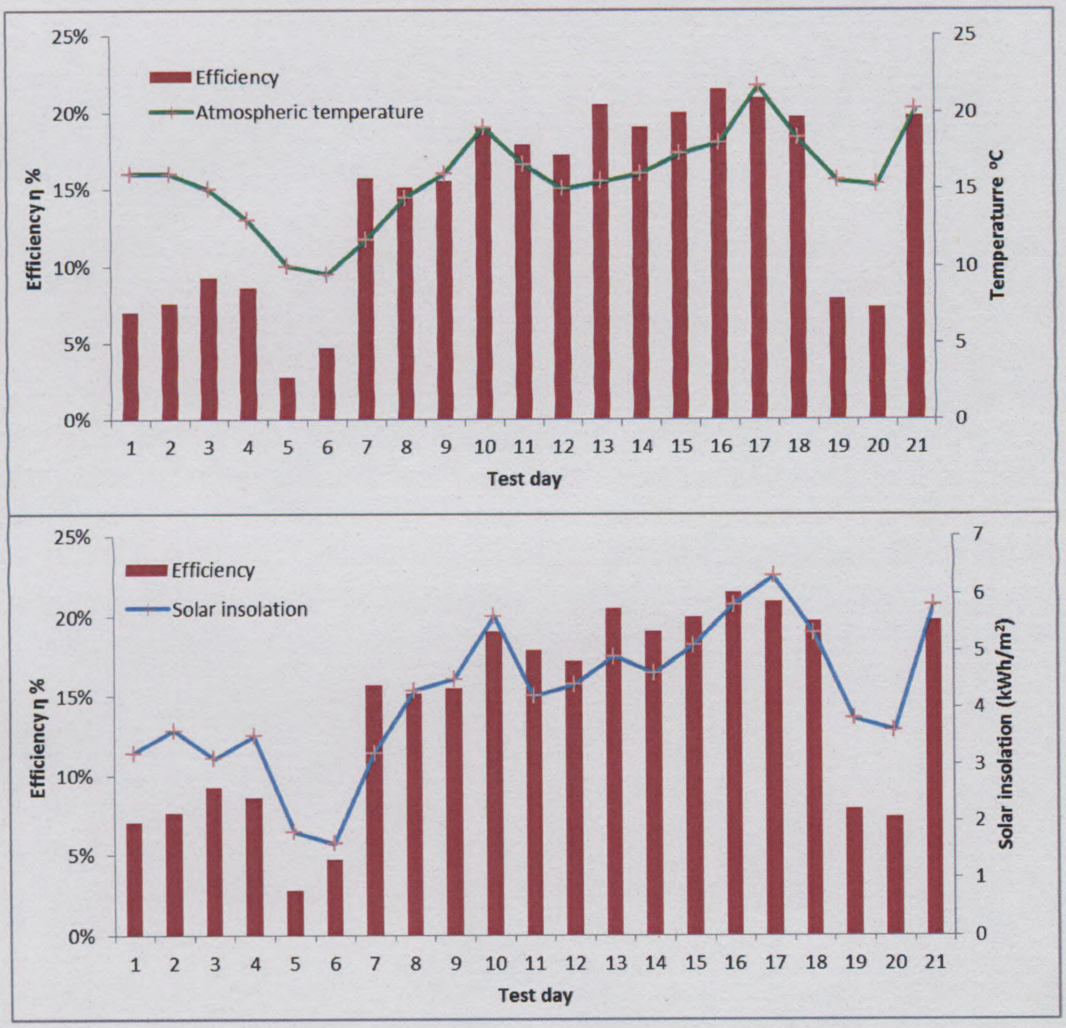

Figure 4-8: Variation of efficiency with a) atmospheric temperature and b) solar radiation June 2 to June 30.

4.3 PROTOTYPE SOLAR STILL PERFORMANCE

4.3.1 WEATHER CONDITIONS

During the prototype solar still unit testing period, weather conditions were satisfactory. Solar radiation data is a fundamental requirement when working on the design and the performance analysis of solar passive technologies. It is therefore necessary to determine the beam and diffuse components of global solar radiation on a horizontal surface in order to use these values to estimate the incoming radiation on a tilted surface.

Figure 4-9 and Figure 4-10 show the variation of the measured solar radiation on typical dates of 18 November 2014 and 25 November 2014 at the Cape Peninsula University of Technology Bellville Campus. These days, from 7:00 to 18:00 were chosen to demonstrate the extent of variation in the magnitude of beam, diffuse and direct solar radiation on a given day. The variation of the estimated incident radiation on the transparent cover inclined at 53° was calculated using the process described in 3.3.1 and plotted. The plots obtained have almost similar trends for the other days of test.

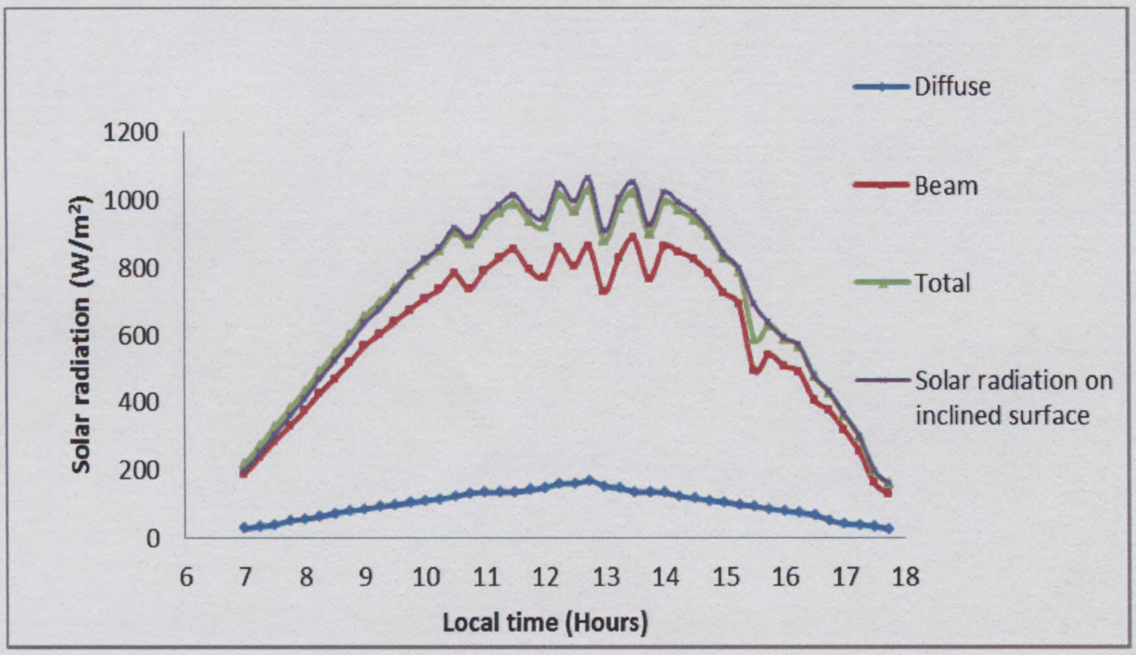

Figure 4-9: Variation of beam, diffuse and direct solar radiation with local time on 18 November 2014.

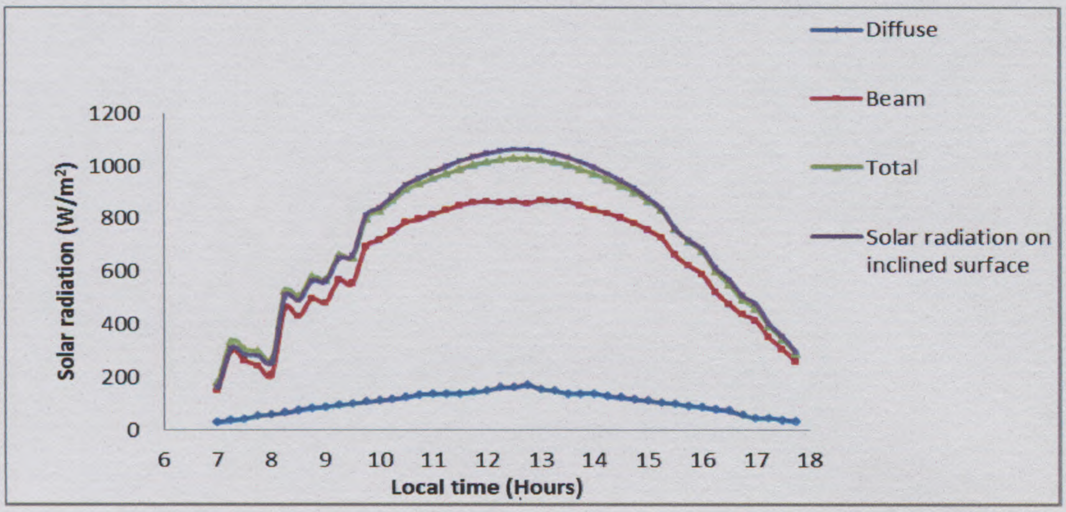

Figure 4-10: Variation of beam, diffuse and direct solar radiation with local time on 25 November 2014.

It is observed that beam radiation was always higher than diffuse radiation throughout the day. This is because on sunny days, most of the solar radiation is beam radiation and diffuse radiation accounts for only about five to twenty per cent of the total solar radiation (Goswami & Kreith: 2007). During some of the days such as the 18-11, solar radiation was intermittent especially around noon. This fluctuation was due to partly cloudy sky conditions.

In Figure 4-11 both measured and calculated data of solar radiation were compared. A reasonably good fit is observed between the two. The difference is due to the atmospheric conditions variation from the ASHRAE standard definition of "clear sky "in Cape Town on that day.

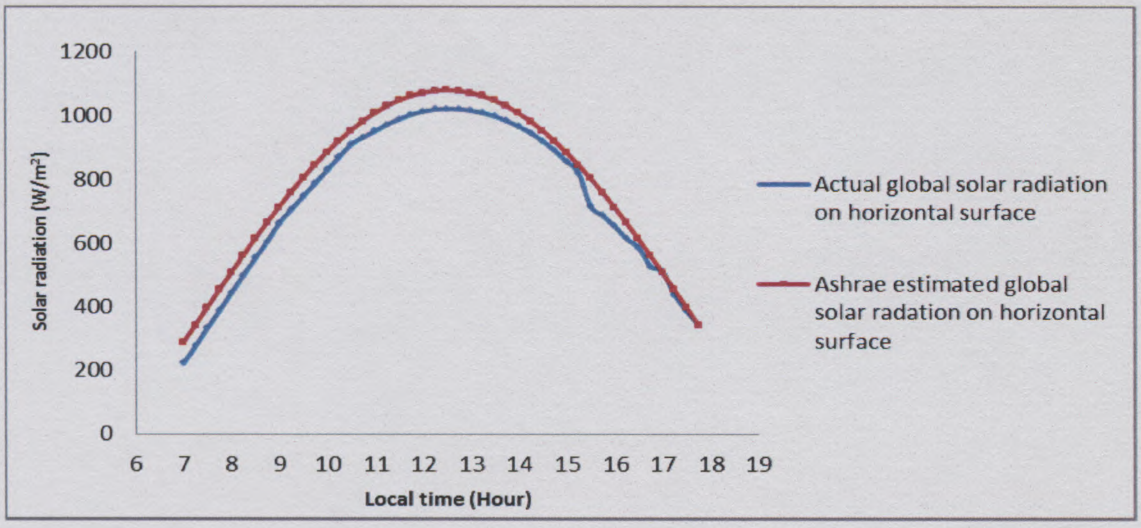

Figure 4-11: Comparison between estimated ASHRAE global solar radiation and measured global solar radiation on the 22 November 2014

See Figure 4-12 for the hourly mean solar intensity and ambient temperature over the test period and APPENDIX E for the meteorological data for the test period. The daily insolation ranged from 6.9 kWh/m^2 to 8.01 kWh/m^2 during the test period (Figure 4-13).

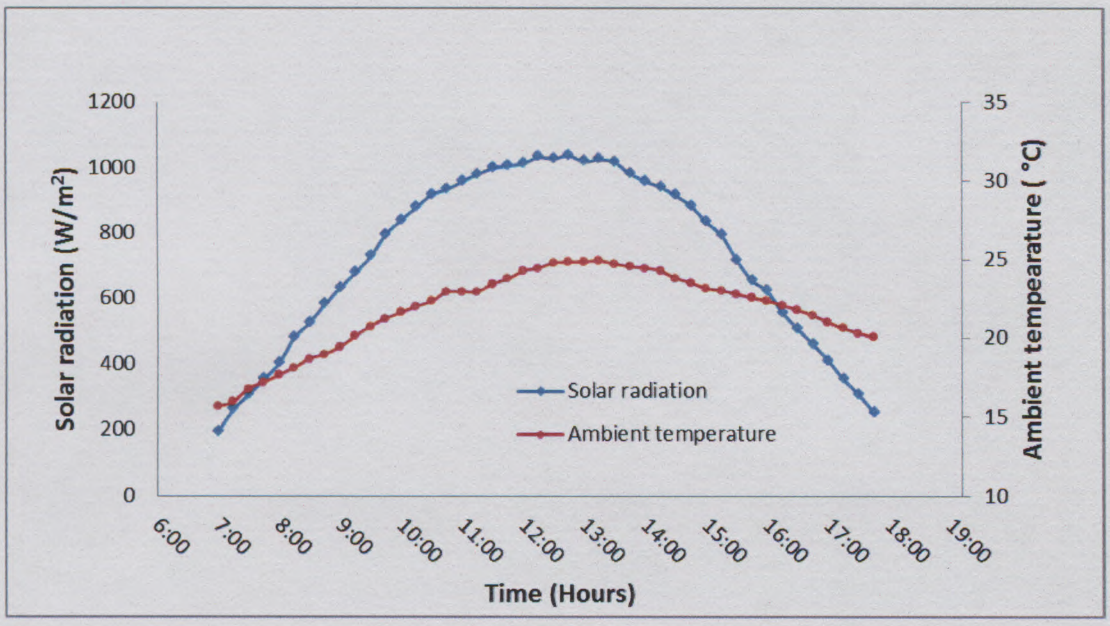

Figure 4-12: Hourly mean solar intensity and ambient temperature over the test period

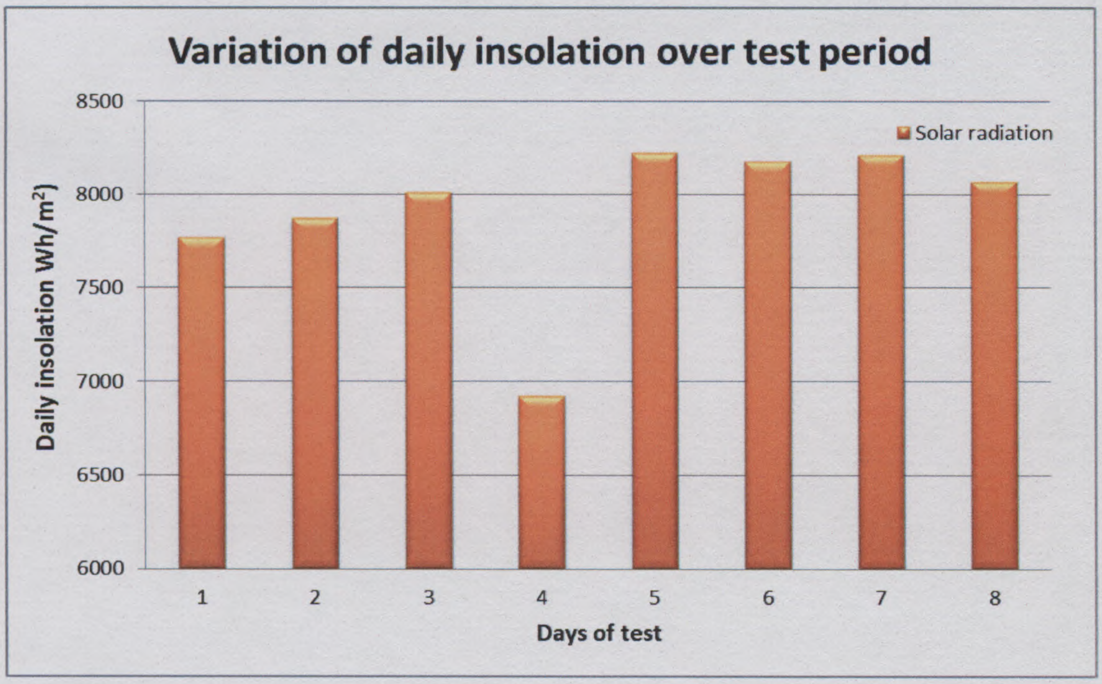

Figure 4-13: Variation of daily insolation over the days of test (November 18 to November 25)

At the test location, ambient temperature was relatively high, ranging from 9.97 °C to 30.68 °C while on a daily basis, the range of average air temperature was within 15.67°C to 24.90°C.

The variation of daily average solar intensity and ambient temperature is shown in Figure 4-14. It is observed that there is generally an increase of solar radiation and ambient temperature day after day.

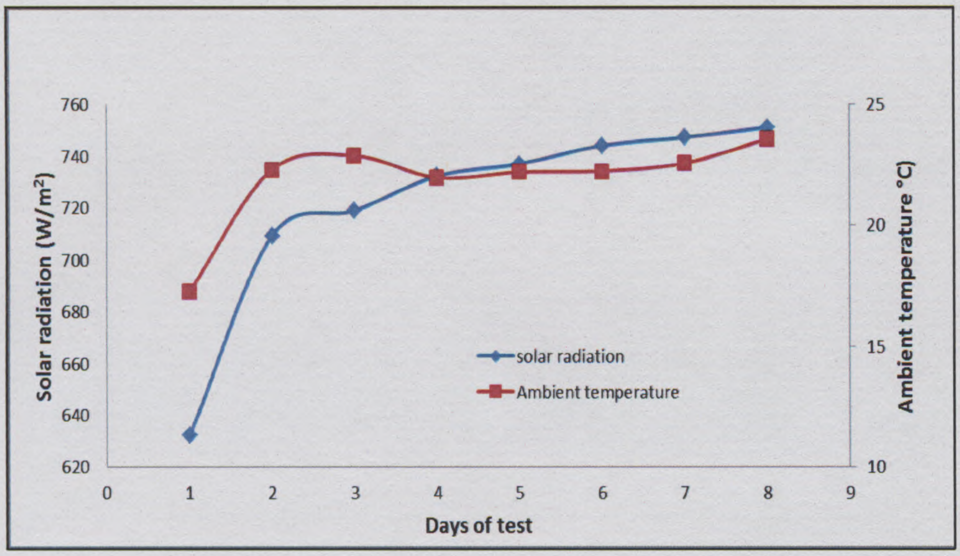

Figure 4-14: Daily average solar radiation and ambient temperature

Generally ambient temperature increases with increasing solar radiation over the days. However, a slight decrease of average ambient temperature is observed between the third and fourth day of test. This may be due to a relatively high wind speed on these days as seen in Figure 4-15.

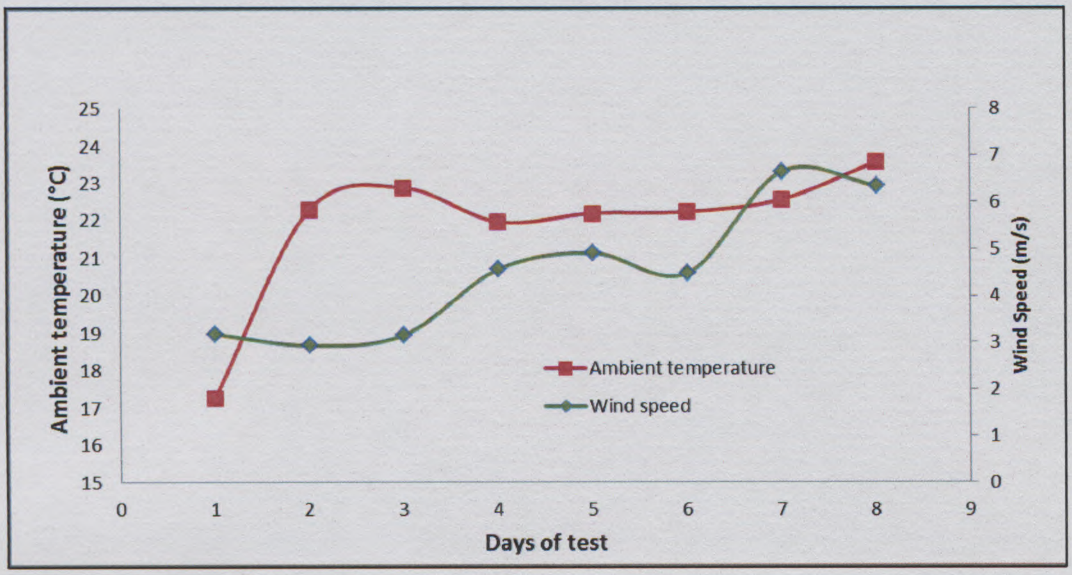

Figure 4-15: Daily average ambient temperature and wind speed

During the test period, wind speed varied between 0.58 m/s to 8.8 m/s while average daily wind speed ranged from 2.93 m/s to 6.64 m/s.

According to previous research, meteorological data have a significant effect on the thermal performance of the solar still as will be discussed in the next section.

4.3.2 TEMPERATURES ON THE STILL

When incident on the different components of the solar still, solar radiation is converted to heat which results in the rise of temperature of the components. More specifically, the distillation process is driven by the difference between the temperature of the water in the evaporation chamber and that of the condensing chamber and transparent covers. The rate of evaporation-condensation increases as this temperature difference increases. Moreover, temperature difference between the solar still system and the ambient conditions increase the heat loss. Analysing the temperature of the system components with respect to climatic parameters is therefore necessary.

The water temperature is one of the main parameters that dictates the productivity of the solar still. Figure 4-16 presents the variation according to time of the incident solar radiation intensity, the ambient temperature and the water temperature on the 22 November 2014 (test day 5) as a sample of the testing period.

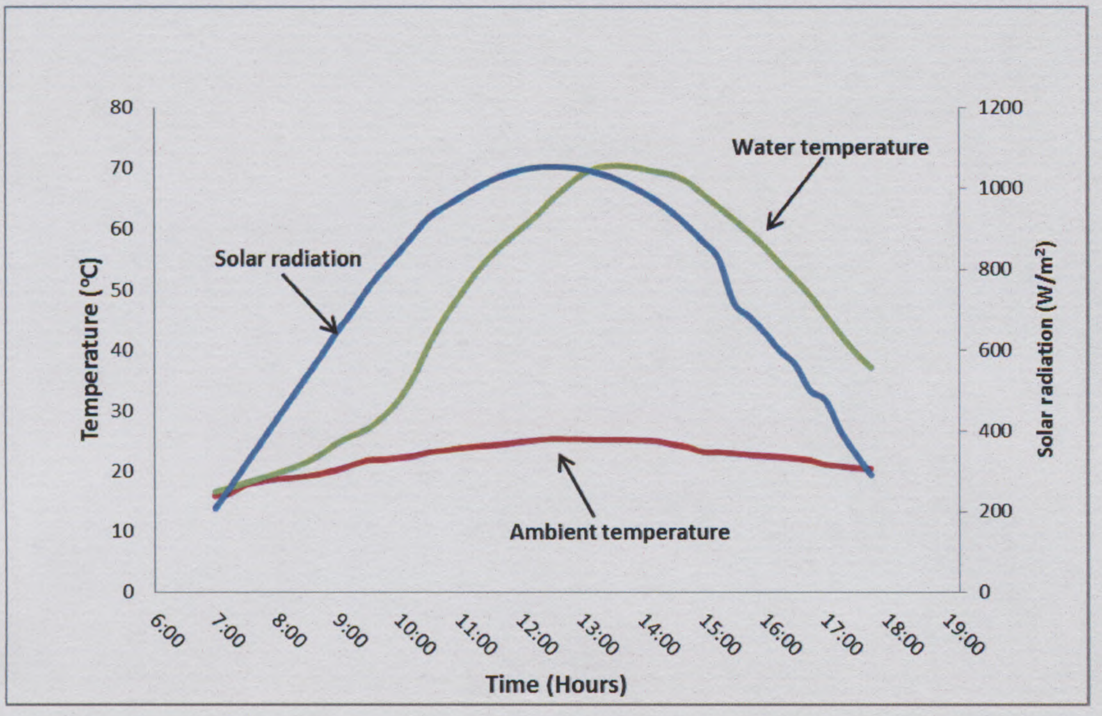

Figure 4-16: Variation of water temperature solar radiation and ambient temperature on 22 November 2014

It is noted that water temperature follows the same trends as solar radiation and ambient temperature. The rise in temperature is observed in the range of 17°C to 70°C with the peak of water temperature occuring at about one hour after noon.

Figure 4-17 shows the behaviour of the temperature of the evaporator chamber such as the basin temperature and the water temperature with the incident solar radiation on the 22 November 2014. It is observed that the variations of the different tempreratures in Figure 4-17 are similar to that of the incident solar radiation. This shows relationship between the incident solar radiation absorbed by the basin , the water and the air inside the evaporator chamber along the day and their temperature variations.

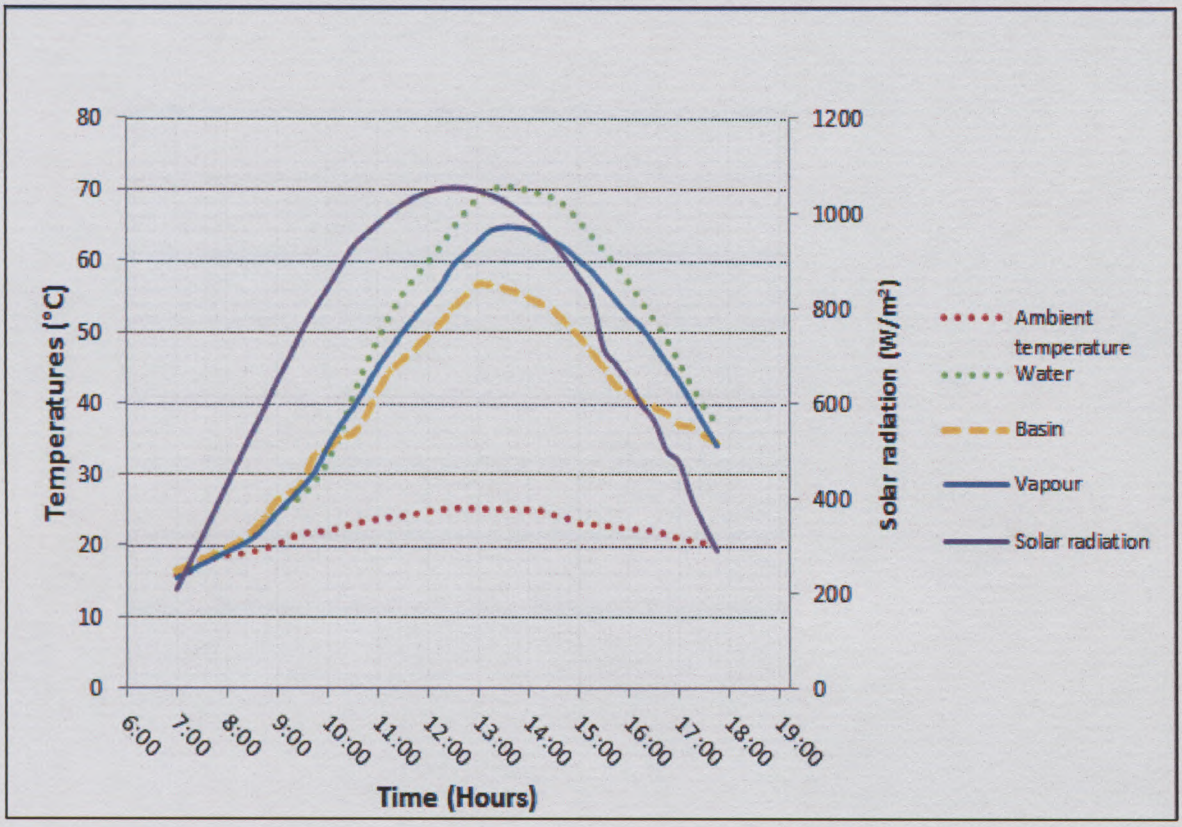

Figure 4-17: Solar still components temperature (basin, vapour)

Figure 4-18 shows the relationship between the inner and the outer transparent cover temperatures at the front of the still, the external condenser temperature at the back of the still and the solar radiation and ambient temperature on the day of 22 November 2014.

During the test, the outer cover temperature ranged from 19.56 °C in the morning to a maximum temperature of 28.31 °C at 13:15.. It is observed that throughout the day, the general overall temperature is close to that of the ambient air.

However, the outer cover temperature was seen to be fluctuating along the day. This may be due to the intermittent wind speed as shown in Figure 4-19. It can be observed that the cover temperature varies inversely as the intermittent wind speed. It is therefore concluded as expected that the outer cover temperature is influenced by solar radiation, ambient temperature and wind speed.

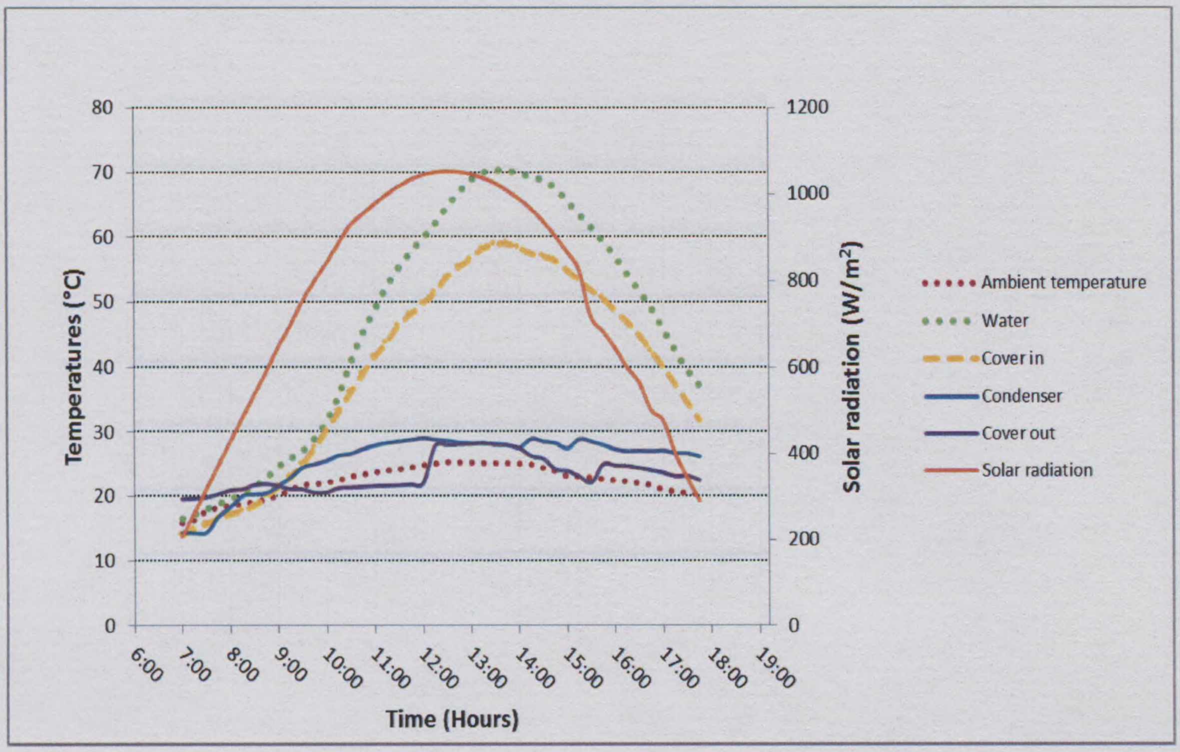

Figure 4-18: Solar still components temperature (covers, condenser)

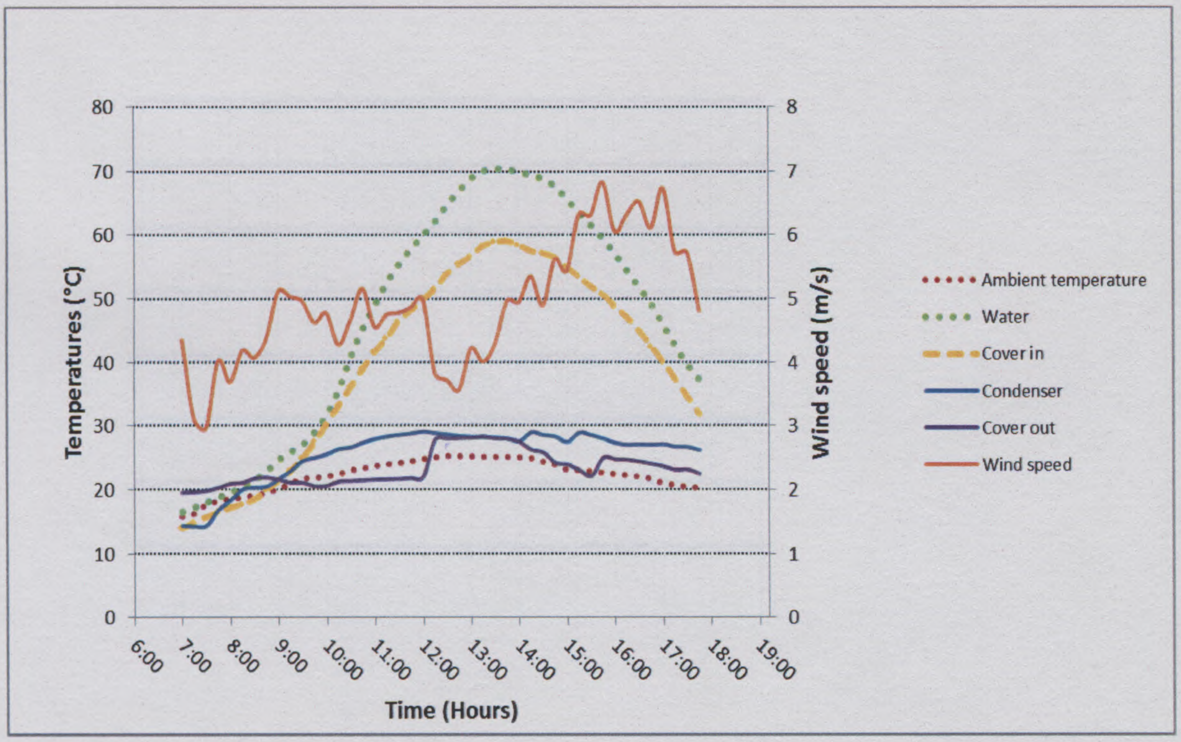

Figure 4-19: Relationship between solar still components temperature (covers, condenser) and wind speed

Throughtout the day, the inner cover temperature is lower than the water temperature, with an average temperature difference of 10 °C between the two. It peaked at a temperature of 59 °C between 13:00 and 14:00.

From the inner cover temperature curve which resembles that of solar radiation, it can be concluded that there is a direct relationnship between solar radiation and the variation of inner cover temperature. This relationship is due to the greenhouse effect inside the enclosure of the still. It also explains the relatively high temperature difference between the inner and outer covers temperatures.

The external condenser temperature shown in Figure 4-18 and Figure 4-19 ranged from a minimum value of 14.28 °C to a maximum of 29.06 °C.

It is noted that throughout the day, the external condenser temperature is lower than that of the evaporator chamber conponents. This temperature is closer to the ambient temperature and outer cover temperature, though it is slightly higher than these. This is due to the fact that this condenser was shielded from solar radiation , and therefore directly exposed to ambient temperature and wind only. These kept the condenser, which is influenced by the wind and ambient temperature, at relatively low temperature.

Figure 4-20 shows the summary of the solar still's components temperatures on the typical chosen day of test.

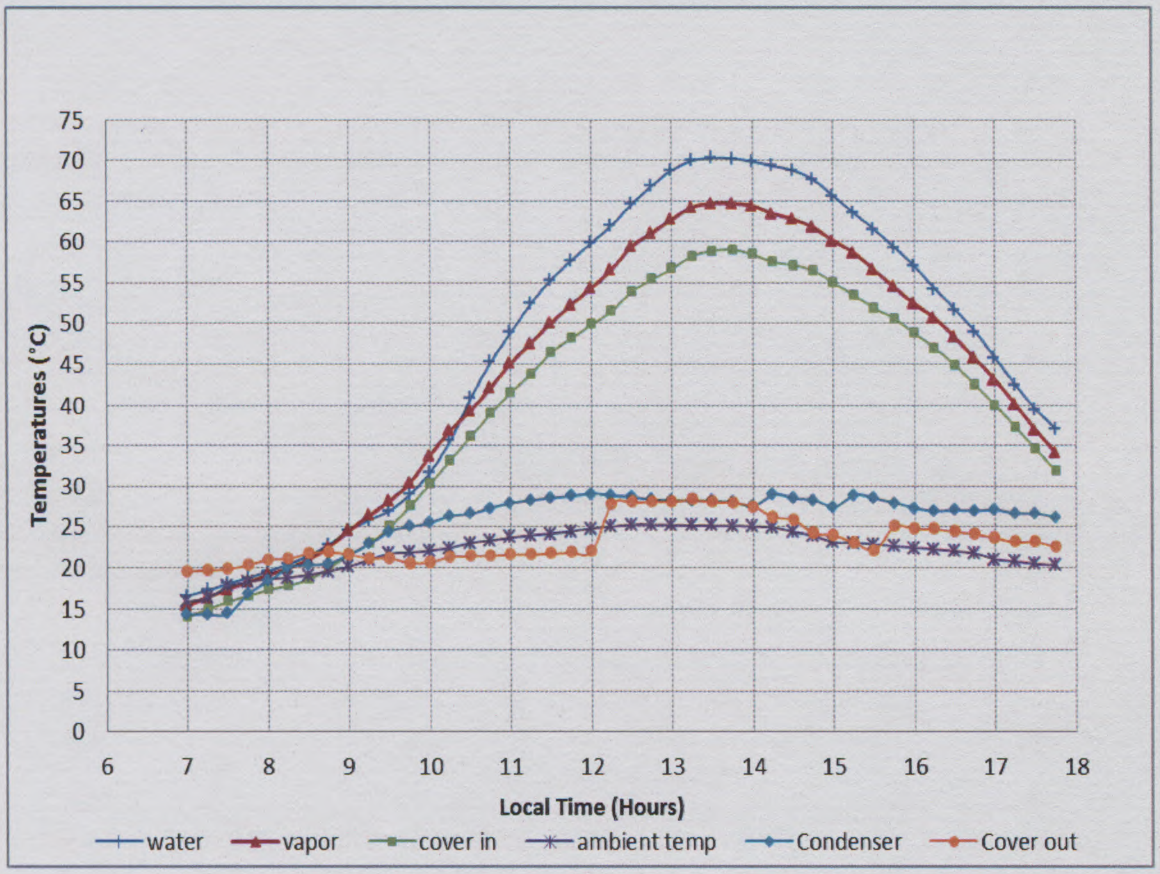

Figure 4-20: Solar still's components temperatures

As stated above, the distillation process is driven by the difference in temperature between the water and the condensing surfaces. Figure 4-21shows the variation in temperature difference between the water surface and the inner transparent cover (T_w -T_{gi}), the water surface and the external condenser (T_w -T_{co}), and the external condenser and ambient temperature (T_{co}- T_a).

It is noted that there is a considerabe difference between the temperature gradients with the highest being at noon at a value of 30,84 °C. This is due to the greenhouse effect inside the still which keeps the inner transparent cover temperature relatively high and close to the water temperature, and to the condensing temperature kept relatively low with because of its high thermal conductivity, shielding, wind speed and ambient temperature.

The condenser temperature is shown to be lower that that of ambient temperature from 7:00 to 8:00. A reverse trend is observed after this time due to heat transfer and diffusion from the evaporator chamber through the slot on the back wall of the basin. Nevertheless, the absolute value of (T_{co}- T_a) was relatively low and constant not exceeding 7 °C.

It can therefore be predicted that the yield of distillate obtained from the external condenser would be higher than that obtained through the transparent cover. The next section will discuss this.

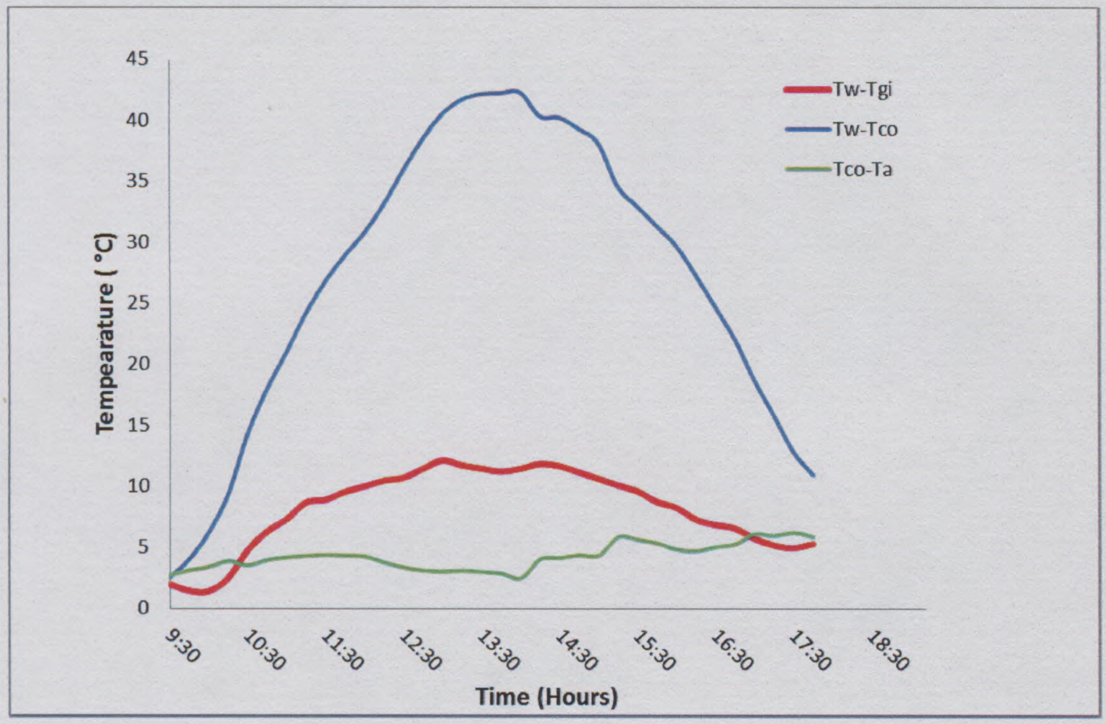

Figure 4-21: Variation of (Tw -Tgi), (Tw -Tco) and (Tco- Ta) over time on 22 November 2014

4.3.3 SOLAR STILL PRODUCTIVITY

This section presents and discusses the productivity of distillate of the solar still as well as the influence of different parameters on this production.

4.3.3.1 DISTILLATE PRODUCTION

Figure 4-22 shows the variation of instantaneous water collection on the typical day of the 22 November 2014, and its relationship to solar radiation, ambient temperature and the still temperatures. The comparison between the collection from the back condenser and the transparent cover is presented. It is observed that during the day, the external condenser yields more distillate than the front cover.

Additionally, Figure 4-22 shows the instantaneous distillate output and its relationship to solar radiation, ambient temperature and solar still temperatures on the 22 November 2014. It is notable that the major distillate production takes place between 13:00 and 14:00, one hour after the peak of solar radiation in the day. This is due to the high amount of heat stored inside the basin, which raised the evaporation rate. The peak distillate from the front cover is 250ml while that from the external condenser is 400ml.

It can be seen that as solar radiation increases between 7:00 and 12:00, there was a gentle increase in distillate productivity since within that time range, solar radiation is mainly used for heating the water inside the basin. Once this water reaches a temperature above 55°C, a significant rise (<300ml) in distillate production per measurement interval of one hour occurs.

From 14:00, the decline in solar still production is due to the decrease of evaporation rate, as the energy input from direct solar radiation is reduced. As sundown is approached, the system tends to switch from the use of solar energy input towards that of the sensible heat stored in the water in the basin.

Ambient temperature and outer cover temperature show a nearly constant behaviour throughout the day and seem to have little to no influence on the productivity of the solar still. Wind speed does not seem to have an influence on the productivity as well. The inside still temperature however shows a bigger correlation with productivity.

The main parameters affecting the productivity are the variation of solar radiation intensity and the water temperature in the basin from which the vapour temperature, the inner cover temperature and the external condenser temperature are dependent. It is to be noted that the external condenser temperature variation depends on ambient temperature and wind speed as discussed in section 4.3.2.

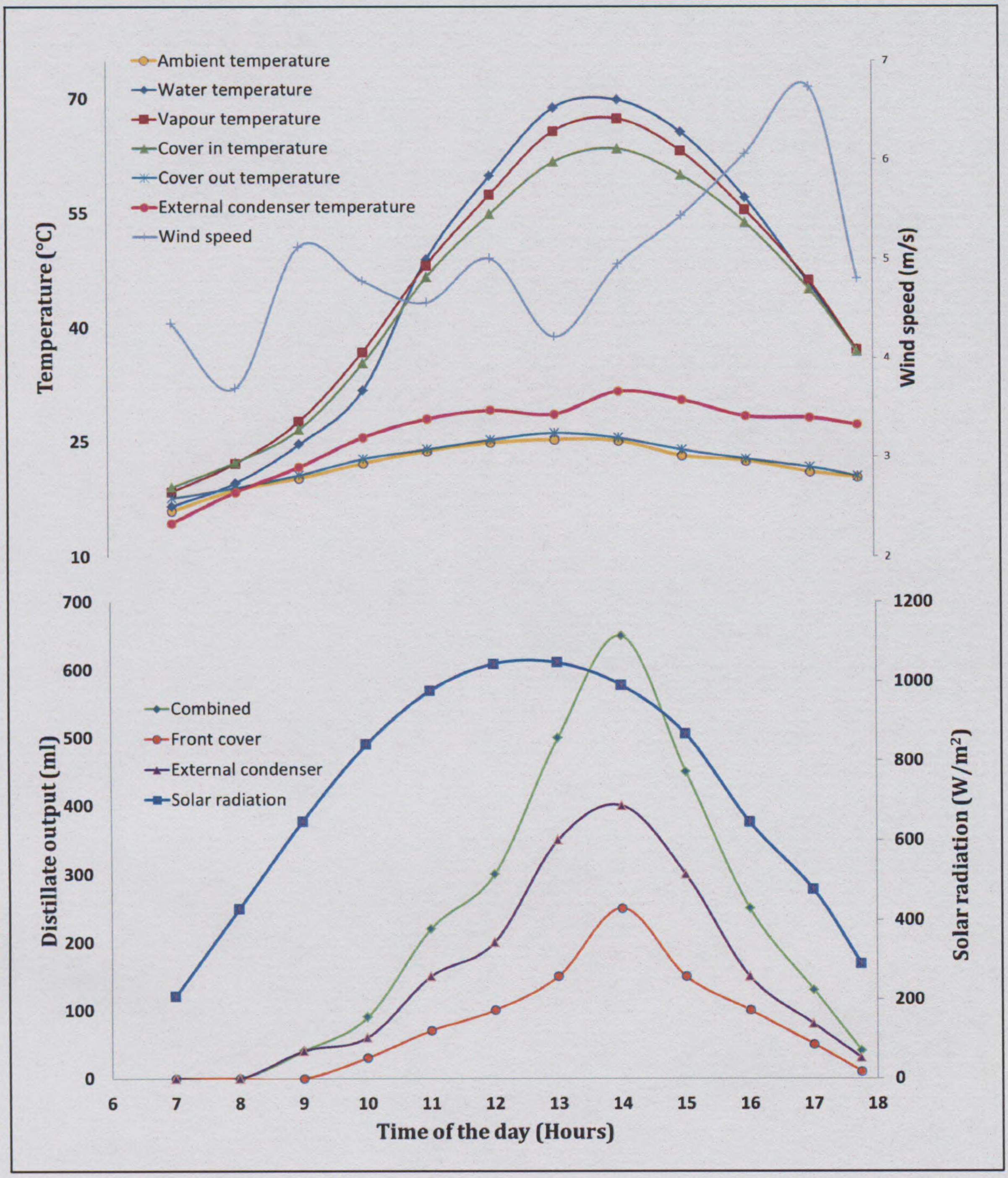

Figure 4-22: Variation of instantaneous distillate output with climatic parameters and solar still temperatures on 22 November 2014

Figure 4-23 presents the combined distillate output over time on the 22 November 2014. It compares the distillate output from the front cover and that from the external condenser.

From 9:00 to 12:00 a slow rise of production rate is noted while the higher inclination of the curves between 12:00 and 16:00 indicate a significant increase of distillate output over a short period of time. This is the timespan in which the solar still attains its highest efficiency (see section 4.3.4).

The nearly constant variation of the yields after 16:00 illustrates the progressive shift from the input from direct solar energy towards the use of the sensible heat stored in water and in the still.

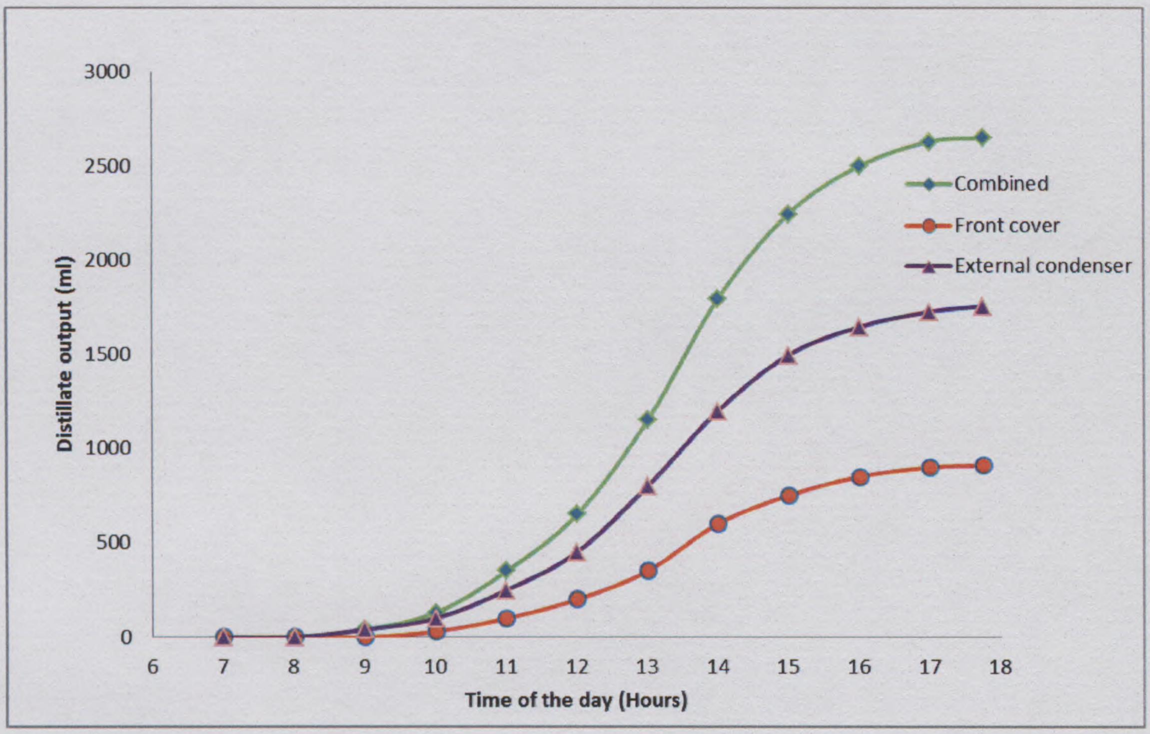

Figure 4-23: Combined distillate output over time on the 22 November 2014

Figure 4-24 shows the variation of distillate yield with solar radiation over the test period. It is generally seen that the productivity in the days having high solar radiation intensity is higher than that having low intensity. This variation is due to the relationship existing between the heat capacity stored inside the solar still and the evaporation rate of the water inside the basin.

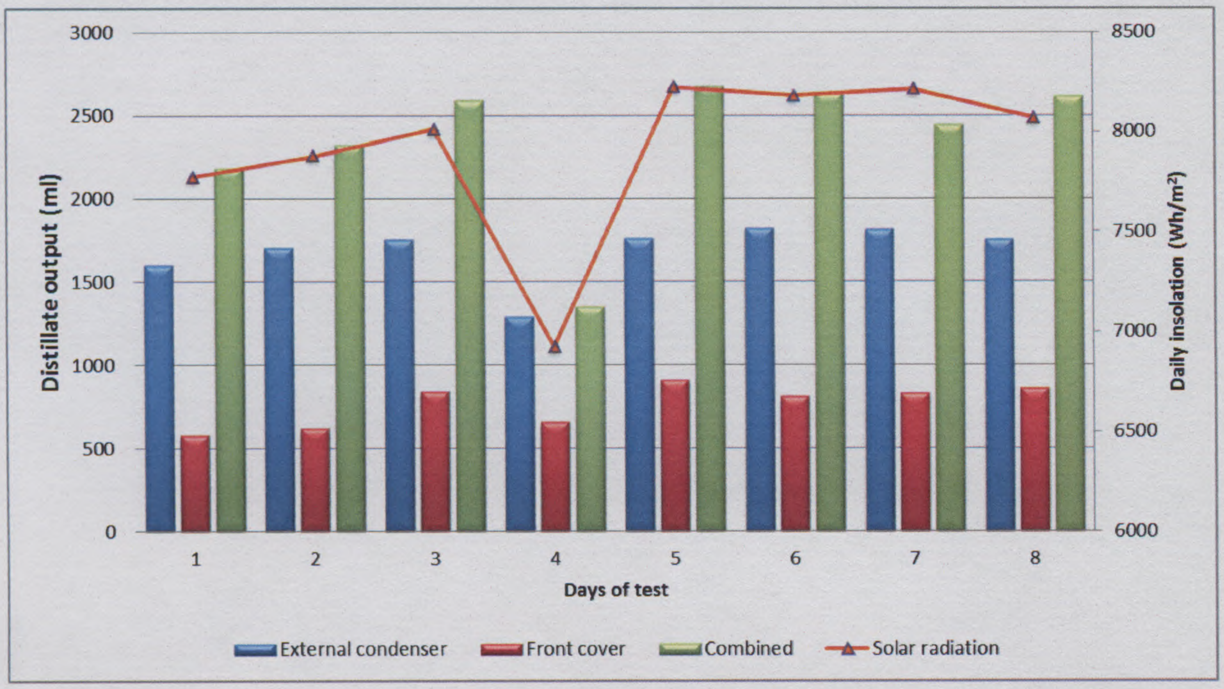

Figure 4-24: Variation of distillate yield and solar radiation over the days of test

4.3.4 EFFICIENCY OF THE STILL

In order to determine if the designed unit uses the solar energy effectively, it is necessary to calculate its energy efficiency.

An approximate estimation of the overall efficiency can be calculated using equation (3-29). For unity conformity, the distillate output in millilitres was converted to kilograms by generally assuming that 1kg of water =1000ml.

Figure 4-25 presents the variation of the instantaneous efficiency of the solar still unit on the 22 November 2014. On that day, the instantaneous efficiency reached a maximum value of 40%. The efficiency was relatively high because of the low angles of incidence at solar noon. Therefore, the transmission of solar radiation through the transparent covers was relatively high. It is observed that solar still instantaneous efficiency is varying according to the solar radiation intensity incident on the still surface as also shown in Figure 4-8.

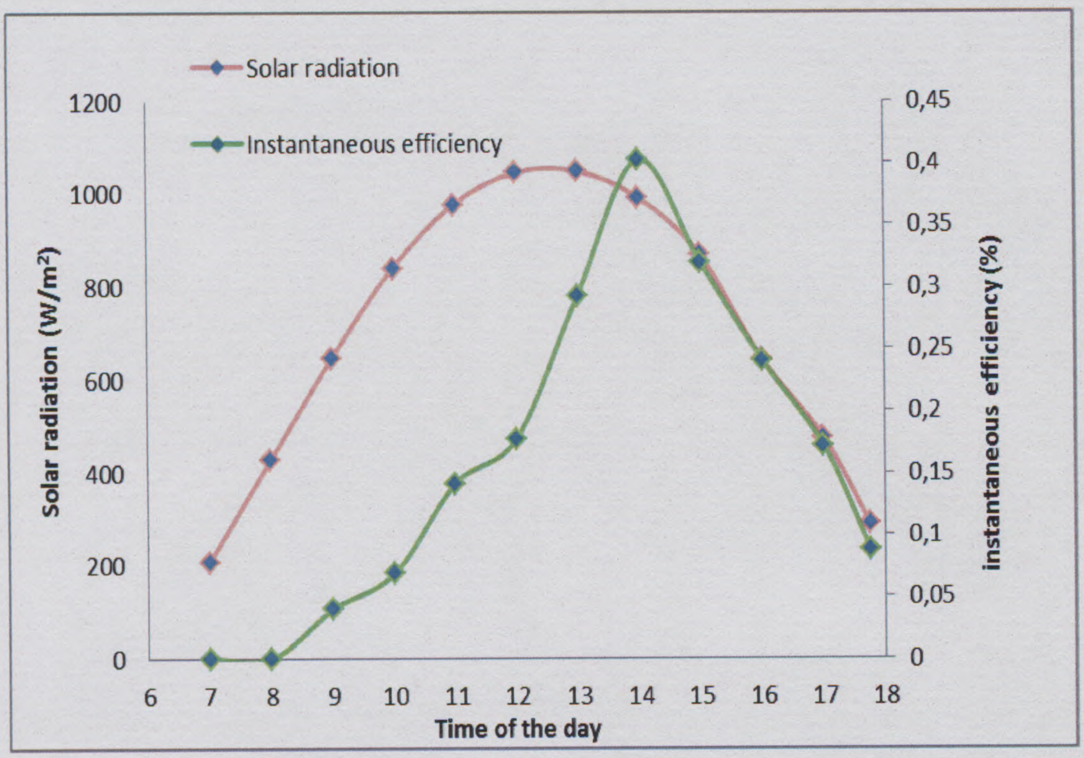

Figure 4-25: Instantaneous efficiency and solar radiation on the 22 November 2014

Figure 4-26 shows the variation of water temperature and ambient temperature with energy efficiency over time. It is observed that water temperature of at least 50 °C is necessary in the basin in order to start reaching satisfactory values of efficiency in the still. Ambient temperature remains nearly constant during the day, although a slight increase is observed between 12:00 and 14:00 where the highest water temperature and energy efficiency values are recorded.

It can therefore be assumed that the water temperature level from which solar distillation process can be assumed to be efficient is 50 °C.

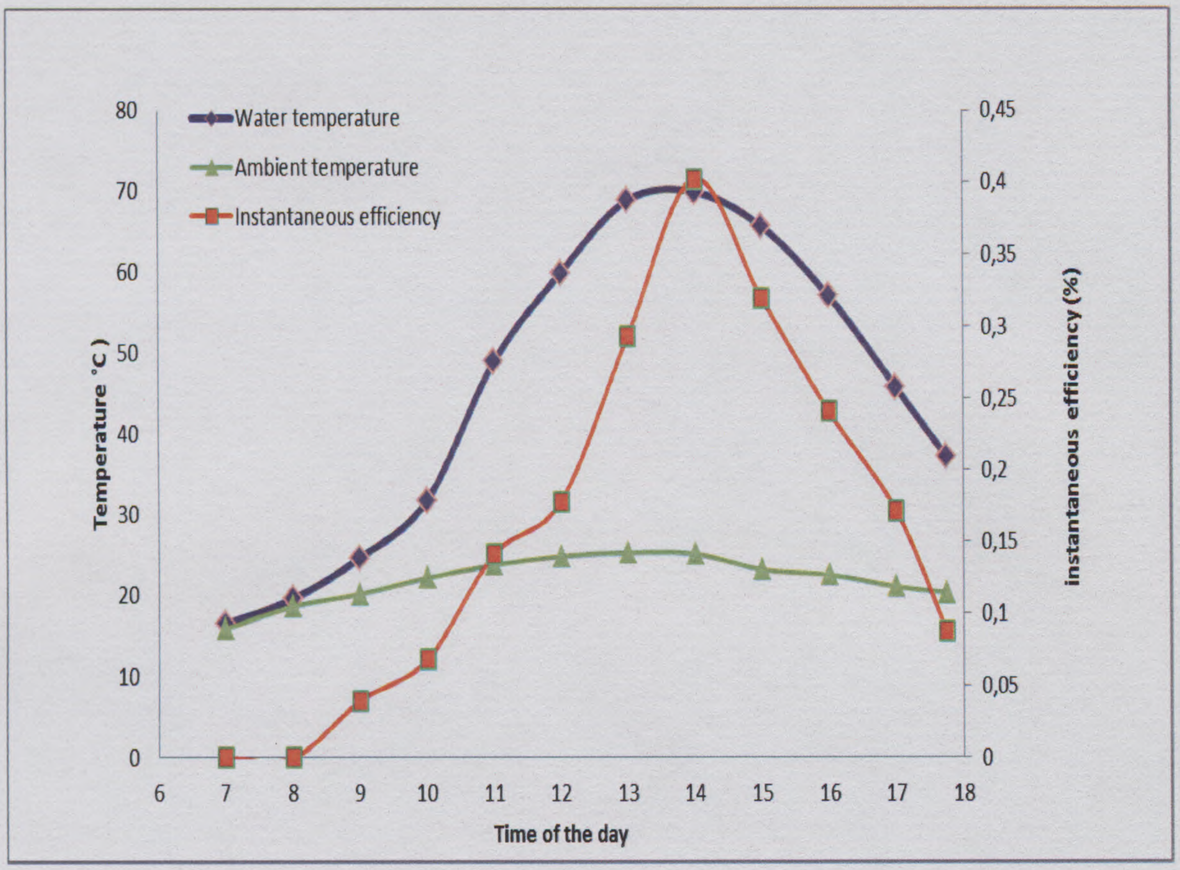

Figure 4-26: Variation of energy efficiency with water and ambient temperature

Figure 4-27 shows the variation of energy efficiency with temperature gradients between the water in the evaporator surface and the condensing surfaces (cover in and external condenser). It is clear that the difference in temperature between the water and the external condenser has an effect on the efficiency of the solar still unit. As this temperature difference varies during the day, so does the instantaneous efficiency. The high temperature of water due to the absorbed solar radiation and the low temperature of the condenser due to shield, ambient temperature and wind blowing contribute to the production of large amount of distillate output. This leads to increased efficiency.

In the same way, the temperature difference between the water surface and the inner transparent cover is a parameter that affects the overall efficiency of the solar still. It drives the distillation process and condensation on the front cover.

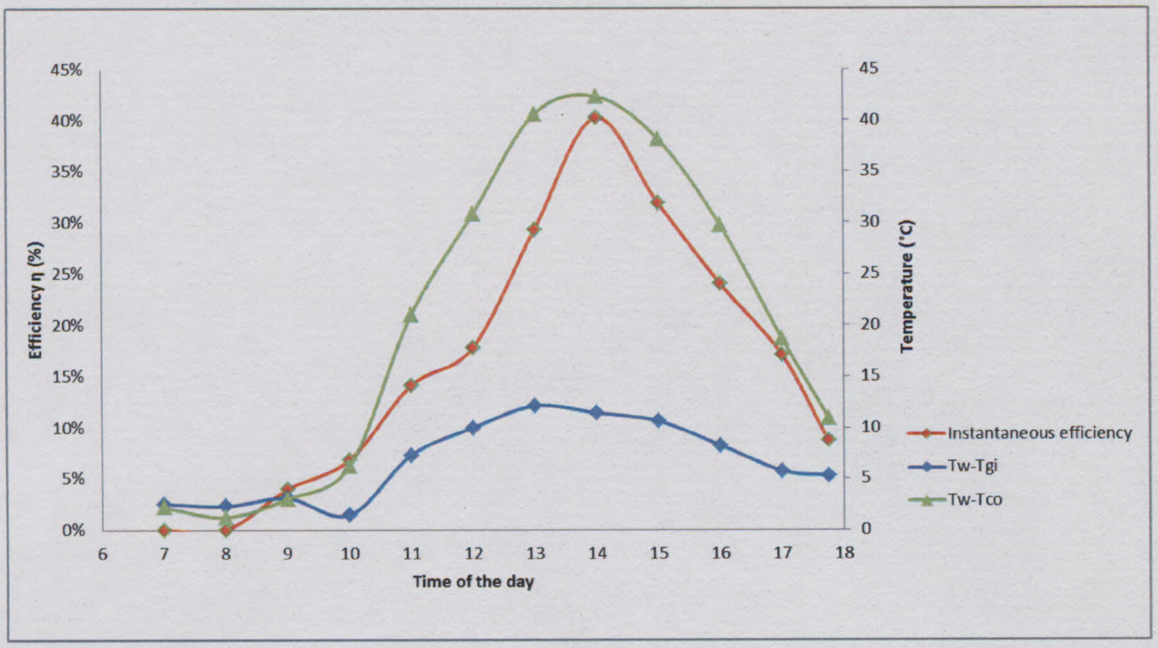

Figure 4-27: Variation of energy efficiency with (Tw -Tgi) and (Tw -Tco)

As mentioned in the previous section, the time range from 7:00 to 12:00 is mainly used for heating up the water in the basin, which causes a low efficiency as the distillate collected is low. However, higher efficiency is obtained from 12:00 to 16:00 since it is the timespan during which there is more yield of distillate per hour. On the 22 November 2014 the efficiency between 12:00 and 16:00 ranged between 20 and 40%.

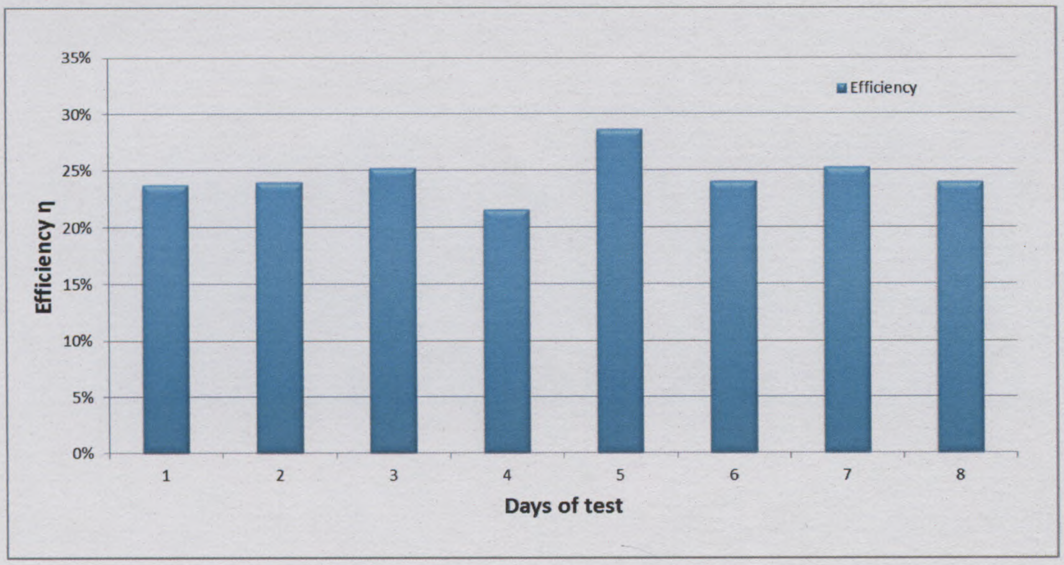

Figure 4-28: Daily efficiencies over test period

Thus, in order to determine the daily efficiency of the solar still over the test period (Figure 4-28), the mean values of efficiency each day were determined by calculating the average of the instantaneous efficiencies corresponding to the timespan of efficient distillate output (12:00 to 16:00). The daily efficiencies ranged between 21% on day 4 (lowest solar radiation intensity and 29% on day 5 (highest solar radiation intensity).

These obtained efficiencies are however still lower than those reported in previous investigations. For example, El Bahi and Inan (1999) reported an efficiency of 48% when coupling the basin solar still with a separate condenser. Moreover when cooling this external condenser with continuous flowing water, they increased the efficiency to up to 70%.

In the case of this study, it can be hypothesised that the low efficiency is partly due to the large gap between the evaporation tray and the transparent cover and the external condenser surfaces. With a large angle of inclination of 53°, the walls shadow the evaporation tray to some extent. Moreover, the time elapsed by the saturated air to reach the condensing surfaces is greater, which lowers the air movement inside the still. This issue may be solved by integrating stepped evaporation trays inside the unit while still coupling it with an external condenser. This would allow the still to be inclined at the optimal angle for receiving maximal solar radiation, while decreasing the air gap between the evaporation and condensing surfaces.

4.4 WATER QUALITY

On one test day (18 November), water from the lake of CPUT was loaded in the basin. The quality of the collected water was analysed as compared to the initial water quality. Total dissolved solids, pH and the quantity of microorganisms were assessed. These experiments were all done in the laboratory of Food Technology of the CPUT. The obtained measurements results confirm that the solar still prototype is efficient in the improvement of water quality. As this series of test is not part of the main scope of this study, the results will not be discussed in this chapter. The reports of the water quality improvement are found in APPENDIX F.

4.5 SUMMARY

Experimental results from the testing of the model and prototype solar stills under Cape Town conditions during the month of June (model) and the month of November (prototype) have been presented in this chapter. On both solar stills, the relationship between climatic conditions such as solar radiation and ambient temperature were pointed out and confirmed. That of wind speed was also observed, but to a certain limit.

Due to its larger size, better insulation and better testing climatic conditions (high solar radiation intensity), the prototype solar still yielded as expected more distillate than the model. Its daily energy efficiency also showed to be higher (values ranging between 21 and 29% while that of the model ranged between 3.5 and 21%). However, it has to be noted that no provision was made to collect distillate from the front cover of the model unit; therefore it can be assumed that the actual efficiency of the model would be slightly higher than the reported one.

The greenhouse effect (which is due to insulation, double glazing and external condenser) made the temperature difference between evaporation and condensing surfaces higher. This showed to be effective since it could lead the still to achieve better overall performance. However, the performance of the unit is still lower than previously investigated solar stills with separate condensers. One of the main reasons may be the large gap between the evaporation and condensing surfaces.

CHAPTER 5 CONCLUSIONS AND RECOMMENDATIONS

5.1 SUMMARY

Several methods such as distillation can be used to improve the quality of drinking water. Amongst distillation methods, solar distillation has the potential to be one of the most economical solutions for overcoming the issue of water and energy crisis.

The present study sought to make a contribution towards the global efforts to tackle the water crisis problem by developing a solar distillation system with the aim of increasing the availability of safe drinking water. To achieve this goal, basic principles of solar distillation were presented and explained in order to understand the science driving the process, and some parameters affecting its performance were investigated. Then, a solar distillation unit was designed, fabricated, experimentally tested during day time and its performance was analysed under Cape Town conditions.

A model of this unit was used for experiments in winter time (June). This model was tested without insulation and with a single glazing, while the prototype was tested in spring time (November). This was done in order to evaluate to a certain extent the effect of insulation and number of glazing cover on the productivity of a solar still unit.

A series of experiments were performed in order to collect climatic measurements (solar radiation, ambient temperature, wind speed…) as well as the solar still operation measurements necessary to analyse the performance of the units.

5.2 CONCLUSIONS

On the basis of the results obtained in this study, the following conclusions can be drawn:

- The nature of the incident solar radiation has significant effects on the thermal performance of the water in the basin and on the temperature of the different components of the solar still throughout the day.

- The experiments confirmed the expected influence of solar radiation on the distillate production of the solar still.

- There is a significant interaction between the distillate production and the temperature difference of the evaporation chamber and the condensation chamber. More distillate yield was obtained through the external condenser than through the inner transparent cover since the temperature difference between the water surface and the external condenser was always higher than the temperature difference between the water surface and the inner cover surface. The external condenser and the inner cover contributed respectively 69% and 31% of the total distilled water collected from the still.

- It was observed that the temperature of the inner condensing cover was comparable to that of the water inside the basin while the temperature of the external condenser remained comparable to that of the ambient air. This shows the effectiveness of the solar shield placed above the external condense, which keeps it relatively cool (a good condition for water condensation).

- The efficiency of the studied solar still units was found to range from 3.5% to 21% for the solar still model and 21% to 29% for the prototype.

- The applied techniques such as the external condenser, double glazing, insulation and low level of water proved to be effective. However, the distillate output of the still (about 2.5 kg/m^2) is insufficient for supplying a family of four. With an evaporation area of 1.056 m^2, this unit can supply 2 persons in drinking water.

5.3 RECOMMENDATIONS FOR FUTURE RESEARCH

- In an attempt to further improve the performance of this solar still design, the basin may be lined with an aluminium tray in order to improve its heat capacity. Moreover, the use of high heat capacity material in the evaporation tray may be investigated for improving solar still performance.

- A Thermodynamic and optical analysis of the designed solar still may be performed using computational simulation, and the model could be validated using the experimental results from this study.

- Future work may attempt to design and build a unit with the particular design presented in this study, so that it could be operated at sub atmospheric conditions in order to increase the evaporation rate inside the evaporation chamber. The unit would have to be airtight and leakage proof.

- An evaporative cooling system used to cool the external condenser would be more effective than the cooling of the collecting jar. Such a system may be designed and implemented in order to increase the solar still's productivity.

- An appropriate drainage system may be designed and implemented in the solar still unit to avoid accumulation of residue when working with brackish or saline water sources.

- Stepped evaporation trays may be integrated in the unit in order to reduce the gap between evaporation and condensing surfaces.

REFERENCES

- Abdallah, S. & Badran, O.O. 2008. Sun tracking system for productivity enhancement of solar still. *Desalination*, 220(1–3): 669–676.

- Abu-Arabi, M., Zurigat, Y.H., Al-Hianai, H., Al-Hiddabi, S. 2002. Modelling and performance analysis of a solar desalination unit with double-glass cover cooling. *Desalination*, 143: 173-182.

- *Abu-Hijleh*, B.A., *Rababa'h*, H.M. 2003. Experimental study of a solar still with sponge cubes in basin. *Energy conversion and Management.* 44 (9), 1411-1418.

- Aimiuwu, V.O. 2008. An Energy-Saving Ceramic Cooler for Hot arid Regions. In H.M. Oluseyi, editor, *Proceedings of the National Society of Black Physicist*s, volume 991 of American *Institure of Physics Conference Series*: 75-81.

- Ali, H.M. 1991. Experimental study on air motion effect inside the solar still on still performance. *Energy Conversion and Management*, 32(1): 67–70.

- ASHRAE: American Society of Heating, Refrigeration and Air conditioning Engineers 2009. *ASHRAE Handbook Fundamentals*, Chapter 14.

- Bacha, H., Dammak, T., Ben Abdalah, A.A., Maalej, A.Y. & Ben Dhia, H. 2007. Desalination unit coupled with solar collectors and a storage tank: modelling and simulation. *Desalination*, 206(1–3): 341–352

- Badran, O.O. 2007. Experimental study of the enhancement parameters on a single slope solar still productivity. *Desalination*, 209: 136–143.

- Benhammou, M., Draoui, B. 2013. Effect of double glazing on the thermal performances of a solar still coupled to a condenser. *ISESCO Journal of science and Technology*, 9(15): 2-8.

- Bhattacharyya, A. 2013. Solar stills foe desalination of water in rural households. *International Journal of Environment and Sustainability*. 2(1): 21-30.

- Blanco,J., Malato, S., Fernández-Ibañez, P., Alarcón, D., Gernjak, W., Maldonado, M.I. 2009. Review of feasible solar energy applications to water processes. *Renewable and Sustainable Energy Reviews*, 13 (6-7): 1437–1445.

- Bundschuh, J., Hoinkis, J. 2012. *Renewable energy applications for freshwater production. Sustainable Energy Development*. London: CRC Press INC.
- Campbell Scientific. 03101 R.M Young Anemometer https://s.campbellsci.com/ documents/af/manuals/03002.pdf [Accessed 12/12/2014].

- Cooper, P.I. 1969. Digital simulation of transient solar still performance. *Solar Energy*, 12: 313-331.

- Delyannis, E.2003. Historic background of desalination and renewable energies. *Solar Energy*. 75: 357-366.

- Dimri, V., Sarkar, B., Singh, U., Tiwari, G.N. 2008. Effect of condensing cover material on yield of an active solar still: an experimental validation. *Desalination*, 227: 178-189.

- EIA (Energy Information Administration): International Energy Outlook. 2013. Energy Information Administration, Office of Integrated Analysis of Forecasting, US Department of Energy, Washington, DC, DOE/EIA-0484(2013), 2013, (accessed 13 January 2014), <http://www.eia.doe.gov/oiaf/ieo/index.html>.

- EIA (Energy Information Administration): International Energy Outlook. 2013. Future world energy demand driven by trend in developing countries. *Today in energy,* (accessed 15 January 2014), <http://www.eia.gov/todayinenergy/detail.cfm?id=14011>.

- Eibling, J.A., Talbert, S.G., Löf, G.O.G. 1971. Solar stills for community use –digest of technology. Solar Energy, 13: 625-632.

- El-Bahi, A., Inan, D. 1999. Analysis of a parallel double glass solar still with separate condenser. *Renewable Energy*, 17 (4): 509-521.

- El-Sebaii, A.A. 2004. Effect of wind speed on active and passive solar stills. *Energy conversion & Management*, 45: 1187-1204.

- Ettouney, H.M., El Dessouky, H.t., Faibish, R.S., Gowin, P.J. 2002. Evaluating the Economics of Desalination. Chemical Engineering Progress, 98(12): 32-40.

- Fath, H.E.S., Elsherbiny, S.M. 1993. Effect of adding a passive condenser on solar still performance. Energy Conversion and Management, 34: 63-72.
- Goswami, D.Y., Kreith, F. 2007 (eds). Handbook of Energy Efficiency and Renewable Energy. CRC Press: Boca Raton, FL.
- Gnanadason, M.K., Kumar, P.S., Sivaraman, G. 2011. Design and performance analysis of a modified vacuum single basin solar still. *Smart Grid and Renewable Energy*, 2: 388-395.
- Gude, V.G., Nirmalakhandan, N., Deng, S. 2010. Renewable and sustainable approaches for desalination. *Renewable and Sustainable Energy Reviews*. 14: 2641-2654.
- Gueymard, C.A. 2004. The sun's total and spectral irradiance for solar energy applications and solar radiation models. *Solar Energy*, 76: 423-453.
- Gupta, B., Mandraha, T.K., Edla, P.J., Pandya, M. 2013. Thermal modelling and efficiency of solar water distillation: A review. *American Journal of Engineering Research*. 2(12): 203-213.
- Hollands, K.G.T. 1963. The regeneration of lithium chloride brine in a solar still for use in solar air conditioning. *Solar Energy*, 7: 39.
- Hottel, H.C., Woertz, B.B. 1942. Performance of Flat-Plate solar heat Exchangers. Trans.ASME, 14: 91-104
- Huth, T., Perrone, D., Brown, C., Lettenmaier, D. 2012. *Water-energy nexus: Solutions to meet a growing demand*. Washington DC: American Geophysical Union (AGU).
- Ismail, B.I. 2009. Design and performance of a transportable hemispherical solar still. *Renewable Energy*, 34: 145-150.
- Kalidasa Murugavel, K., Chockalingam, Kn.K.S.K., Srithar, K. 2008. Progresses in improving the effectiveness of the single basin passive solar still. *Desalination*, 220: 677-686.
- Kalogirou, S.A. 2005. Seawater desalination using renewable energy sources. *Progress in Energy and Combustion Science*. 31 (3): 242-281.

- Kanyarusoke, K.E., Gryzagoridis, J., Oliver, G. 2012. Issues in solar tracking for sub-sahara Africa. *Proceeding of Southern African Solar Energy Conference*. Stellenbosch South Africa, May 2012.

- Kane, R.P. 2005. Sun-earth relation: Historical development and present status – a brief review. *Advances in Space Research*, 35: 866-881.

- Kaushal, A. Varun. 2010. Solar stills: A review. *Renewable and Sustainable Energy Reviews*, 14: 446–453.

- Khalifa, A.J.N., Hamood, A.M. 2009a. On the verification of the effect of water depth on the performance of basin type solar still. *Solar Energy*, 83: 1312–1321.

- Khalifa, A.J.N., Hamood, A.M. 2009b. Effect of insulation thickness on the productivity of basin type solar stills: An experimental verification under local climate. *Energy Conversion and Management*, 50(9): 2457-2461.

- Kipp & Zonen CMP06 Pyranometer, http://www.ames.si/files/attachments/KippZonen_Brochure_Pyranometers.pdf [Accessed 12/12/2014].

- Kipp & Zonen SP-LITE silicon pyranometer. http://s.campbellsci.com/documents/us/manuals/sp-lite.pdf. [Accessed 12/12/2014].

- Kondratyev, K. Y.1969. *Radiation in the Atmosphere*, Academic: New York.

- Kumar, D., Himanshu, P., Ahmed, Z. 2013. Performance analysis of single slope solar still. International Journal of Emerging Technology and Advanced Engineering, 3 (3): 66-72.

- Liu, B.Y.H., Jordan, R.C. 1960. The Interrelationship and Characteristic Distribution of Direct, Diffuse and Total Solar Radiation. Solar Energy, 4(3): 1-30.

- Malik, M.A.S., Tiwari, G.N., Kumar, A., Sodha, M.S. 1982. Active and passive solar distillation: A review. In *Solar distillation*. UK: Permagon Press.

- Malik, M.A.S., Tran, V. 1973. A simple mathematical model for predicting the nocturnal output of a solar still. *Solar Energy*, 14: 371-385.

- Mohammedi, K., Talamali, A., Smaili, Y., Saadoun, I., Ait-Aider, A. 2013. Environmental impact of seawater desalination plants: case study in Algeria. *American Journal of Environmental Protection*. 2 (6): 141-148.
- Morse, R.N., Read, W.R.W. 1968. A rational basis for the engineering development of a solar still. *Solar Energy*, 12(1): 5.
- Mowla, D., Karimi, G. 1995. Mathematical modelling of solar stills in Iran. *Solar Energy*, 55(5): 389-393.
- Nafey, A.S., Abdelkader, M., Abdelmotalip, A., Mabrouk, A.A. 2001. Solar still productivity enhancement. *Energy Conversion Management*, 42(11): 1401-1408.
- Perez, R. P., Ineichen, R., Seals, J., Michalsky, and R. Stewart. 1990. 'Modeling Daylight Availability and Irradiance Components from Direct and Global Irradiance. Solar Energy, 44(5): 271-289.
- Phadatare, M.K., Verma, S.K. 2007. Influence of water depth on internal heat and mass transfer in a plastic solar still. *Desalination*, 217 (1-3): 267-275.
- Pillai, R., Libin, A.T., Mani, M. 2013. Study into solar-still performance under sealed and unsealed conditions. *International Journal of Low-Carbon Technologies*, 00: 1-11.
- Sanshi, A.K. 1981. Effect of various dyes on solar distillation. *Solar Energy*, 27: 51–65.
- Sampathkumar, K., Arjunan, T. V., Pitchandi, P., Senthilkumar, P. 2010. Active solar distillation - A detailed review. *Renewable and Sustainable Energy Reviews*. 14: 1503–1526.
- Sharma, M.R. and Pal, R.S. 1965. Total, direct and diffuse solar radiation in the tropics. *Solar Energy*, 9: 183-192.
- Soliman, S.H. 1972. Effect of wind on solar distillation. *Solar Energy*, 13: 403-415.
- Talbert, S. G., Eibling, J. A., Löf, G.O.G. 1970. *Manual on Solar Distillation of Saline Water*. Springfield, VA, USA: National Technical Information Service.
- Tanaka, H., Nakatake, Y. 2006. Theoretical analysis of a basin type solar still with internal and external reflectors. *Desalination*, 186: 280-299.

- Tanaka, H. 2010. Monthly optimum inclination of glass cover and external reflector of a basin type solar still with internal and external reflector. *Solar Energy*, 84: 1959-1966.
- Thevenard, D. 2009. *Updating the ASHRAE climatic data for design and standards (RP-1453)*. ASHRAE Research Project, Final Report.
- Tiwari, G.N., Tripathi, R. 2003. Study of heat and mass transfer in indoor conditions for distillation.
- Tiwari, G.N. 2006. *Solar Energy Technology Advances*. New York: Nova Science Publishers, Inc.
- Tiwari, G.N., Dimri, V., Chel, A. 2009. Parametric study of an active and passive solar distillation system: energy and Exergy analysis. *Desalination*, 242: 1-18.
- Tiwari, G.N., Tiwari, A.K. 2008. *Solar distillation practice for water desalination systems*. Anshan: Tunbridge wells, UK.
- UNICEF and WHO, Progress on sanitation and drinking water: 2012 Update. 2012, p 2.
- Von Uexkull, O. 2004. Energy and water: the ignored link. *Refocus*, 40–44
- Wassouf, P., Peska, T., Singh, R., Akbarzadeh, A. 2011. Novel and low cost designs of portable solar stills. *Desalination*, 276: 294-302.
- Wheeler, N.W., Evans, W.W. 1870. *Evaporating and distilling with solar heat*, US Patent No. 102.633
- Yang, K., Huang, G.W., Tamai, N. 2001. A hybrid model for estimating global solar radiation. *Solar Energy*, 70: 13-22.
- Yeh, H.M., Chen L.C. 1985. Basin-type solar distillation with air flow through the still. *Energy*, 10: 1237-1241.
- Yeh, H.M., Chen L.C. 1986. The effect of climatic, design and operational parameters on the performance of wick-type solar distiller. Energy Conservation and Management, 26: 175-180.

APPENDICES

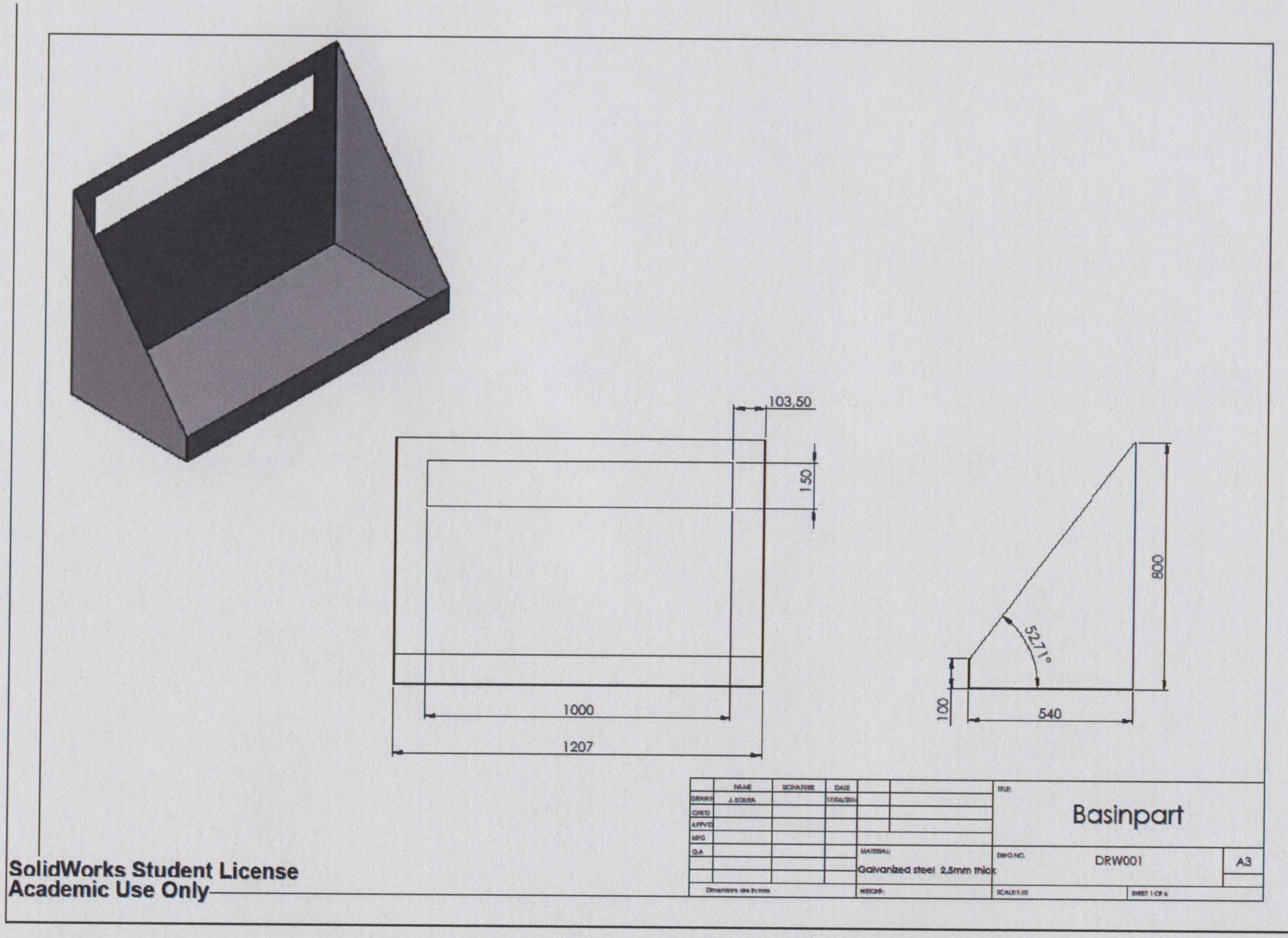

Figure A-5-1: Solar still basin dimensions

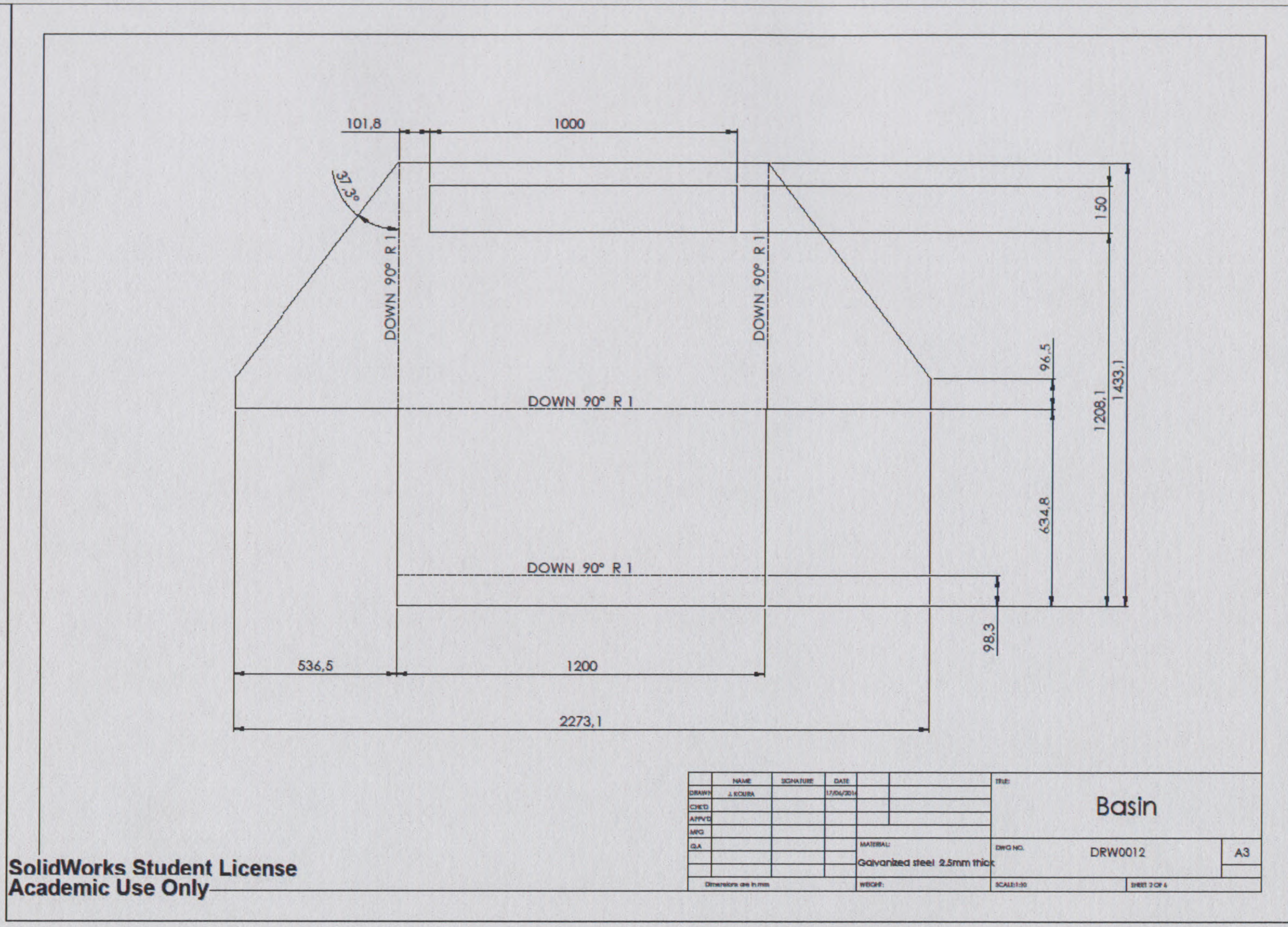

Figure A-5-2: Flat pattern of the basin

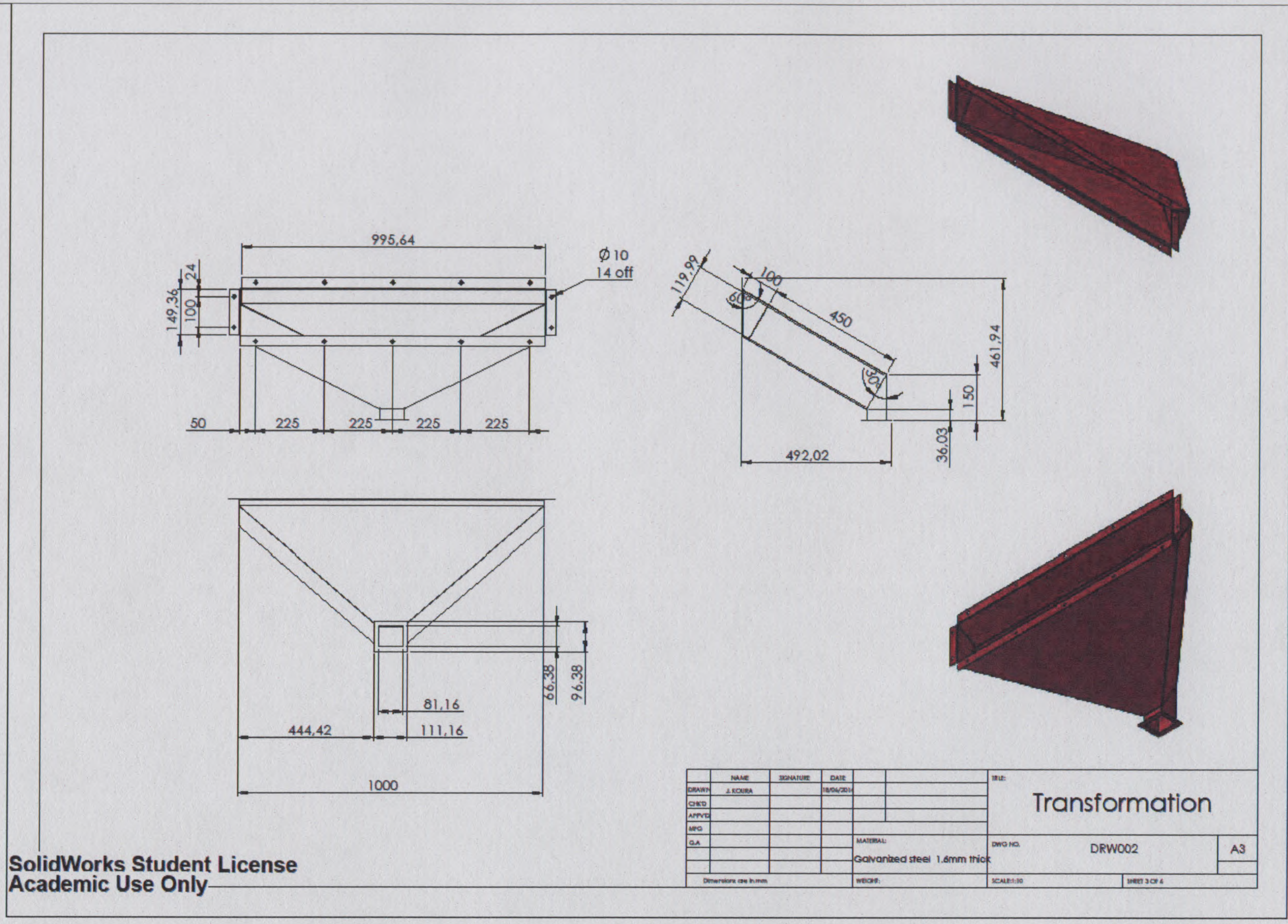

Figure A-5-3: External condenser (Transformation duct) overall dimensions

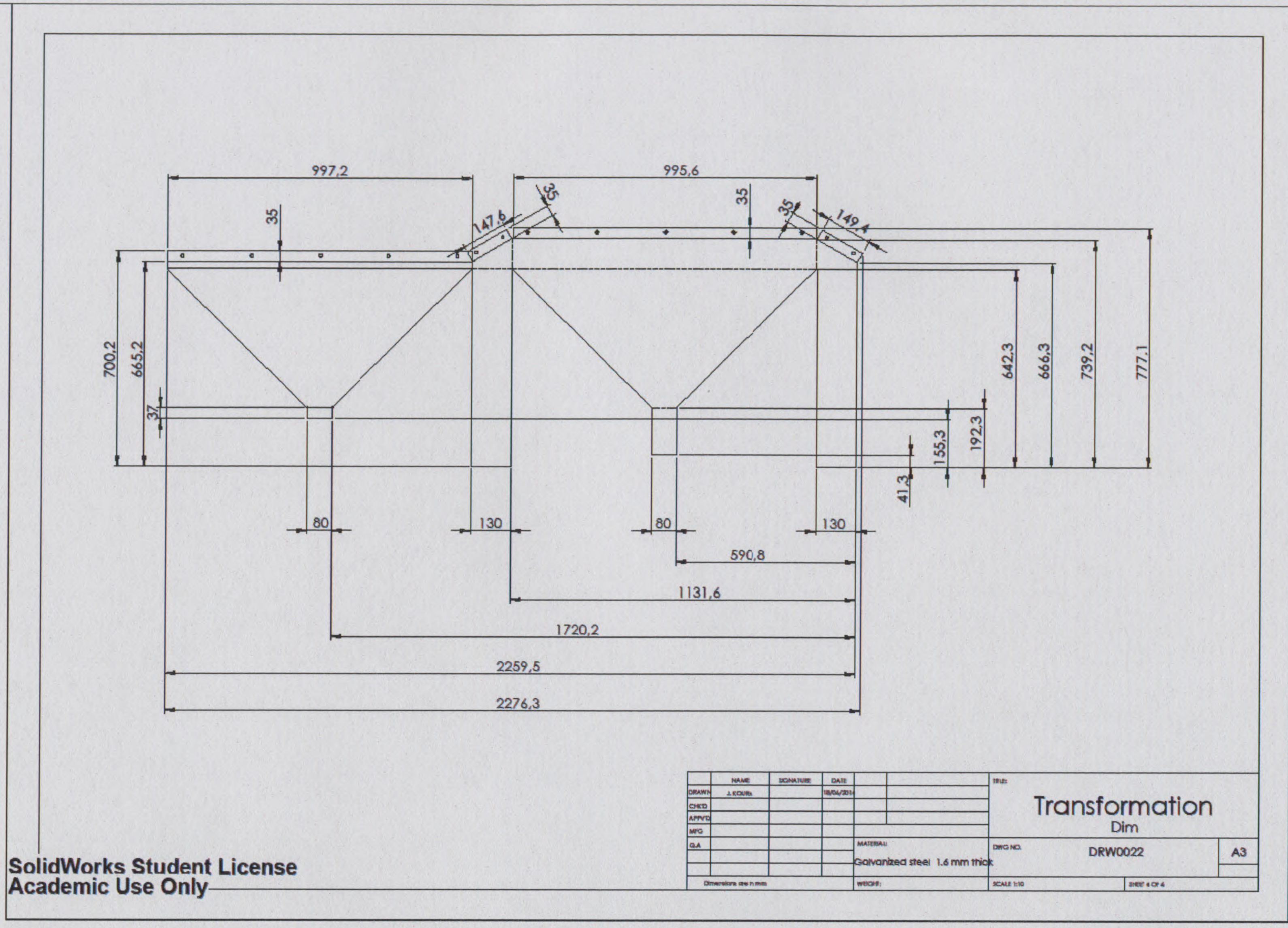

Figure A-5-4: Flat pattern of the transformation duct (external condenser)

Table A- 1: Material cost for construction

Quantity	Material	Cost (Rands)
1	Galvanised steel basin	1870
1	Galvanised steel external condenser	600
2	Sheets of polycarbonate	1500
2	Glass containers	100
1	Tin of high heat resistant and waterproof paint	219
1	Tin of white weatherproof paint	179
3	Sheets of polystyrene 1200x500x25 mm	150
1	Aluminum sheet 1200x600	600
1	PVC pipe 20mm (3m)	30
1	Clear plastic pipes (1m)	25
	Pipe fittings	70
1	PVC ball valve	20
2	Weather resistant silicone sealant tube	250
1	Self-adhesive sponge rubber (10 m)	70
	Flat and angle bars	110
	Screws	25
1	Meshing basket	15
Total		**5883**

B-1: Kipp & Zonen CMP06 pyranometer

Specifications	CMP 3	CMP 6	CMP10 & CMP 11	CMP 21	CMP 22
Classification to ISO 9060:1990	Second Class	First Class	Secondary Standard	Secondary Standard	Secondary Standard
Spectral range (50% points)	300 to 2800 nm	285 to 2800 nm	285 to 2800 nm	285 to 2800 nm	200 to 3600 nm
Sensitivity	5 to 20 μV/W/m²	5 to 20 μV/W/m²	7 to 14 μV/W/m²	7 to 14 μV/W/m²	7 to 14 μV/W/m²
Impedance	20 to 200 Ω	20 to 200 Ω	10 to 100 Ω	10 to 100 Ω	10 to 100 Ω
Expected output range (0 to 1500 W/m²)	0 to 30 mV	0 to 30 mV	0 to 20 mV	0 to 20 mV	0 to 20 mV
Maximum operational irradiance	2000 W/m²	2000 W/m²	4000 W/m²	4000 W/m²	4000 W/m²
Response time (63%) Response time (95%)	< 6 s < 18 s	< 6 s < 18 s	< 1.7 s < 5 s	< 1.7 s < 5 s	< 1.7 s < 5 s
Zero offsets (a) thermal radiation (at 200 W/m²) (b) temperature change (5 K/h)	 < 15 W/m² < 5 W/m²	 < 12 W/m² < 4 W/m²	 < 7 W/m² < 2 W/m²	 < 7 W/m² < 2 W/m²	 < 3 W/m² < 1 W/m²
Non-stability (change/year)	< 1%	< 1%	< 0.5%	< 0.5%	< 0.5%
Non-linearity (100 to 1000 W/m²)	< 1.5%	< 1%	< 0.2%	< 0.2%	< 0.2%
Directional response (up to 80° with 1000 W/m² beam)	< 20 W/m²	< 20 W/m²	< 10 W/m²	< 10 W/m²	< 5 W/m²
Spectral selectivity (350 to 1500 nm)	< 3%	< 3%	< 3%	< 3%	< 3%
Temperature response	< 5% (-10°C to +40°C)	< 4% (-10°C to +40°C)	< 1% (-10°C to +40°C)	< 1% (-20°C to +50°C)	< 0.5% (-20°C to +50°C)
Tilt response (0° to 90° at 1000 W/m²)	< 1%	< 1%	< 0.2%	< 0.2%	< 0.2%
Field of view	180°	180°	180°	180°	180°
Accuracy of bubble level	< 0.2°	< 0.1°	< 0.1°	< 0.1°	< 0.1°
Temperature sensor output				10 K Thermistor (optional Pt-100)	10 K Thermistor (optional Pt-100)
Detector type	Thermopile	Thermopile	Thermopile	Thermopile	Thermopile
Operational temperature range	-40°C to +80°C	-40°C to +80°C	-40°C to +80°C	-40°C to +80°C	-40°C to +80°C
Storage temperature range	-40°C to +80°C	-40°C to +80°C	-40°C to +80°C	-40°C to +80°C	-40°C to +80°C
Humidity range	0 to 100% non-condensing	0 to 100% non-condensing	0 to 100% non-condensing	0 to 100% non-condensing	0 to 100% non-condensing
Ingress Protection (IP) rating	67	67	67	67	67
Recommended applications	Economical solution for routine measurements in weather stations, field testing	Good quality measurements for hydrology networks, greenhouse climate control	Meteorological networks, PV panel and thermal collector testing, materials testing	Meteorological networks, reference measurements in extreme climates, polar or arid	Scientific research requiring the highest level of measurement accuracy and reliability

(Kipp & Zonen, pyranometers. http://www.ames.si/files/attachments/KippZonen_Brochure_Pyranometers.pdf)

B-2: SP-LITE silicon pyranometer

SP-LITE Silicon Pyranometer

2. Sensor Specifications

Electrical

Nominal Impedance:	<50 Ω
Response Time:	<1 second
Sensitivity:	10 μV/(W m^{-2})
Expected signal range: (under atmospheric conditions)	0 – 15 mV
Stability:	<±2% per year
Non-linearity:	<±1% up to 1000 W m^{-2}
Temperature dependence of sensitivity:	<±0.15% /°C

Spectral

Spectral range:	400 to 1100 nm
Detector type:	BPW 34

Directional

Cosine corrected between 80° angle of incidence, error:	within ±10%
Cosine errors averaged over opposite azimuth error (at 60° angle of incidence):	within ±10%
Tilt response:	zero error

Mechanical

Housing material:	Anodized aluminum
Cable material:	Polyurethane
Weight:	110 g
Cable length:	5 m (can be extended up to 100 m)
Physical Dimensions:	See Figure 5

Environmental

Working temperature:	-30 to +70°C

Dimensions

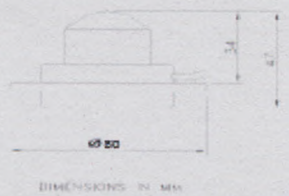

FIGURE 5. Dimensions of SP-LITE with Leveling Device

Campbell Scientific- SP-LITE silicon pyranometer Instruction manual, Revision 7/04,

http://s.campbellsci.com/documents/us/manuals/sp-lite.pdf

B-3: 03101 R.M Young three cup anemometer

Range:	0 to 50 m s^{-1} (112 mph), gust survival 60 m s^{-1} (134 mph)
Sensor:	12 cm diameter cup wheel assembly, 40 mm diameter hemispherical cups
Accuracy:	±0.5 m s^{-1} (1.1 mph)
Turning Factor:	75 cm (2.5 ft)
Distance Constant (63% recovery):	2.3 m (7.5 ft)
Threshold:	0.5 m s^{-1} (1.1 mph)
Transducer:	Stationary coil, 1300 ohm nominal resistance
Output:	AC sine wave signal induced by rotating magnet on cup wheel shaft 100 mV peak-to-peak at 60 rpm; 6 V peak-to-peak at 3600 rpm
Output Frequency:	1 cycle per cup wheel revolution; 0.75 m s^{-1} per Hz
Cup Wheel Diameter:	12 cm (4.7 in)
Weight:	113 g (4 oz)

Campbell Scientific, 03101 R.M. Young Wind Sentry Anemometer, Instruction Manual. https://s.campbellsci.com/documents/af/manuals/03002.pdf

Table C- 1: Value of n by Months

Month	*n* for *i*th day of Month
January	*i*
February	31+ *i*
March	59+ *i*
April	90+ *i*
May	120+ *i*
June	151+ *i*
July	181+ *i*
August	212+ *i*
September	243+ *i*
October	273+ *i*
November	304+ *i*
December	334+ *i*

Table C- 2: Brightness coefficient for Perez Anisotropic Sky

Range of ε	f_{11}	f_{12}	f_{13}	f_{21}	f_{22}	f_{23}
1.000-1.065	**-0.008**	**0.588**	**-0.062**	**-0.060**	**0.072**	**-0.022**
1.065-1.230	**0.130**	**0.683**	**-0.151**	**-0.019**	**0.066**	**-0.029**
1.230-1.500	**0.330**	**0.487**	**-0.221**	**0.055**	**-0.064**	**-0.026**
1.500-1.950	**0.568**	**0.187**	**-0.295**	**0.109**	**-0.152**	**0.014**
1.950-2.800	**0.873**	**-0.392**	**-0.362**	**0.226**	**-0.462**	**0.001**
2.800-4.500	**1.132**	**-1.237**	**-0.412**	**0.288**	**-0.823**	**0.056**
4.500-6.200	**1.060**	**-1.600**	**-0.359**	**0.264**	**-1.127**	**0.131**
6.200-∞	**0.678**	**-0.327**	**-0.250**	**0.156**	**-1.377**	**0.251**

Adapted from Perez et al. (1990)

Table C- 3: Values of optical depths and air mass exponents for days of the year in Cape Town

DAY NUMBER n	BEAM OPTICAL DEPTH τ_b	DIFFUSE OPTICAL DEPTH τ_d	AIR MASS EXP.ab	AIR MASS EXP.ad
1	0,336	2,605	0,633	-0,414
2	0,336	2,605	0,633	-0,414
3	0,336	2,605	0,633	-0,414
4	0,336	2,606	0,633	-0,414
5	0,336	2,606	0,633	-0,414
6	0,335	2,607	0,633	-0,414
7	0,335	2,607	0,632	-0,414
8	0,335	2,608	0,632	-0,414
9	0,335	2,608	0,632	-0,414
10	0,335	2,608	0,632	-0,414
11	0,335	2,609	0,632	-0,414
12	0,335	2,609	0,632	-0,414
13	0,335	2,610	0,632	-0,414
14	0,335	2,610	0,632	-0,414
15	0,335	2,610	0,632	-0,414
16	0,335	2,611	0,632	-0,414
17	0,335	2,611	0,632	-0,414
18	0,335	2,612	0,632	-0,414
19	0,335	2,612	0,632	-0,414
20	0,335	2,613	0,632	-0,414
21	**0,335**	**2,613**	0,631	-0,414
22	0,335	2,613	0,631	-0,415
23	0,335	2,612	0,631	-0,415
24	0,336	2,612	0,631	-0,415
25	0,336	2,611	0,631	-0,415
26	0,336	2,611	0,631	-0,416
27	0,336	2,610	0,631	-0,416
28	0,336	2,610	0,631	-0,416
29	0,337	2,609	0,631	-0,417
30	0,337	2,609	0,631	-0,417
31	0,337	2,608	0,631	-0,417
32	0,337	2,608	0,631	-0,417
33	0,337	2,608	0,631	-0,418
34	0,338	2,607	0,631	-0,418
35	0,338	2,607	0,631	-0,418
36	0,338	2,606	0,631	-0,419
37	0,338	2,606	0,631	-0,419
38	0,338	2,605	0,631	-0,419
39	0,338	2,605	0,631	-0,419
40	0,339	2,604	0,631	-0,420
41	0,339	2,604	0,631	-0,420
42	0,339	2,604	0,631	-0,420
43	0,339	2,603	0,631	-0,421
44	0,339	2,603	0,631	-0,421
45	0,340	2,602	0,631	-0,421
46	0,340	2,602	0,631	-0,421
47	0,340	2,601	0,631	-0,422
48	0,340	2,601	0,631	-0,422
49	0,340	2,600	0,631	-0,422
50	0,341	2,600	0,631	-0,423
51	0,341	2,599	0,631	-0,423
52	**0,341**	**2,599**	0,631	-0,423
53	0,341	2,601	0,631	-0,423
54	0,340	2,603	0,631	-0,423
55	0,340	2,605	0,630	-0,422
56	0,340	2,607	0,630	-0,422
57	0,340	2,608	0,630	-0,422
58	0,339	2,610	0,630	-0,422
59	0,339	2,612	0,629	-0,421
60	0,339	2,614	0,629	-0,421
61	0,338	2,616	0,629	-0,421
62	0,338	2,618	0,629	-0,420
63	0,338	2,620	0,628	-0,420
64	0,338	2,622	0,628	-0,420
65	0,337	2,624	0,628	-0,420
66	0,337	2,626	0,628	-0,419
67	0,337	2,627	0,627	-0,419
68	0,336	2,629	0,627	-0,419
69	0,336	2,631	0,627	-0,419
70	0,336	2,633	0,627	-0,418
71	0,336	2,635	0,626	-0,418
72	0,335	2,637	0,626	-0,418
73	0,335	2,639	0,626	-0,417
74	0,335	2,641	0,626	-0,417
75	0,334	2,643	0,625	-0,417
76	0,334	2,644	0,625	-0,417
77	0,334	2,646	0,625	-0,416
78	0,334	2,648	0,625	-0,416
79	0,333	2,650	0,624	-0,416
80	**0,333**	**2,652**	0,624	-0,416

DAY NUMBER n	BEAM OPTICAL DEPTH τ_b	DIFFUSE OPTICAL DEPTH τ_d	AIR MASS EXP.ab	AIR MASS EXP.ad
81	0,333	2,650	0,625	-0,415
82	0,333	2,647	0,625	-0,415
83	0,333	2,645	0,626	-0,415
84	0,333	2,642	0,626	-0,415
85	0,333	2,640	0,627	-0,414
86	0,333	2,637	0,627	-0,414
87	0,333	2,635	0,628	-0,414
88	0,333	2,632	0,628	-0,414
89	0,333	2,630	0,629	-0,413
90	0,333	2,627	0,629	-0,413
91	0,333	2,625	0,630	-0,413
92	0,333	2,622	0,630	-0,412
93	0,333	2,620	0,631	-0,412
94	0,333	2,617	0,631	-0,412
95	0,333	2,615	0,632	-0,412
96	0,334	2,612	0,632	-0,411
97	0,334	2,610	0,633	-0,411
98	0,334	2,607	0,634	-0,411
99	0,334	2,605	0,634	-0,411
100	0,334	2,602	0,635	-0,410
101	0,334	2,600	0,635	-0,410
102	0,334	2,597	0,636	-0,410
103	0,334	2,595	0,636	-0,410
104	0,334	2,592	0,637	-0,409
105	0,334	2,590	0,637	-0,409
106	0,334	2,587	0,638	-0,409
107	0,334	2,585	0,638	-0,409
108	0,334	2,582	0,639	-0,408
109	0,334	2,580	0,639	-0,408
110	0,334	2,577	0,640	-0,408
111	**0,334**	**2,575**	0,640	-0,408
112	0,334	2,576	0,640	-0,407
113	0,333	2,578	0,640	-0,407
114	0,333	2,579	0,640	-0,406
115	0,333	2,580	0,640	-0,406
116	0,332	2,582	0,640	-0,405
117	0,332	2,583	0,640	-0,405
118	0,332	2,585	0,640	-0,404
119	0,331	2,586	0,640	-0,404
120	0,331	2,587	0,640	-0,403
121	0,330	2,589	0,639	-0,403
122	0,330	2,590	0,639	-0,402
123	0,330	2,591	0,639	-0,402

DAY NUMBER n	BEAM OPTICAL DEPTH τ_b	DIFFUSE OPTICAL DEPTH τ_d	AIR MASS EXP.ab	AIR MASS EXP.ad
124	0,329	2,593	0,639	-0,402
125	0,329	2,594	0,639	-0,401
126	0,329	2,596	0,639	-0,401
127	0,328	2,597	0,639	-0,400
128	0,328	2,598	0,639	-0,400
129	0,327	2,600	0,639	-0,399
130	0,327	2,601	0,639	-0,399
131	0,327	2,602	0,639	-0,398
132	0,326	2,604	0,638	-0,398
133	0,326	2,605	0,638	-0,397
134	0,326	2,606	0,638	-0,397
135	0,325	2,608	0,638	-0,396
136	0,325	2,609	0,638	-0,396
137	0,325	2,611	0,638	-0,395
138	0,324	2,612	0,638	-0,395
139	0,324	2,613	0,638	-0,394
140	0,323	2,615	0,638	-0,394
141	**0,323**	**2,616**	0,638	-0,393
142	0,323	2,617	0,638	-0,393
143	0,322	2,619	0,638	-0,392
144	0,322	2,620	0,637	-0,392
145	0,321	2,622	0,637	-0,391
146	0,321	2,623	0,637	-0,391
147	0,321	2,625	0,637	-0,390
148	0,320	2,626	0,637	-0,390
149	0,320	2,628	0,637	-0,389
150	0,320	2,629	0,637	-0,389
151	0,319	2,631	0,637	-0,388
152	0,319	2,632	0,637	-0,387
153	0,318	2,633	0,637	-0,387
154	0,318	2,635	0,637	-0,386
155	0,318	2,636	0,636	-0,386
156	0,317	2,638	0,636	-0,385
157	0,317	2,639	0,636	-0,385
158	0,316	2,641	0,636	-0,384
159	0,316	2,642	0,636	-0,384
160	0,316	2,644	0,636	-0,383
161	0,315	2,645	0,636	-0,383
162	0,315	2,646	0,636	-0,382
163	0,314	2,648	0,636	-0,382
164	0,314	2,649	0,636	-0,381
165	0,314	2,651	0,636	-0,381
166	0,313	2,652	0,636	-0,380

DAY NUMBER n	BEAM OPTICAL DEPTH τ_b	DIFFUSE OPTICAL DEPTH τ_d	AIR MASS EXP.ab	AIR MASS EXP.ad
167	0,313	2,654	0,635	-0,380
168	0,313	2,655	0,635	-0,379
169	0,312	2,657	0,635	-0,379
170	0,312	2,658	0,635	-0,378
171	0,311	2,660	0,635	-0,378
172	**0,311**	**2,661**	0,635	-0,377
173	0,311	2,659	0,635	-0,377
174	0,311	2,657	0,636	-0,377
175	0,312	2,654	0,636	-0,377
176	0,312	2,652	0,636	-0,377
177	0,312	2,650	0,637	-0,377
178	0,312	2,648	0,637	-0,377
179	0,312	2,646	0,638	-0,377
180	0,312	2,643	0,638	-0,377
181	0,313	2,641	0,638	-0,377
182	0,313	2,639	0,639	-0,377
183	0,313	2,637	0,639	-0,377
184	0,313	2,635	0,639	-0,378
185	0,313	2,632	0,640	-0,378
186	0,313	2,630	0,640	-0,378
187	0,314	2,628	0,641	-0,378
188	0,314	2,626	0,641	-0,378
189	0,314	2,624	0,641	-0,378
190	0,314	2,621	0,642	-0,378
191	0,314	2,619	0,642	-0,378
192	0,314	2,617	0,643	-0,378
193	0,315	2,615	0,643	-0,378
194	0,315	2,613	0,643	-0,378
195	0,315	2,610	0,644	-0,378
196	0,315	2,608	0,644	-0,378
197	0,315	2,606	0,644	-0,378
198	0,315	2,604	0,645	-0,378
199	0,316	2,602	0,645	-0,378
200	0,316	2,599	0,646	-0,378
201	0,316	2,597	0,646	-0,378
202	**0,316**	**2,595**	0,646	-0,378
203	0,316	2,593	0,647	-0,378
204	0,317	2,590	0,647	-0,379
205	0,317	2,588	0,647	-0,379
206	0,317	2,585	0,648	-0,380
207	0,318	2,583	0,648	-0,380
208	0,318	2,581	0,648	-0,380
209	0,318	2,578	0,648	-0,381

DAY NUMBER n	BEAM OPTICAL DEPTH τ_b	DIFFUSE OPTICAL DEPTH τ_d	AIR MASS EXP.ab	AIR MASS EXP.ad
210	0,319	2,576	0,649	-0,381
211	0,319	2,574	0,649	-0,381
212	0,320	2,571	0,649	-0,382
213	0,320	2,569	0,650	-0,382
214	0,320	2,566	0,650	-0,382
215	0,321	2,564	0,650	-0,383
216	0,321	2,562	0,651	-0,383
217	0,321	2,559	0,651	-0,383
218	0,322	2,557	0,651	-0,384
219	0,322	2,554	0,652	-0,384
220	0,322	2,552	0,652	-0,384
221	0,323	2,550	0,652	-0,385
222	0,323	2,547	0,653	-0,385
223	0,323	2,545	0,653	-0,385
224	0,324	2,542	0,653	-0,386
225	0,324	2,540	0,654	-0,386
226	0,325	2,538	0,654	-0,386
227	0,325	2,535	0,654	-0,387
228	0,325	2,533	0,654	-0,387
229	0,326	2,531	0,655	-0,387
230	0,326	2,528	0,655	-0,388
231	0,326	2,526	0,655	-0,388
232	0,327	2,523	0,656	-0,388
233	**0,327**	**2,521**	0,656	-0,389
234	0,327	2,521	0,656	-0,389
235	0,328	2,521	0,656	-0,389
236	0,328	2,521	0,656	-0,390
237	0,328	2,521	0,655	-0,390
238	0,328	2,521	0,655	-0,391
239	0,329	2,521	0,655	-0,391
240	0,329	2,521	0,655	-0,392
241	0,329	2,521	0,655	-0,392
242	0,329	2,521	0,655	-0,393
243	0,330	2,521	0,655	-0,393
244	0,330	2,521	0,654	-0,394
245	0,330	2,521	0,654	-0,394
246	0,330	2,521	0,654	-0,394
247	0,331	2,521	0,654	-0,395
248	0,331	2,521	0,654	-0,395
249	0,331	2,522	0,654	-0,396
250	0,331	2,522	0,654	-0,396
251	0,332	2,522	0,653	-0,397
252	0,332	2,522	0,653	-0,397

DAY NUMBER n	BEAM OPTICAL DEPTH τ_b	DIFFUSE OPTICAL DEPTH τ_d	AIR MASS EXP.ab	AIR MASS EXP.ad
253	0,332	2,522	0,653	-0,398
254	0,332	2,522	0,653	-0,398
255	0,333	2,522	0,653	-0,399
256	0,333	2,522	0,653	-0,399
257	0,333	2,522	0,652	-0,399
258	0,333	2,522	0,652	-0,400
259	0,334	2,522	0,652	-0,400
260	0,334	2,522	0,652	-0,401
261	0,334	2,522	0,652	-0,401
262	0,334	2,522	0,652	-0,402
263	0,335	2,522	0,652	-0,402
264	**0,335**	**2,522**	0,651	-0,403
265	0,335	2,521	0,652	-0,403
266	0,336	2,519	0,652	-0,403
267	0,336	2,518	0,652	-0,404
268	0,336	2,516	0,652	-0,404
269	0,337	2,515	0,652	-0,405
270	0,337	2,513	0,652	-0,405
271	0,337	2,512	0,652	-0,406
272	0,338	2,511	0,652	-0,406
273	0,338	2,509	0,653	-0,406
274	0,338	2,508	0,653	-0,407
275	0,339	2,506	0,653	-0,407
276	0,339	2,505	0,653	-0,408
277	0,339	2,503	0,653	-0,408
278	0,340	2,502	0,653	-0,408
279	0,340	2,501	0,653	-0,409
280	0,340	2,499	0,654	-0,409
281	0,341	2,498	0,654	-0,409
282	0,341	2,496	0,654	-0,410
283	0,341	2,495	0,654	-0,410
284	0,342	2,493	0,654	-0,411
285	0,342	2,492	0,654	-0,411
286	0,342	2,490	0,654	-0,411
287	0,343	2,489	0,654	-0,412
288	0,343	2,488	0,655	-0,412
289	0,343	2,486	0,655	-0,413
290	0,344	2,485	0,655	-0,413
291	0,344	2,483	0,655	-0,413
292	0,344	2,482	0,655	-0,414
293	0,345	2,480	0,655	-0,414
294	**0,345**	**2,479**	0,655	-0,415
295	0,344	2,483	0,655	-0,414

DAY NUMBER n	BEAM OPTICAL DEPTH τ_b	DIFFUSE OPTICAL DEPTH τ_d	AIR MASS EXP.ab	AIR MASS EXP.ad
296	0,344	2,487	0,654	-0,414
297	0,343	2,491	0,653	-0,414
298	0,343	2,496	0,653	-0,413
299	0,342	2,500	0,652	-0,413
300	0,342	2,504	0,652	-0,412
301	0,341	2,508	0,651	-0,412
302	0,341	2,512	0,650	-0,412
303	0,340	2,516	0,650	-0,411
304	0,340	2,521	0,649	-0,411
305	0,339	2,525	0,648	-0,411
306	0,339	2,529	0,648	-0,410
307	0,338	2,533	0,647	-0,410
308	0,338	2,537	0,647	-0,410
309	0,337	2,541	0,646	-0,409
310	0,337	2,546	0,645	-0,409
311	0,336	2,550	0,645	-0,408
312	0,336	2,554	0,644	-0,408
313	0,335	2,558	0,643	-0,408
314	0,335	2,562	0,643	-0,407
315	0,334	2,566	0,642	-0,407
316	0,334	2,571	0,642	-0,406
317	0,333	2,575	0,641	-0,406
318	0,333	2,579	0,640	-0,406
319	0,332	2,583	0,640	-0,405
320	0,332	2,587	0,639	-0,405
321	0,331	2,591	0,638	-0,404
322	0,331	2,596	0,638	-0,404
323	0,330	2,600	0,637	-0,404
324	0,330	2,604	0,637	-0,403
325	**0,329**	**2,608**	0,636	-0,403
326	0,329	2,608	0,636	-0,403
327	0,329	2,607	0,636	-0,404
328	0,330	2,607	0,636	-0,404
329	0,330	2,607	0,636	-0,404
330	0,330	2,607	0,636	-0,405
331	0,330	2,606	0,636	-0,405
332	0,331	2,606	0,635	-0,406
333	0,331	2,606	0,635	-0,406
334	0,331	2,606	0,635	-0,406
335	0,331	2,605	0,635	-0,407
336	0,332	2,605	0,635	-0,407
337	0,332	2,605	0,635	-0,407
338	0,332	2,605	0,635	-0,408

DAY NUMBER n	BEAM OPTICAL DEPTH τ_b	DIFFUSE OPTICAL DEPTH τ_d	AIR MASS EXP.ab	AIR MASS EXP.ad
339	0,332	2,604	0,635	-0,408
340	0,333	2,604	0,635	-0,409
341	0,333	2,604	0,635	-0,409
342	0,333	2,603	0,635	-0,409
343	0,333	2,603	0,635	-0,410
344	0,333	2,603	0,635	-0,410
345	0,334	2,603	0,634	-0,411
346	0,334	2,602	0,634	-0,411
347	0,334	2,602	0,634	-0,411
348	0,334	2,602	0,634	-0,412
349	0,335	2,602	0,634	-0,412
350	0,335	2,601	0,634	-0,412
351	0,335	2,601	0,634	-0,413

DAY NUMBER n	BEAM OPTICAL DEPTH τ_b	DIFFUSE OPTICAL DEPTH τ_d	AIR MASS EXP.ab	AIR MASS EXP.ad
352	0,335	2,601	0,634	-0,413
353	0,336	2,601	0,634	-0,414
354	0,336	2,600	0,634	-0,414
355	**0,336**	**2,6**	0,634	-0,414
356	0,336	2,600	0,634	-0,414
357	0,336	2,601	0,634	-0,414
358	0,336	2,601	0,634	-0,414
359	0,336	2,602	0,633	-0,414
360	0,336	2,602	0,633	-0,414
361	0,336	2,603	0,633	-0,414
362	0,336	2,603	0,633	-0,414
363	0,336	2,603	0,633	-0,414
364	0,336	2,604	0,633	-0,414
365	0,336	2,604	0,633	-0,414

D.1. Solar radiation incident on transparent cover

Initial data

Day: 21 June 2014

Latitude: L= -33.93°

Longitude: Long=18.46°

Cover inclination angle: β=53°

Solar constant: I_{SC}=1367 W/m^2

Ground reflectance: ρ=0.2

Local time: 12:00

Measured diffuse radiation incident on horizontal surface at 12:00: I_d= 29.45 W/m^2

Measured total radiation incident on horizontal surface at 12:00: I_h= 498.65 W/m^2

Calculated beam radiation incident on horizontal surface at 12:00: I_b= I_h-I_d = 469.2W/m^2

Sun angles calculation

Declination angle: δ=23.45 x sin [360x (284+n)/365] *Eq (3-6)*

On the 21 June, n=172 from Table C-1 in *Appendix C*

δ=23.45°

Hour angle: ω=15(t-t_{noon}) *Eq (3-7)*

t=12.0h

t_{noon} =720+4 x longitude- equation of time *Eq (3-8)*

Equation of time = 9.87 sin 2B -7.53 cos B -1.5 sin B *Eq (3-9)*

B=360 x (n-81)/365 = 360 x (172 -81)/365 *Eq (3-10)*

B=89.75.

Therefore,

Equation of time = 9.87 x sin (2x89.75) – 7.53 x cos (89.75) -1.5 sin (89.75)

Equation of time= -1.4474.

And,

t_{noon} = 795.287 minutes = 13.254h

ω = 15 (12.0-13.254)

ω = -18.82°

Incident angle of beam radiation: $\theta_i = \cos^{-1}$ [cos (L+β) x cos δ x cos ω + sin (L+β) x sin δ] *Eq (3-4)*

$\theta_i = \cos^{-1}$ [cos (-33.93+ 53) x cos 23.45 x cos (-18.82) + sin (-33.93 + 53) x sin 23.45]

θ_i = 60.11°

Cos θ_i = 0.951

Zenith angle: $\theta_z = \cos^{-1}$ [cos L x cos δ x cos ω + sin L x sin δ]

$\theta_z = \cos^{-1}$ [cos (-33.93) x cos 23.45 x cos (-18.82) + sin (-33.93) x sin 23.45] *Eq (3-5*

θ_z = 60.107

Cos θ_z = 0.5.

Beam radiation calculation

$I_{Tb} = R_b \times I_b$ *Eq (3-2)*

$R_b = \cos \theta_i / \cos \theta_z = 0.951/0.5$

$R_b = 1.908$

$I_{Tb} = 1.908 \times 469.2$

$I_{Tb} = 895.08\ W/m^2$

Diffuse radiation calculation

$I_{Td} = I_d [(1 - F_1) \times (1 + \cos \beta)/2 + F_1 (a/b) + F_2 \sin \beta]$ *Eq (3-12)*

$a = \max (0; \cos \theta_i) = \max (0; 0.951)$ *Eq (3-13)*

$a = 0.951$

$b = \max (0; \cos \theta_z) = \max (0; 0.5)$ *Eq (3-14)*

$b = 0.5$.

$F_1 = \max [0; (f_{11} + \Delta f_{12} + \pi\ \theta_z f_{13}/180)]$ *Eq (3-20)*

$F_2 = f_{21} + \Delta f_{22} + \pi\ \theta_z f_{23}/180$ *Eq (3-21)*

$\Delta = m \times I_d/I_{on}$ *Eq (3-17)*

$m = 1/ \cos \theta_z = 1/0.5$ *Eq (3-18)*

$m = 2\ kg$

$I_{on} = I_{sc} (1 + 0.033 \cos (360n/365) \times \cos \theta_z$ *Eq (3-19)*

$I_{on} = 661.31\ W/m^2$

$\Delta = 2.01 \times 29.45/663.33$

$\Delta = 0.088$

The brightness coefficients f_{11}, f_{12}, $f_{13,}$ f_{21}, f_{22} and $f_{23,}$ depend on the clearness parameter ε.

$$\varepsilon = [(I_d + I_{b.n})/ I_d + 5.535 \times 10^{-6} \times \theta_z^3]/ (1+ 5.535 \times 10^{-6} \times \theta_z^3) \qquad \textit{Eq (3-15)}$$

$$I_{b.n} = I_b/ \cos \theta_z = 469.2 / 0.5 \qquad \textit{Eq (3-16)}$$

$$I_{b.n} = 938.4 \ W/m^2$$

$$\varepsilon = [(29.45 + 938.4)/ 29.45 + 5.535 \times 10^{-6} \times 60.18^3]/ (1+ 5.535 \times 10^{-6} \times 60.18^3)$$

$$\varepsilon = 15.44.$$

From Table C.2 of Appendix C, ε = 15.44 is in the range [6.200; +$^{\infty}$]

$$f_{11} = 0.678; f_{12} = -0.327; f_{13} = -0.25$$

$$f_{21} = 0.156; f_{22} = -1.377; f_{23} =0.251$$

Therefore:

$$F_1 = \max [0; (0.678+ 0.088 \times -0.327+ \pi \times 60.18 \times (-0.25)/180)]$$

$$F_1 = \max (0; 0.387)$$

$$F_1 = 0.387$$

$$F_2 = 0.156 + 0.088 \times (-1.377) + \pi \times 60.18 \times 0.251/180$$

$$F_2 = 0.298$$

$$I_{Td} = 29.45 [(1- 0.387) \times (1 + \cos 53)/2 + 0.387 (0.951/0.5) +0.298 \sin 53]$$

$\underline{I_{Td} = 45.1 \ W/m^2}$

Reflected radiation calculation

$$I_{Trefl}= I_h \rho_g (1- \cos\beta)/2 = 498.65 \times 0.2 \times (1- \cos53)/2 \qquad \textit{Eq (3-22)}$$

I_{Trefl}= 19.855 W/m^2

Total solar radiation incident on the transparent cover

$I_T = I_{Tb} + I_{Td} + I_{Trefl}$ *Eq (3-23)*

I_T = 895.08 + 45.1 + 19.855

I_T = 960.017 W/m^2.

D.2. Estimated solar radiation using the ASHRAE model method

Initial data

Day: 21 June 2014, n=172

Local time: 12:00

Latitude: L= -33.93°

Beam and diffuse radiation estimation

$E_b = I_{on} \times \exp[-\tau_b \times m^{ab}]$

$E_b = I_{on} \times \exp[-\tau_d \times m^{ad}]$

I_{on} and m were calculated in the sample calculation D.1 as:

I_{on} = 663.33 W/m^2

m= 2 kg

From Table C-3 in Appendix C. at day number n= 172,

$\tau_b = 0.311$, $\tau_d = 2.661$

ab = 0.635 , ad = 0.377.

Therefore:

$E_b = 661.31 \times \exp(-0.311\times 2^{0.635})$

$\underline{E_b = 408.06\ W/m^2}$

$E_d = 661.31 \times \exp(-2.661 \times 2^{-0.377})$

$\underline{E_d = 85.21\ W/m^2}$

Estimated total solar radiation:

$E = E_b + E_d$

$E = 408.06 + 85.21$

$\underline{E = 493.27\ W/m^2}$

D.3. Solar still productivity

Initial Data

Area of the transparent cover: A =0.27 m^2

Hourly instantaneous water collection (21/06/2014)

Time	Volume (ml)
8:30	0
9:00	10
10:00	41
11:00	87
12:00	152
13:00	234
14:00	313
15:00	383
16:00	448
17:00	502

The solar still productivity on this day is expressed as:

$P_d = \Sigma V_i/A$ *Eq (3-27)*

$= 502/0.27$

$=1859\ ml/m^2$

$\underline{P_d = 1.86\ l/m^2}$

D.4. Energy efficiency calculation

Energy efficiency (21/06/2014)

Initial data

Average water temperature during the day: T_W= 36°C

Total collected volume: V_t = 0.502 Litres

Area of the transparent cover: A= 0.27 m^2

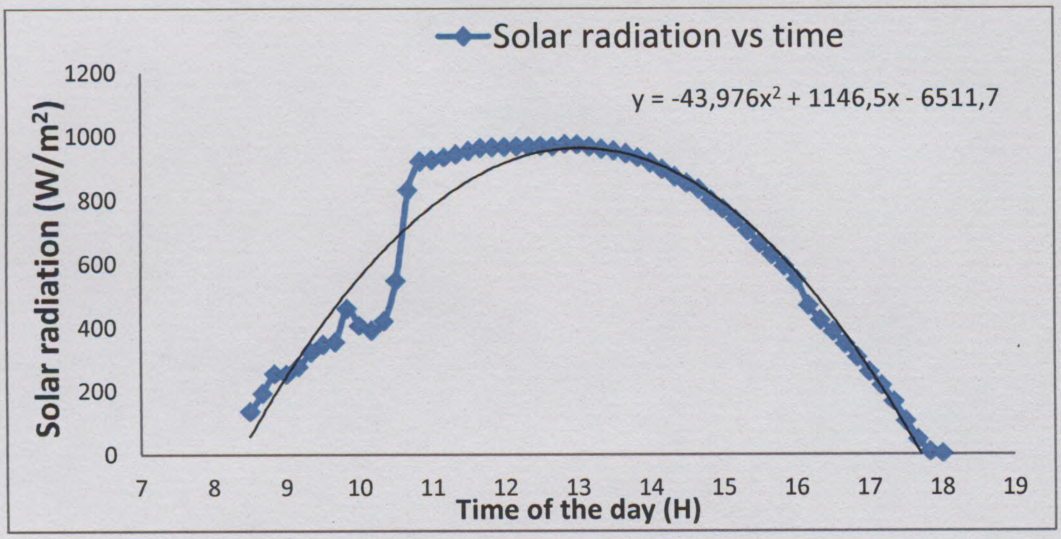

Solar radiation curve on the 21 June 2014

Amount of solar energy incident on transparent cover (daily insolation) =Area under the curve

-Integral of y=f(t) between sunrise and sunset hour

$$I = \int_{8.5}^{18} [-43.976t^2 + 1146.5t - 6511.7]\, dt$$

$$I = \left[-\frac{1}{3} \times 43.976t^3 + \frac{1}{2} \times 11446.5t^2 - 6511.7t\right]_{8.5}^{18}$$

$I = 5967.45\ Wh/m^2 = 21482.784\ kJ/m^2$.

Latent heat of evaporation of the water in the basin depending on its average temperature

Eq (3-30) $h_{fg} = 2.4935 \times 10^6 \times [1 - 9.4779 \times 10^{-4}T + 1.3132 \times 10^{-7}T^2 - 4.7974 \times 10^{-9}T^3]$

for $T < 70$ °C

At Tv = 36 °C,

<u>h_{fg}= 2408.29 kJ/kg</u>

<u>Mass of collected water</u>

It was assumed that 1 kg of distilled water = 1 Litre of distilled water

m= 0.502 kg

$$\text{Efficiency of solar still} = \frac{\text{Energy used in vaporising water}}{\text{Amount of solar energy incident on transparent cover}}$$

$$\eta = \frac{m \times h_{fg}}{A \times \int I} \qquad \textit{Eq (3-29)}$$

$$\eta = \frac{0.502 \times 2408.29}{0.27 \times 21482.784}$$

$$\boldsymbol{\eta = 20.8 \approx 21\%}$$

Table E- 1: Measured data on 2 June 2014:

Local Time	Meteorological factors							
	Solar radiation (beam) I_b [W/m^2]	Solar radiation (diffuse) I_d [W/m^2]	Solar radiation (total horizontal) I_h [W/m^2]	Solar radiation (total inclined) I_T [W/m^2]	Air temp [°C]	Wind speed [m/s]	Basin temp [°C]	Distillate output [ml]
9:00	55,215	19,14	74,355	209,16	13,59	5,244	15,015	0
9:10	62,86	22,59	85,45	218,86	13,61	4,839		
9:20	68,25	19,6	87,85	215,12	13,71	4,36		
9:30	95,87	26,08	121,95	285,37	13,97	4,5		
9:40	97,11	31,29	128,4	283,59	14,02	5,182		
9:50	95,72	33,28	129	273,12	14,24	4,699		
10:00	93,11	36,69	129,8	263,60	14,45	4,301	18,564	5
10:10	102,76	30,79	133,55	276,77	14,59	4,235		
10:20	176,89	27,31	204,2	434,42	14,81	5,037		
10:30	246,32	24,03	270,35	570,61	15,46	5,186		
10:40	136,4	20,1	156,5	323,31	15,26	5,02		
10:50	108,22	17,58	125,8	255,71	14,89	5,217		
11:00	128,35	19,7	148,05	296,48	14,96	4,57	22,471	15
11:10	373,18	29,87	403,05	794,22	15,68	5,993		
11:20	468,39	34,66	503,05	978,71	16,54	5,88		
11:30	478,86	32,09	510,95	984,01	17,11	5,186		
11:40	489,59	32,51	522,1	994,53	17,46	5,201		
11:50	510,41	36,04	546,45	1029,30	17,58	6,014		
12:00	548,14	41,01	589,15	1098,37	17,96	6,187	25,123	30
12:10	542,94	53,51	596,45	1102,33	18,16	6,392		
12:20	339,48	50,82	390,3	715,47	17,6	7,415		
12:30	598,87	53,58	652,45	1187,27	18,28	6,619		
12:40	344,61	30,99	375,6	682,93	17,97	6,932		
12:50	236,19	29,81	266	485,23	17,5	6,34		
13:00	204,55	34,9	239,45	434,76	17,29	6,836	31,485	50
13:10	165,52	37,93	203,45	367,40	17,04	7,115		
13:20	147,81	37,19	185	333,87	17,04	6,761		
13:30	106,82	36,13	142,95	249,80	16,85	6,905		
13:40	96,82	40,68	137,5	238,30	16,83	6,144		
13:50	92,17	40,28	132,45	229,86	16,81	6,415		
14:00	179,5	32,1	211,6	388,86	17,06	5,922	30,678	65
14:10	152,88	23,52	176,4	327,53	17,26	6,107		
14:20	126,12	25,18	151,3	281,88	17,15	6,347		
14:30	85,43	23,67	109,1	198,37	16,96	6,874		
14:40	74,12	22,18	96,3	176,10	16,88	6,571		
14:50	71,65	20,5	92,15	170,47	16,77	8,05		
15:00	78,93	24,67	103,6	192,63	16,76	7,445	28,142	75
15:10	99,3	19,65	118,95	233,08	16,77	7,755		
15:20	179,88	25,82	205,7	409,06	17	8,84		
15:30	72,83	18,57	91,4	178,38	16,7	9,01		
15:40	59,065	18,54	77,605	152,17	16,43	8,45		
15:50	40,105	13,63	53,735	106,86	16,14	9,01		
16:00	24,28	10,82	35,1	66,48	16,02	7,562	24,147	85
16:10	19,135	10,52	29,655	55,91	16,09	7,937		
16:20	14,632	7,678	22,31	43,22	16,01	5,604		
16:30	13,273	6,357	19,63	39,44	15,93	5,676		
16:40	17,655	8,37	26,025	53,99	15,86	6,119		
16:50	21,12	10,74	31,86	67,97	15,91	7,93		
17:00	19,765	9,39	29,155	65,62	15,69	8,2	20,421	90

Table E- 2: Measured data on 3 June 2014

Local Time	Meteorological factors							
	Solar radiation (beam) I_b [W/m²]	Solar radiation (diffuse) I_d [W/m²]	Solar radiation (total horizontal) I_h [W/m²]	Solar radiation (total inclined) I_T [W/m²]	Air temp [°C]	Wind speed [m/s]	Basin temp [°C]	Distillate output [ml]
9:00	44,74	20,54	65,28	179,24	13,19	4,497	17,41	0
9:10	37,895	14,57	52,465	133,53	13,04	4,465		
9:20	56,56	20,14	76,7	184,74	13	5,161		
9:30	94,63	36,32	130,95	298,41	13,23	5,194		
9:40	74,86	23,34	98,2	218,29	13,31	5,385		
9:50	140,09	35,26	175,35	385,94	13,66	4,895		
10:00	129,48	36,82	166,3	353,27	13,96	4,701	19.56	10
10:10	86,44	27,86	114,3	236,98	13,79	5,206		
10:20	169,37	37,38	206,75	428,20	14,16	4,472		
10:30	354,33	59,27	413,6	842,50	15,03	5,299		
10:40	448,3	81,6	529,9	1041,50	15,32	5,755		
10:50	375,79	75,96	451,75	876,75	15,78	5,021		
11:00	109,74	39,96	149,7	282,71	15,17	4,936	25,28	25
11:10	81,41	25,44	106,85	202,26	14,91	5,109		
11:20	71,49	23,26	94,75	177,12	14,94	4,981		
11:30	88,77	28,68	117,45	216,96	15,21	5,139		
11:40	89,02	32,03	121,05	220,18	15,05	5,344		
11:50	147,76	42,34	190,1	345,43	15,1	4,654		
12:00	104,07	34,88	138,95	249,43	15,02	5,206	28,45	40
12:10	52,525	18,11	70,635	126,43	14,54	4,482		
12:20	59,625	18,93	78,555	140,22	14,31	4,674		
12:30	113,4	31,9	145,3	258,46	13,96	4,366		
12:40	544,64	78,56	623,2	1126,36	15,23	4,509		
12:50	566,9	78,75	645,65	1157,37	16,13	5,292		
13:00	274,58	64,47	339,05	606,55	15,97	6,622	32,587	55
13:10	161,11	48,79	209,9	367,60	15,47	7,266		
13:20	193,59	52,01	245,6	440,56	14,58	6,831		
13:30	312,67	67,53	380,2	681,20	15,04	5,467		
13:40	302,15	66,65	368,8	662,12	15,52	4,951		
13:50	212,67	58,53	271,2	479,14	15,56	5,587		
14:00	238,67	61,13	299,8	541,35	15,63	5,536	31,13	70
14:10	344,72	66,13	410,85	749,44	16,18	4,96		
14:20	237,94	59,46	297,4	543,45	16,35	4,539		
14:30	468,2	80,3	548,5	1010,22	17,63	5,542		
14:40	344,79	74,76	419,55	774,03	18,18	5,555		
14:50	374,48	74,42	448,9	837,59	17,79	6,697		
15:00	283,77	56,98	340,75	647,56	17,88	5,585	26,14	90
15:10	69,71	21,39	91,1	172,05	16,93	6,237		
15:20	101,55	30,9	132,45	252,41	16,06	6,586		
15:30	85,48	28,37	113,85	219,00	15,18	5,317		
15:40	252,15	48	300,15	601,64	14,98	5,234		
15:50	152,93	38,97	191,9	384,23	15,25	4,635		
16:00	190,67	41,03	231,7	476,22	15,15	5,148	25,47	100
16:10	123,05	29,8	152,85	319,95	15,07	4,392		
16:20	74,34	19,01	93,35	200,47	15,14	3,725		
16:30	37,61	10,34	47,95	105,91	15,43	5,08		
16:40	24,411	7,964	32,375	70,37	15,47	5,042		
16:50	50,145	20,14	70,285	155,64	15,48	6,29		
17:00	35,885	20,77	56,655	122,65	15,5	5,533	21,45	110

Table E- 3: Measured data on 4 June 2014

Local Time	Meteorological factors							
	Solar radiation (beam) I_b [W/m^2]	Solar radiation (diffuse) I_d [W/m^2]	Solar radiation (total horizontal) I_h [W/m^2]	Solar radiation (total inclined) I_T [W/m^2]	Air temp [°C]	Wind speed [m/s]	Basin temp [°C]	Distillate output [ml]
9:00	25,6	11,35	36,95	101,62	11,45	5,024	18,01	0
9:10	20,89	9,74	30,63	76,19	12,04	5,337		
9:20	12,688	5,132	17,82	42,18	12,65	4,109		
9:30	16,683	6,932	23,615	52,99	12,66	4,769		
9:40	31,77	10,6	42,37	93,69	12,32	4,104		
9:50	20,657	7,768	28,425	59,90	12,06	3,936		
10:00	24,28	9,39	33,67	68,74	11,97	3,945	20,06	10
10:10	34,34	14,3	48,64	96,17	11,9	3,437		
10:20	33,875	11,62	45,495	93,42	11,93	4,207		
10:30	85,13	30,82	115,95	230,19	12,17	4,056		
10:40	90,11	28,64	118,75	234,29	12,57	3,873		
10:50	78,46	25,79	104,25	202,55	12,99	6,187		
11:00	57,345	21,22	78,565	149,93	12,55	5,033	26,27	25
11:10	74,24	30,66	104,9	195,71	12,37	4,642		
11:20	48,23	20,22	68,45	126,82	12,15	4,43		
11:30	74	26,85	100,85	185,87	12,49	4,041		
11:40	124,32	43,78	168,1	305,67	13,08	4,26		
11:50	104,47	44,03	148,5	265,36	13	4,729		
12:00	138,91	47,14	186,05	333,43	13	4,991	28,41	40
12:10	136,09	47,41	183,5	326,36	13,41	4,97		
12:20	174,66	44,49	219,15	401,05	14,21	4,84		
12:30	66,6	26	92,6	163,27	13,19	5,601		
12:40	47,855	19,45	67,305	118,28	12,15	3,959		
12:50	187,12	28,28	215,4	395,26	12,26	2,628		
13:00	411,68	41,62	453,3	828,45	14,02	2,297	32,08	55
13:10	513,88	43,02	556,9	1011,60	15,3	6,61		
13:20	334,77	53,13	387,9	703,99	15,47	6		
13:30	131,56	47,69	179,25	312,90	14,47	6,638		
13:40	224,76	48,69	273,45	496,31	14,42	6,872		
13:50	440,82	50,28	491,1	900,00	14,58	6,33		
14:00	303,17	54,28	357,45	654,49	14,77	6,954	31,98	75
14:10	459,98	51,12	511,1	946,31	15,47	6,072		
14:20	368,64	43,31	411,95	769,34	15,73	4,946		
14:30	176,15	36,95	213,1	399,40	14,93	6,266		
14:40	303,42	44,88	348,3	660,16	15,2	5,382		
14:50	229,81	40,54	270,35	516,36	15,32	6,055		
15:00	269,41	40,84	310,25	600,46	15,33	5,435	25,79	90
15:10	296	39,75	335,75	659,25	15,25	7,131		
15:20	230,73	35,22	265,95	528,46	15,25	5,759		
15:30	158,9	36,4	195,3	382,72	14,76	5,774		
15:40	204,45	43,4	247,85	493,62	14,98	5,794		
15:50	198,41	35,69	234,1	483,14	15,2	5,141		
16:00	58,42	24,56	82,98	159,24	14,59	4,832	24,15	105
16:10	59,09	25,91	85	165,81	14,33	5,127		
16:20	45,07	16,72	61,79	125,46	14,2	5,459		
16:30	28,76	12,48	41,24	84,49	14,09	5,146		
16:40	29,125	10,65	39,775	85,74	13,9	4,411		
16:50	42,14	16,73	58,87	130,87	13,79	5,576		
17:00	17,22	8,43	25,65	57,92	13,75	5,771	22,01	115

Table E- 4: Measured data on 5 June 2014

Local Time	Meteorological factors							
	Solar radiation (beam) I_b [W/m^2]	Solar radiation (diffuse) I_d [W/m^2]	Solar radiation (total horizontal) I_h [W/m^2]	Solar radiation (total inclined) I_T [W/m^2]	Air temp [°C]	Wind speed [m/s]	Basin temp [°C]	Distillate output [ml]
9:00	143,95	37,3	181,25	550,87	9,5	3,064	18,5	0
9:10	27,49	8,27	35,76	94,73	9,03	2,858		
9:20	11,39	5,68	17,07	39,49	8,73	2,332		
9:30	33,39	15,76	49,15	109,44	8,82	3,204		
9:40	52,65	11,05	63,7	150,93	9,23	1,532		
9:50	99,28	19,82	119,1	271,64	8,87	2,693		
10:00	114,96	20,89	135,85	302,31	8,82	3,951	20,5	10
10:10	73,92	26,03	99,95	202,10	8,98	3,445		
10:20	78,86	26,74	105,6	215,50	9,18	4,368		
10:30	312,25	38,95	351,2	739,63	9,74	4,669		
10:40	381,95	51,15	433,1	888,35	10,5	4,368		
10:50	398,92	74,93	473,85	929,16	11,39	3,246		
11:00	246,84	59,41	306,25	591,16	10,96	3,377	26,3	25
11:10	488	81,9	569,9	1095,73	11,75	3,32		
11:20	317,3	80,8	398,1	743,65	11,78	3,4		
11:30	265,48	63,57	329,05	618,53	11,78	3,032		
11:40	102,79	23,71	126,5	241,90	11,52	3,021		
11:50	74,47	19,48	93,95	173,27	11	3,026		
12:00	57,7	15,11	72,81	133,36	11	1,471	29,05	40
12:10	58,255	11,87	70,125	131,92	10,6	1,173		
12:20	24,46	13,55	38,01	62,63	9,69	3,455		
12:30	52,53	23,22	75,75	133,27	9,7	3,173		
12:40	343,6	47,25	390,85	715,27	10,55	2,331		
12:50	500,25	86,9	587,15	1055,62	11,5	2,69		
13:00	530,95	87	617,95	1110,89	12,78	2,417	33,17	60
13:10	331,74	70,51	402,25	722,36	12,62	2,426		
13:20	275,5	86,6	362,1	630,51	12,86	2,722		
13:30	91,16	39,04	130,2	226,65	12,67	1,897		
13:40	194,4	39	233,4	426,93	12,74	1,484		
13:50	198,25	47,6	245,85	448,01	12,87	2,454		
14:00	181,1	38,6	219,7	404,65	12	2,671	31,2	80
14:10	15,012	6,988	22	39,12	10,81	3,776		
14:20	14,703	3,947	18,65	34,11	8,2	2,163		
14:30	75,32	17,18	92,5	175,35	8,19	1,128		
14:40	210,64	31,36	242	462,17	9,12	0,903		
14:50	38,09	16,33	54,42	99,69	10,06	1,001		
15:00	34,855	12,64	47,495	88,71	9,96	1,103	26,1	95
15:10	48,395	27,35	75,745	131,25	10,04	0,67		
15:20	81,68	32,97	114,65	215,84	10,58	1,032		
15:30	54,58	22,58	77,16	141,39	10,55	1,342		
15:40	71,37	24,23	95,6	187,53	10,73	1,716		
15:50	23,94	20,16	44,1	72,04	10,37	2,116		
16:00	27,49	18,35	45,84	83,51	10,29	2,047	24,68	110
16:10	44,725	17,8	62,525	123,41	10,13	2,063		
16:20	112,85	116,6	229,45	439,20	10,55	1,775		
16:30	65,65	159,5	225,15	516,79	10,72	1,673		
16:40	51,56	71,69	123,25	241,18	10,73	1,577		
16:50	14,409	5,621	20,03	44,60	10,09	2,156		
17:00	8,369	4,316	12,685	28,47	9,53	1,854	22,64	120

Table E- 5: Measured data on 6 June 2014

Local Time	Meteorological factors							
	Solar radiation (beam) I_b [W/m^2]	Solar radiation (diffuse) I_d [W/m^2]	Solar radiation (total horizontal) I_h [W/m^2]	Solar radiation (total inclined) I_T [W/m^2]	Air temp [°C]	Wind speed [m/s]	Basin temp [°C]	Distillate output [ml]
9:00	30,74	17,78	48,52	66,30	9,64	2,988	13,42	0
9:10	35,98	21,94	57,92	79,86	9,78	3,411		
9:20	43,88	25,31	69,19	94,50	9,99	3,049		
9:30	47,81	29,67	77,48	107,15	10,25	3,619		
9:40	50,96	31,07	82,03	113,10	10,56	3,314		
9:50	65,11	35,52	100,63	136,15	10,93	2,618		
10:00	69,85	38	107,85	145,85	11,02	3,531	15,34	0
10:10	87,83	41,31	129,14	170,45	11,14	3,571		
10:20	116,38	47,76	164,14	211,90	11,49	2,843		
10:30	106,01	47,07	153,08	200,15	11,76	2,332		
10:40	130,74	40,13	170,87	211,00	11,74	3,113		
10:50	278,28	47,36	325,64	373,00	12,46	2,965		
11:00	163,97	41,99	205,96	247,95	12,43	2,809	18,65	0
11:10	378,4	47,5	425,9	473,40	13,31	2,962		
11:20	405,09	35,98	441,07	477,05	13,66	3,433		
11:30	420,39	31,23	451,62	482,85	13,95	3,163		
11:40	431,45	30	461,45	491,45	13,95	3,515		
11:50	440,71	30,07	470,78	500,85	14,05	3,289		
12:00	447,07	30,89	477,96	508,85	13,9	3,889	21,46	0
12:10	455,02	32,04	487,06	519,10	14,39	3,601		
12:20	457,32	32,89	490,21	523,10	14,87	3,277		
12:30	458,07	33,99	492,06	526,05	14,85	2,856		
12:40	456,98	34,86	491,84	526,70	15,12	2,67		
12:50	464,49	36,63	501,12	537,75	15	3,117		
13:00	432,72	37,19	469,91	507,10	15	3,782	23,51	20
13:10	398,92	38,09	437,01	475,10	15,29	3,555		
13:20	113,82	23,34	137,16	160,50	14,83	3,045		
13:30	82,9	39,65	122,55	162,20	14,69	2,952		
13:40	69,16	44,92	114,08	159,00	14,7	3,096		
13:50	104,55	43,05	147,6	190,65	14,86	2,709		
14:00	138,04	41,23	179,27	220,50	15,16	2,71	22,12	20
14:10	498,75	66,45	565,2	330,41	16,35	2,533		
14:20	427,38	69,56	496,94	566,50	17,32	3,101		
14:30	251,89	49,03	300,92	349,95	16,37	2,753		
14:40	176,44	38,58	215,02	253,60	16,02	3,15		
14:50	227,45	50,7	278,15	328,85	16,37	3,088		
15:00	331,09	60,88	391,97	452,85	16,72	2,79	22,03	20
15:10	149,71	37,27	186,98	224,25	16,24	3,185		
15:20	227,49	46,18	273,67	319,85	16,04	2,754		
15:30	233,21	53,12	286,33	339,45	15,87	3,113		
15:40	163,75	40,25	204	244,25	16	2,888		
15:50	37,81	27,37	65,18	92,55	15,36	3,203		
16:00	88,11	32,22	120,33	152,55	15,13	2,763	21,42	20
16:10	76,42	41,99	118,41	160,40	15,39	3,383		
16:20	45,69	63,93	109,62	173,55	15,44	2,986		
16:30	35,8	104	139,8	182,20	15,46	2,46		
16:40	31,24	60,11	91,35	116,70	15,09	3,376		
16:50	21,95	53,4	75,35	94,85	14,8	2,574		
17:00	11,26	37,06	48,32	75,38	14,55	2,704	19,12	20

Table E- 6: Measured data on 9 June 2014

Local Time	Meteorological factors							
	Solar radiation (beam) I_b [W/m^2]	Solar radiation (diffuse) I_d [W/m^2]	Solar radiation (total horizontal) I_h [W/m^2]	Solar radiation (total inclined) I_T [W/m^2]	Air temp [°C]	Wind speed [m/s]	Basin temp [°C]	Distillate output [ml]
9:00	54,59	19,28	73,87	219,45	8,6	3,667	12,92	0
9:10	21,961	6,759	28,72	77,36	8,55	2,616		
9:20	31,76	9,17	40,93	103,39	8,6	1,801		
9:30	35,135	11,88	47,015	110,46	9,19	1,805		
9:40	78,03	25,02	103,05	233,67	10,13	3,662		
9:50	76,29	27,96	104,25	224,69	9,18	6,765		
10:00	107,59	26,21	133,8	294,72	8,03	6,263	15,01	0
10:10	119,69	40,61	160,3	332,86	8,33	4,054		
10:20	141,83	34,77	176,6	369,60	8,65	2,526		
10:30	90,19	33,16	123,35	246,90	8,76	2,351		
10:40	104,77	37,13	141,9	279,70	9,06	1,625		
10:50	185,63	42,92	228,55	454,23	9,7	1,729		
11:00	279,5	51,75	331,25	657,97	12,18	1,395	19,37	0
11:10	83,08	25,22	108,3	207,95	10,95	3,517		
11:20	23,53	9,85	33,38	62,72	9,79	4,987		
11:30	19,471	6,779	26,25	49,29	8,9	3,455		
11:40	62,56	22,59	85,15	157,21	8,87	1,769		
11:50	168,35	48,05	216,4	397,36	9,56	1,056		
12:00	93,22	32,48	125,7	228,03	9,79	1,785	21,5	0
12:10	93,72	31,43	125,15	226,00	9,53	2,346		
12:20	159,41	43,99	203,4	366,99	9,9	1,614		
12:30	289,73	56,47	346,2	636,24	10,98	0,795		
12:40	155,69	44,91	200,6	358,12	11,19	0,881		
12:50	21,1	8,49	29,59	52,50	9,44	3,785		
13:00	30,155	9,52	39,675	70,87	8,58	2,158	23,51	20
13:10	293,95	76,75	370,7	663,64	9,81	1,334		
13:20	170,64	55,91	226,55	399,15	10,16	2,091		
13:30	75,46	30,34	105,8	186,27	9,96	2,249		
13:40	60,425	19,44	79,865	142,63	9,34	2,392		
13:50	63,76	24,49	88,25	156,78	8,97	2,4		
14:00	127,07	45,28	172,35	306,57	9,24	2,186	22,09	30
14:10	197,63	55,17	252,8	455,73	10,09	1,878		
14:20	184,33	41,07	225,4	421,53	10,49	1,061		
14:30	82,28	33,17	115,45	208,56	10,52	2,133		
14:40	31,64	14,98	46,62	80,22	10,11	2,803		
14:50	82,05	24,45	106,5	199,04	10,09	1,236		
15:00	157,33	38,07	195,4	370,84	10,51	2,233	21,98	30
15:10	54,415	23,95	78,365	139,94	10,05	2,291		
15:20	77,05	34,4	111,45	201,35	10,21	1,903		
15:30	35,97	18,8	54,77	98,56	10,04	1,96		
15:40	29,055	10,45	39,505	78,26	9,81	2		
15:50	40,77	13,16	53,93	109,11	9,46	1,43		
16:00	81,42	26,28	107,7	220,13	9,74	0,528	21,3	30
16:10	80,41	28,89	109,3	219,77	10,12	0,704		
16:20	68,99	23,86	92,85	191,95	10,44	0,788		
16:30	100,7	84,6	185,3	368,01	10,79	0,43		
16:40	71,76	41,44	113,2	235,44	10,55	1,714		
16:50	15,005	6,52	21,525	47,70	9,85	1,66		
17:00	7,402	4,468	11,87	24,89	9,68	1,262	20,5	30

Table E- 7: Measured data on 10 June 2014

Local Time	Meteorological factors							
	Solar radiation (beam) I_b [W/m^2]	Solar radiation (diffuse) I_d [W/m^2]	Solar radiation (total horizontal) I_h [W/m^2]	Solar radiation (total inclined) I_T [W/m^2]	Air temp [°C]	Wind speed [m/s]	Basin temp [°C]	Distillate output [ml]
9:00	51,26	20,67	71,93	212,42	7,174	3,971	11,36	0
9:10	91,31	27,94	119,25	328,51	7,617	3,814		
9:20	160,85	44,65	205,5	497,61	8,28	3,354		
9:30	160,12	38,88	199	477,18	8,89	2,896		
9:40	111,41	37,39	148,8	338,26	8,77	3,595		
9:50	124,6	40,4	165	362,33	9,1	2,973		
10:00	130,64	40,26	170,9	366,55	9,24	2,619	15,24	20
10:10	151,96	47,04	199	415,45	9,48	2,482		
10:20	277,77	59,28	337,05	704,82	10,25	3,251		
10:30	397,26	67,59	464,85	953,73	11	3,342		
10:40	384,79	64,11	448,9	912,67	10,97	4,02		
10:50	246,1	52,45	298,55	595,26	10,84	3,737		
11:00	349,3	58,7	408	811,53	11,31	3,689	20,34	40
11:10	353,01	53,89	406,9	804,73	11,74	2,924		
11:20	433,04	44,91	477,95	943,25	11,96	3,018		
11:30	319,27	39,93	359,2	702,19	12,16	3,044		
11:40	279,41	37,89	317,3	613,57	11,7	3,461		
11:50	483,09	49,61	532,7	1017,83	12,08	3,982		
12:00	474,28	35,17	509,45	968,11	12,76	3,236	25,63	60
12:10	492,32	33,83	526,15	993,26	12,9	3,165		
12:20	491,61	34,34	525,95	985,92	13,02	3,1		
12:30	495,68	36,17	531,85	990,58	12,82	3,531		
12:40	493,19	40,61	533,8	987,44	13,23	3,025		
12:50	478,71	40,44	519,15	956,85	13,35	3,14		
13:00	500,34	40,71	541,05	995,66	13,59	3,188	28,46	90
13:10	516,98	45,12	562,1	1031,60	13,8	3,151		
13:20	536,36	53,59	589,95	1085,76	13,97	3,393		
13:30	396,45	48,8	445,25	819,28	13,64	3,026		
13:40	422,77	46,33	469,1	867,43	13,95	3,28		
13:50	380,85	44,35	425,2	788,86	13,81	3,001		
14:00	273,38	43,52	316,9	589,79	13,65	2,7	30,86	125
14:10	271,18	53,67	324,85	602,73	13,79	2,281		
14:20	160,25	48,85	209,1	379,00	13,32	2,827		
14:30	178,42	49,83	228,25	418,17	13,19	3,004		
14:40	385,33	63,57	448,9	850,43	14,18	2,076		
14:50	503,55	65,8	569,35	1094,19	14,53	2,599		
15:00	431,45	64,65	496,1	959,49	14,82	2,522	29.55	155
15:10	356,11	54,29	410,4	805,86	14,52	2,953		
15:20	325,4	44,1	369,5	740,54	14,92	2,649		
15:30	303,57	36,43	340	695,51	14,92	2,676		
15:40	278,85	32,6	311,45	648,67	14,64	2,964		
15:50	253,75	31,05	284,8	603,21	14,56	2,438		
16:00	227,95	30,8	258,75	556,76	14,15	2,322	24,12	180
16:10	177,84	53,41	231,25	476,35	13,93	2,005		
16:20	58,55	144,9	203,45	410,89	14,56	1,399		
16:30	9	168,1	177,1	376,30	14,35	1,393		
16:40	7,55	142	149,55	332,59	13,93	1,781		
16:50	6,4	119	125,4	297,91	14,13	0,859		
17:00	6,05	93,1	99,15	248,15	14,25	1,626	22,42	200

Table E- 8: Measured data on 11 June 2014

Local Time	Meteorological factors							
	Solar radiation (beam) I_b [W/m^2]	Solar radiation (diffuse) I_d [W/m^2]	Solar radiation (total horizontal) I_h [W/m^2]	Solar radiation (total inclined) I_T [W/m^2]	Air temp [°C]	Wind speed [m/s]	Basin temp [°C]	Distillate output [ml]
9:00	68,17	13,8	81,97	255,06	7,477	1,588	12,46	0
9:10	88,075	14,73	102,805	296,96	8,09	1,463		
9:20	125,77	15,48	141,25	385,29	8,33	1,284		
9:30	129,835	16,17	146,005	378,10	8,96	1,509		
9:40	157,14	16,91	174,05	434,42	9,62	1,196		
9:50	203,66	17,74	221,4	535,92	10,28	1,464		
10:00	181,93	18,42	200,35	467,92	10,86	1,469	15,84	25
10:10	177,56	19,3	196,86	446,46	11,5	1,523		
10:20	198,63	20,17	218,8	485,04	12,55	1,329		
10:30	306,72	20,88	327,6	711,36	13,39	1,17		
10:40	392,83	21,97	414,8	885,11	14	1,325		
10:50	404,99	22,86	427,85	895,89	14,74	1,109		
11:00	415,68	23,72	439,4	904,42	15,09	1,465	20,67	50
11:10	427,19	24,81	452	915,82	15,56	1,27		
11:20	438,94	25,86	464,8	928,38	16,24	1,19		
11:30	450,21	26,84	477,05	940,57	17,08	1,11		
11:40	462,32	27,58	489,9	954,80	16,61	1,311		
11:50	475,32	28,63	503,95	971,89	16,42	1,641		
12:00	484,89	29,46	514,35	982,74	16,09	2,642	26,3	70
12:10	492,9	30,6	523,5	991,88	16,61	1,753		
12:20	496,82	31,73	528,55	994,16	16,42	1,963		
12:30	497,88	32,42	530,3	991,50	16,74	1,265		
12:40	498,75	33,3	532,05	989,90	18,8	0,516		
12:50	498,24	33,81	532,05	986,34	18,27	0,606		
13:00	495,38	33,82	529,2	978,87	19,04	0,556		
13:10	494,14	34,41	528,55	976,41	19,77	0,903	28,41	120
13:20	492,02	34,78	526,8	973,15	19,28	1,433		
13:30	488,45	35,1	523,55	968,24	19,09	2,008		
13:40	482,39	35,56	517,95	959,96	18,96	2,063		
13:50	474,91	35,74	510,65	949,67	18,64	2,389		
14:00	465,31	35,74	501,05	936,10	18,18	2,301	31,56	155
14:10	453,45	35,65	489,1	918,97	18,82	1,768		
14:20	440,48	34,97	475,45	899,67	18,94	1,871		
14:30	424,48	34,62	459,1	875,59	19,05	1,393		
14:40	408,09	33,81	441,9	850,60	19,49	1,145		
14:50	391,11	32,94	424,05	829,91	18,69	1,568		
15:00	372,32	32,08	404,4	800,39	18,84	1,942	30,72	195
15:10	353,2	31,2	384,4	770,22	18,7	1,877		
15:20	332,42	30,18	362,6	736,38	18,17	1,295		
15:30	311,6	29,45	341,05	702,60	18,17	2,245		
15:40	287,48	28,62	316,1	661,27	17,83	1,172		
15:50	263,09	27,71	290,8	620,26	17,61	1,704		
16:00	237,14	27,51	264,65	574,21	17,34	1,646	27,41	230
16:10	182,81	55,49	238,3	490,51	17,13	1,948		
16:20	47,65	164,1	211,75	448,60	16,92	1,67		
16:30	31,25	187,3	184,55	502,90	17,13	1,378		
16:40	28,25	159,6	157,6	455,61	17	0,956		
16:50	24,32	131,2	130,4	398,18	16,96	1,141		
17:00	22,45	104,8	104,65	348,41	16,66	1,365	22,69	260

Table E- 9: Measured data on 12 June 2014

Local Time	Meteorological factors							
	Solar radiation (beam) I_b [W/m^2]	Solar radiation (diffuse) I_d [W/m^2]	Solar radiation (total horizontal) I_h [W/m^2]	Solar radiation (total inclined) I_T [W/m^2]	Air temp [°C]	Wind speed [m/s]	Basin temp [°C]	Distillate output [ml]
9:00	25,835	9,09	34,925	107,61	9,7	1,525	13,57	0
9:10	28,295	10,3	38,595	106,00	10,14	1,916		
9:20	35,395	12,49	47,885	122,05	10,89	1,903		
9:30	49,555	17,48	67,035	161,12	13,57	2,095		
9:40	59,505	21,47	80,975	185,18	15,89	2,563		
9:50	66,76	23,84	90,6	199,50	16,47	2,503		
10:00	78,19	27,36	105,55	225,48	17,2	1,746	15,95	30
10:10	71,23	27,17	98,4	202,53	18,31	1,542		
10:20	77,18	29,92	107,1	214,88	18,97	2,124		
10:30	90,87	33,03	123,9	251,48	18,81	1,478		
10:40	96,43	34,52	130,95	261,56	19,25	2,12		
10:50	103,17	36,48	139,65	274,78	20,22	2,895		
11:00	106,86	36,94	143,8	279,49	20,83	2,649	21,78	55
11:10	112,61	39,09	151,7	290,86	21,11	2,688		
11:20	122,88	42,87	165,75	313,66	21,28	2,572		
11:30	144,26	49,04	193,3	361,77	21,37	2,817		
11:40	154,31	51,99	206,3	382,35	21,58	2,738		
11:50	130,92	46,43	177,35	325,70	21,98	2,6		
12:00	148,38	52,37	200,75	365,34	22,4	2,359	27,4	95
12:10	163,8	55,15	218,95	396,51	22,87	2,403		
12:20	151,63	53,37	205	368,56	23,16	2,103		
12:30	145,78	53,47	199,25	355,82	23,26	2,085		
12:40	156,96	56,49	213,45	379,79	23,28	2,886		
12:50	221,19	63,61	284,8	509,69	23,14	2,875		
13:00	230,56	64,49	295,05	527,56	23,13	3,11	29,52	130
13:10	215,36	64,49	279,85	498,42	23,52	2,454		
13:20	170,82	55,68	226,5	402,79	24,01	3,024		
13:30	125,46	46,04	171,5	304,45	24,63	2,836		
13:40	78,89	30,91	109,8	195,60	25,4	3,245		
13:50	61,13	22,12	83,25	149,66	25,99	2,095		
14:00	57,88	19,52	77,4	140,23	25,83	3,055	32,67	175
14:10	74,04	25,11	99,15	180,22	26,27	3,558		
14:20	80,48	31,07	111,55	202,38	26,16	3,341		
14:30	119,49	37,21	156,7	288,61	26,73	2,119		
14:40	114,15	40	154,15	284,24	26,84	1,381		
14:50	87,6	31,8	119,4	222,31	26,46	1,217		
15:00	73,31	25,74	99,05	186,97	26,86	1,55	31,83	215
15:10	85,24	27,36	112,6	215,74	27,13	0,963		
15:20	101,71	32,14	133,85	259,27	25,79	2,257		
15:30	105,05	32,9	137,95	270,77	25,12	2,74		
15:40	102,49	31,76	134,25	267,61	24,99	3,554		
15:50	93,92	28,78	122,7	249,04	24,71	3,08		
16:00	87,31	26,39	113,7	235,40	24,9	2,458	28,31	250
16:10	77,58	24,12	101,7	214,66	24,72	2,371		
16:20	66,03	20,57	86,6	187,38	24,34	1,791		
16:30	56,455	17,66	74,115	164,93	23,57	1,93		
16:40	47,655	15,14	62,795	140,48	22,82	2,948		
16:50	38,865	12,71	51,575	119,71	21,49	2,618		
17:00	32,115	10,25	42,365	103,54	20,64	2,021	23,8	280

Table E- 10: Measured data on 13 June 2014

Local Time	Meteorological factors							
	Solar radiation (beam) I_b [W/m^2]	Solar radiation (diffuse) I_d [W/m^2]	Solar radiation (total horizontal) I_h [W/m^2]	Solar radiation (total inclined) I_T [W/m^2]	Air temp [°C]	Wind speed [m/s]	Basin temp [°C]	Distillate output [ml]
9:00	25,835	9,09	34,925	110,02	12,62	2,979	15,26	20
9:10	28,295	10,3	38,595	107,70	12,74	2,029		
9:20	35,395	12,49	47,885	123,56	12,78	3,02		
9:30	49,555	17,48	67,035	162,75	12,8	3,349		
9:40	59,505	21,47	80,975	186,74	12,91	3,293		
9:50	66,76	23,84	90,6	200,94	13,02	3,777		
10:00	78,19	27,36	105,55	226,92	13,08	4,099	17,64	50
10:10	71,23	27,17	98,4	203,67	13,34	2,832		
10:20	77,18	29,92	107,1	215,98	13,61	2,691		
10:30	90,87	33,03	123,9	252,55	13,75	3,007		
10:40	96,43	34,52	130,95	262,61	13,97	2,835		
10:50	103,17	36,48	139,65	275,82	14,26	1,864		
11:00	106,86	36,94	143,8	280,51	14,57	2,175	23,47	75
11:10	112,61	39,09	151,7	291,87	14,59	2,198		
11:20	122,88	42,87	165,75	314,69	14,67	2,484		
11:30	144,26	49,04	193,3	362,91	14,82	2,599		
11:40	154,31	51,99	206,3	383,52	15,31	2,079		
11:50	130,92	46,43	177,35	326,65	15,61	2,3		
12:00	148,38	52,37	200,75	366,36	15,71	2,12	29,09	115
12:10	163,8	55,15	218,95	397,59	15,8	2,18		
12:20	151,63	53,37	205	369,51	15,98	2,364		
12:30	145,78	53,47	199,25	356,70	16,06	1,521		
12:40	156,96	56,49	213,45	380,70	15,93	2,035		
12:50	221,19	63,61	284,8	510,88	16,2	1,909		
13:00	230,56	64,49	295,05	528,75	16,85	1,885	31,21	150
13:10	215,36	64,49	279,85	499,48	16,54	2,439		
13:20	170,82	55,68	226,5	403,60	16,78	1,863		
13:30	125,46	46,04	171,5	305,03	16,9	1,928		
13:40	78,89	30,91	109,8	195,96	16,84	2,08		
13:50	61,13	22,12	83,25	149,92	16,66	1,891		
14:00	57,88	19,52	77,4	140,45	16,35	2,122	34,36	195
14:10	74,04	25,11	99,15	180,49	16,26	1,608		
14:20	80,48	31,07	111,55	202,67	16,27	2,456		
14:30	119,49	37,21	156,7	289,00	16,33	2,27		
14:40	114,15	40	154,15	284,60	16,42	2,034		
14:50	87,6	31,8	119,4	222,57	16,52	1,886		
15:00	73,31	25,74	99,05	187,17	16,44	1,436	33,52	235
15:10	85,24	27,36	112,6	215,96	16,68	1,234		
15:20	101,71	32,14	133,85	259,52	16,91	1,094		
15:30	105,05	32,9	137,95	271,01	16,81	1,676		
15:40	102,49	31,76	134,25	267,82	16,63	1,598		
15:50	93,92	28,78	122,7	249,21	16,55	1,665		
16:00	87,31	26,39	113,7	235,54	16,45	2,065	30	270
16:10	77,58	24,12	101,7	214,76	16,32	1,451		
16:20	66,03	20,57	86,6	187,44	16,23	1,254		
16:30	56,455	17,66	74,115	164,95	16,21	1,131		
16:40	47,655	15,14	62,795	140,42	16,05	0,884		
16:50	38,865	12,71	51,575	119,61	16,02	0,939		
17:00	32,115	10,25	42,365	103,38	15,98	0,822	25,49	300

Table E- 11: Measured data on 17 June 2014

Local Time	Meteorological factors							
	Solar radiation (beam) I_b [W/m^2]	Solar radiation (diffuse) I_d [W/m^2]	Solar radiation (total horizontal) I_h [W/m^2]	Solar radiation (total inclined) I_T [W/m^2]	Air temp [°C]	Wind speed [m/s]	Basin temp [°C]	Distillate output [ml]
9:00	65,16	13,34	78,5	256,81	9,59	1,004	16,61	20
9:10	80,33	14,28	94,61	283,20	10,86	0,502		
9:20	105,73	15,16	120,89	336,64	12,55	0		
9:30	121,34	16,07	137,41	364,01	13,67	0		
9:40	132,94	16,85	149,79	380,03	14,87	0		
9:50	180,7	17,85	198,55	488,94	15,36	0		
10:00	169,62	18,68	188,3	446,91	15,56	0	18,99	50
10:10	167,065	19,53	186,595	429,56	15,35	0,148		
10:20	177,195	20,52	197,715	443,88	15,54	0,114		
10:30	233,65	21,4	255,05	561,50	16,91	0,232		
10:40	367,12	22,28	389,4	842,20	16,59	0,793		
10:50	397,41	23,29	420,7	892,85	18,15	0,798		
11:00	411,86	24,29	436,15	909,38	16,46	1,414	24,82	80
11:10	415,42	25,18	440,6	903,73	17,38	1,095		
11:20	427,28	25,97	453,25	916,24	16,94	1,521		
11:30	439,29	26,86	466,15	929,88	17,16	1,577		
11:40	450,26	27,69	477,95	942,04	17,81	1,088		
11:50	455,7	28,6	484,3	944,12	18,69	1,37		
12:00	464,58	29,62	494,2	954,06	18,11	1,568	30,44	120
12:10	473,06	30,34	503,4	963,66	18,34	1,539		
12:20	478,96	31,49	510,45	969,78	18,35	1,38		
12:30	480,68	32,32	513	968,47	18,81	1,737		
12:40	480,45	33,1	513,55	964,49	18,11	1,705		
12:50	477,55	33,8	511,35	956,48	18,46	1,697		
13:00	477,54	33,81	511,35	954,16	19,3	1,78	32,56	150
13:10	484,09	34,21	518,3	965,90	18,74	2,253		
13:20	479,25	34,5	513,75	957,10	18,5	2,699		
13:30	473,73	34,77	508,5	948,10	18,4	2,671		
13:40	467,63	34,77	502,4	938,72	18,62	2,288		
13:50	459,02	34,83	493,85	925,68	18,71	2,469		
14:00	448,6	34,85	483,45	910,07	18,19	2,726	35,71	200
14:10	436,57	34,78	471,35	892,10	18,33	2,887		
14:20	423,58	34,77	458,35	873,08	18,57	2,948		
14:30	407,25	34,05	441,3	847,22	18,84	2,705		
14:40	390,5	33,55	424,05	826,70	18,81	2,623		
14:50	373,71	32,79	406,5	800,39	18,44	3,2		
15:00	356,13	32,02	388,15	772,68	18,37	3,061	34,87	240
15:10	336,92	31,03	367,95	741,42	18,5	2,911		
15:20	316,28	30,07	346,35	707,15	17,76	3,526		
15:30	294,12	29,28	323,4	669,61	17,78	2,688		
15:40	270,58	28,67	299,25	628,81	17,67	2,607		
15:50	247,32	27,88	275,2	589,43	17,35	3,446		
16:00	221,98	27,92	249,9	543,93	17,42	2,899	31,35	275
16:10	165,55	58,6	224,15	456,39	17,21	2,648		
16:20	37,85	161,4	199,25	417,17	17,04	2,673		
16:30	2,05	171,8	173,85	373,75	16,98	2,943		
16:40	3,2	144,9	148,1	332,82	16,84	2,632		
16:50	4,25	119	123,25	291,49	16,49	3,07		
17:00	4,6	93,5	98,1	244,33	16,31	2,504	26,84	300

Table E- 12: Measured data on 18 June 2014

Local Time	Meteorological factors							
	Solar radiation (beam) I_b [W/m^2]	Solar radiation (diffuse) I_d [W/m^2]	Solar radiation (total horizontal) I_h [W/m^2]	Solar radiation (total inclined) I_T [W/m^2]	Air temp [°C]	Wind speed [m/s]	Basin temp [°C]	Distillate output [ml]
9:00	32,37	10,95	43,32	135,96	12,3	4,022	17,54	0
9:10	41,39	16,97	58,36	160,09	12,47	2,934		
9:20	35,965	10,97	46,935	122,31	12,47	2,933		
9:30	37,835	13,48	51,315	123,58	12,53	2,607		
9:40	35,09	11,08	46,17	107,25	12,64	2,892		
9:50	36,37	11,45	47,82	106,78	12,82	3,311		
10:00	27,335	8,78	36,115	80,80	12,84	3,561	19,92	20
10:10	34,775	11,17	45,945	99,87	12,8	3,046		
10:20	42,8	11,8	54,6	116,98	13,06	1,724		
10:30	51,065	15,12	66,185	138,03	13,35	2,853		
10:40	53,795	17,84	71,635	145,51	13,37	3,706		
10:50	53,55	21,01	74,56	147,26	13,3	5,046		
11:00	52,11	27,87	79,98	144,79	13,11	4,442	25,75	60
11:10	101,82	33,18	135	260,94	13,1	2,701		
11:20	133	52	185	346,87	13,48	4,287		
11:30	182,75	45,35	228,1	435,23	13,82	4,272		
11:40	269,58	57,12	326,7	625,71	14,42	4,587		
11:50	157,92	44,18	202,1	376,44	14,57	4,851		
12:00	379,31	55,79	435,1	828,88	15,14	3,606	31,37	110
12:10	501,84	45,06	546,9	1043,62	15,61	5,265		
12:20	331,59	45,16	376,75	711,93	16,1	5,072		
12:30	102,8	43,05	145,85	259,95	15,8	3,824		
12:40	114,37	41,73	156,1	279,16	16,16	4,38		
12:50	89,39	31,86	121,25	217,06	16,56	6,204		
13:00	51,45	19,64	71,09	127,10	16,37	5,954	33,49	190
13:10	121,16	33,99	155,15	279,46	16,24	5,674		
13:20	109,24	38,46	147,7	263,31	16,45	6,489		
13:30	162,72	44,08	206,8	380,72	16,68	6,291		
13:40	149,23	40,97	190,2	343,42	17,01	5,619		
13:50	116,79	45,61	162,4	289,21	16,97	6,212		
14:00	58,88	22,17	81,05	146,21	16,61	7,42	34,64	260
14:10	56,095	20,16	76,255	138,61	15,05	7,005		
14:20	39,905	17,79	57,695	104,55	13,42	5,46		
14:30	24,28	9,62	33,9	62,37	13,26	5,359		
14:40	29,975	9,76	39,735	74,33	13,29	5,889		
14:50	54,095	21,54	75,635	140,83	13,18	6,946		
15:00	69,2	21,65	90,85	172,88	13,07	5,28	32,76	320
15:10	81,82	30,23	112,05	212,99	13,2	4,292		
15:20	29,415	13,86	43,275	78,33	13,3	2,727		
15:30	45,285	17,04	62,325	122,05	13,29	2,21		
15:40	51,455	19,14	70,595	140,19	13,26	2,192		
15:50	39,45	16,05	55,5	106,69	13,32	1,874		
16:00	41,075	13,42	54,495	113,25	13,26	1,641	30,39	370
16:10	16,888	7,602	24,49	48,39	13,15	1,91		
16:20	18,77	8,35	27,12	54,94	12,77	2,42		
16:30	20,514	7,251	27,765	59,33	12,68	2,236		
16:40	17,379	7,296	24,675	53,41	12,59	1,848		
16:50	10,76	4,885	15,645	34,81	12,46	2,528		
17:00	9,67	4,09	13,76	32,40	12,37	3,406	24,88	400

Table E- 13: Measured data on 19 June 2014

Local Time	Meteorological factors							
	Solar radiation (beam) I_b [W/m^2]	Solar radiation (diffuse) I_d [W/m^2]	Solar radiation (total horizontal) I_h [W/m^2]	Solar radiation (total inclined) I_T [W/m^2]	Air temp [°C]	Wind speed [m/s]	Basin temp [°C]	Distillate output [ml]
9:00	68,2	18,67	86,87	283,77	11,81	0,936	15,35	0
9:10	84,195	19,1	103,295	296,45	12,37	1,733		
9:20	106,26	20,58	126,84	344,35	12,93	1,786		
9:30	124,22	22,13	146,35	377,70	13,45	1,71		
9:40	134,595	22,23	156,825	388,65	14,02	1,688		
9:50	182,32	24,03	206,35	497,25	14,4	1,789		
10:00	197,1	39,8	236,9	534,78	15,29	1,255	17,43	18
10:10	195,22	38,28	233,5	515,17	15,75	1,277		
10:20	186,39	26,56	212,95	471,94	15,28	1,904		
10:30	240,41	26,09	266,5	583,14	14,96	1,914		
10:40	361,66	26,09	387,75	836,77	15,4	1,705		
10:50	395,32	26,73	422,05	891,60	15,61	2,526		
11:00	412,03	27,42	439,45	912,68	15,68	1,799	22,53	53
11:10	422,14	29,46	451,6	922,32	15,75	1,906		
11:20	433,66	31,74	465,4	936,01	14,97	2,123		
11:30	441,27	33,13	474,4	941,34	16	2,064		
11:40	450,66	36,59	487,25	953,86	15,1	2,326		
11:50	476,39	41,86	518,25	1007,22	15,06	2,781		
12:00	521,82	49,13	570,95	1096,20	15,25	2,707	27,45	95
12:10	427,3	51,55	478,85	907,63	15,53	2,381		
12:20	508,6	59,2	567,8	1067,10	15,97	1,027		
12:30	401,99	39,11	441,1	832,82	15,47	1,768		
12:40	100,44	17,66	118,1	222,70	14,1	2,001		
12:50	455,52	37,93	493,45	919,79	14,13	2,675		
13:00	451,42	38,88	490,3	911,17	14,63	2,885	29,30	165
13:10	346,98	34,32	381,3	712,87	14,67	2,345		
13:20	304,97	35,53	340,5	635,28	14,42	1,926		
13:30	507,14	50,41	557,55	1038,40	16,1	1,251		
13:40	524,52	53,33	577,85	1077,23	17,41	1,611		
13:50	469,44	45,31	514,75	965,92	16,98	1,64		
14:00	455,22	49,98	505,2	948,88	15,73	2,716	30,31	230
14:10	445,82	48,08	493,9	933,56	16,31	2,02		
14:20	431,5	52,15	483,65	916,63	16,5	2,444		
14:30	422,83	46,32	469,15	899,51	17,33	2,148		
14:40	414,73	41,37	456,1	885,08	17	2,771		
14:50	387,01	40,14	427,15	836,81	16,36	2,589		
15:00	369,82	40,63	410,45	811,62	16,46	2,152	28,67	280
15:10	343,68	38,57	382,25	765,10	15,58	3,155		
15:20	319,06	38,84	357,9	726,67	14,59	3,324		
15:30	210,03	33,62	243,65	499,59	14,35	3,28		
15:40	244,07	40,03	284,1	588,02	14,21	3,275		
15:50	101,96	27,24	129,2	264,84	13,82	2,393		
16:00	164,13	32,92	197,05	416,87	13,91	1,663	26,59	325
16:10	183,12	60,73	243,85	499,10	14,26	1,878		
16:20	71,45	114,1	185,55	357,70	13,83	2,163		
16:30	45,1	50,85	95,95	174,62	13,63	1,497		
16:40	33,745	36,82	70,565	131,15	13,39	2,036		
16:50	29,805	38,5	68,305	130,21	13,35	1,891		
17:00	34,945	18,64	53,585	123,12	13,28	1,521	21,77	350

Table E- 14: Measured data on 20 June 2014

Local Time	Meteorological factors							
	Solar radiation (beam) I_b [W/m^2]	Solar radiation (diffuse) I_d [W/m^2]	Solar radiation (total horizontal) I_h [W/m^2]	Solar radiation (total inclined) I_T [W/m^2]	Air temp [°C]	Wind speed [m/s]	Basin temp [°C]	Distillate output [ml]
9:00	29,105	10,14	39,245	123,59	9,83	2,492	18,68	0
9:10	37,53	13,55	51,08	142,83	9,98	2,422		
9:20	52,385	19,24	71,625	184,41	10,07	2,899		
9:30	62,47	23,48	85,95	207,39	10,52	2,987		
9:40	71,01	26,54	97,55	224,20	10,92	2,233		
9:50	83,93	30,42	114,35	253,39	11,08	2,563		
10:00	102,92	36,68	139,6	299,85	11,48	1,946	21,06	30
10:10	96,78	36,87	133,65	276,92	11,72	1,646		
10:20	77,19	30,56	107,75	216,70	11,45	2,776		
10:30	70,88	27,37	98,25	193,79	11,42	2,938		
10:40	70,25	27,6	97,85	189,03	11,42	2,86		
10:50	76,71	26,89	103,6	205,70	11,57	2,563		
11:00	92,03	32,27	124,3	242,70	11,88	1,707	26,89	70
11:10	117,11	41,99	159,1	304,98	12,1	1,913		
11:20	124,19	46,91	171,1	322,61	12,45	1,247		
11:30	127,54	46,21	173,75	325,25	12,63	1,515		
11:40	121,53	46,77	168,3	311,01	12,54	2,035		
11:50	128,73	50,17	178,9	327,25	12,82	1,513		
12:00	122,73	47,37	170,1	309,38	13,05	1,644	32,51	110
12:10	149,42	54,48	203,9	368,71	13,34	1,18		
12:20	197,76	63,14	260,9	471,13	13,63	1,411		
12:30	224,44	65,91	290,35	523,53	13,78	1,913		
12:40	276,99	65,86	342,85	629,24	13,96	2,513		
12:50	294,27	63,93	358,2	657,90	14,26	2,63		
13:00	271,84	64,81	336,65	615,32	14,81	1,739	34,63	200
13:10	195,22	62,63	257,85	458,92	14,62	1,779		
13:20	197,8	60,5	258,3	460,97	14,4	2,205		
13:30	184,35	59,7	244,05	434,92	14,9	1,113		
13:40	181,91	57,69	239,6	428,45	14,99	1,084		
13:50	158,97	55,18	214,15	382,68	14,79	1,535		
14:00	144,95	51,2	196,15	351,96	14,93	0,923	35,78	250
14:10	159	51,8	210,8	381,48	15,47	0,767		
14:20	174,79	52,06	226,85	414,64	15,2	1,229		
14:30	169,87	50,98	220,85	406,40	15,2	1,477		
14:40	145,54	46,96	192,5	356,11	15,95	0,61		
14:50	153,39	45,66	199,05	373,10	15,5	1,576		
15:00	162,88	44,77	207,65	394,72	15,58	1,217	33,9	330
15:10	158,61	43,54	202,15	388,65	15,28	1,255		
15:20	136,49	39,21	175,7	341,54	16,06	0,128		
15:30	120,81	34,89	155,7	307,09	15,77	0,584		
15:40	93,07	31,73	124,8	247,55	15,53	0,033		
15:50	77,26	28,39	105,65	212,12	15,53	0,274		
16:00	61,65	23,35	85	167,85	15,55	0,167	31,53	380
16:10	61,98	20,27	82,25	173,60	15,88	0,047		
16:20	52,1	16,65	68,75	149,06	15,78	0,541		
16:30	40,71	14,25	54,96	117,70	15,47	0,633		
16:40	30,055	10,87	40,925	90,21	15,22	1,005		
16:50	26,285	9,66	35,945	82,24	15,09	0,208		
17:00	25,545	8,5	34,045	82,70	15,04	0,101	26,02	400

Table E- 15: Measured data on 21 June 2014

Local Time	Meteorological factors							
	Solar radiation (beam) I_b [W/m^2]	Solar radiation (diffuse) I_d [W/m^2]	Solar radiation (total horizontal) I_h [W/m^2]	Solar radiation (total inclined) I_T [W/m^2]	Air temp [°C]	Wind speed [m/s]	Basin-Water temp [°C]	Distillate output [ml]
8:30	10.11	10,34	20.45	133,64	7,926	0,431	14,1	0
9:00	63,83	13,79	77,62	320,78	13,43	0	20,68	10
9:10	78	14,55	92,55	330,61	14,89	0		
9:20	99,46	15,43	114,89	369,02	15,9	0,016		
9:30	115,12	15,97	131,09	386,33	16,81	0,06		
9:40	123,18	16,5	139,68	383,10	17,02	0,122		
9:50	169,15	17,4	186,55	486,00	17,07	0,188		
10:00	153,095	18,28	171,375	422,63	17,31	0,482	29,14	41
10:10	150,58	19,34	169,92	400,79	18,33	0,891		
10:20	166,65	20,46	187,11	426,30	17,9	1,389		
10:30	227,14	21,21	248,35	552,19	17,58	1,692		
10:40	332.120	22,13	354.25	835,61	16,81	1,866		
10:50	369.360	22,76	392.12	921,93	16,53	1,644		
11:00	378.5	23,63	402.13	923,23	16,91	1,329	31,96	87
11:10	398.56	24,59	423.15	929,70	16,83	1,493		
11:20	423.940	25,29	449.23	937,42	17,92	1,1		
11:30	433.51	26,12	459.63	948,12	17,87	1,037		
11:40	459,68	27,17	486,85	956,30	17,66	1,239		
11:50	465,12	28,38	493,5	958,96	17,94	0,858		
12:00	469,2	29,45	498,65	960,02	18,46	1,173	42,3	152
12:10	473,4	30,6	504	962,63	17,87	1,498		
12:20	476,15	31,65	507,8	963,42	18,23	1,331		
12:30	478,86	32,79	511,65	965,34	18,43	1,119		
12:40	480,99	33,01	514	965,82	18,91	0,84		
12:50	485,9	33,75	519,65	973,32	18,94	0,614		
13:00	486,3	33,8	520,1	972,22	21,18	0,307	48,88	234
13:10	482,94	34,06	517	965,28	21,86	0,24		
13:20	479,04	34,51	513,55	958,54	20,47	0,278		
13:30	475,53	34,77	510,3	953,20	21,73	0,377		
13:40	469,63	34,77	504,4	943,86	22,22	0,453		
13:50	461,33	34,92	496,25	931,07	22,86	0,054		
14:00	450,58	34,97	485,55	914,33	20,61	0,324	43,24	313
14:10	437,13	34,77	471,9	892,85	21,09	0,376		
14:20	422,06	34,64	456,7	869,10	20,8	0,96		
14:30	408,63	33,97	442,6	848,42	20,81	0,448		
14:40	392,84	33,76	426,6	824,52	21,86	0,317		
14:50	371,91	32,94	404,85	790,14	22,38	0,298		
15:00	354,8	32,05	386,85	763,72	21,32	0,581	39,48	383
15:10	334,89	31,21	366,1	732,20	21,53	0,897		
15:20	313,36	30,24	343,6	697,48	20,83	1,28		
15:30	290,35	29,45	319,8	660,10	20,89	0,841		
15:40	269,7	28,7	298,4	627,85	20,69	1,052		
15:50	248,06	27,89	275,95	593,43	20,17	1,733		
16:00	223,58	28,12	251,7	554,10	19,15	2,778	38,54	448
16:10	171,67	55,58	227,25	499,42	18,27	2,053		
16:20	45,15	157	202,15	301,76	17,82	2,135		
16:30	3,9	173,5	177,4	203,31	17,53	1,96		
16:40	3,55	148	151,55	172,85	17,27	1,935		
16:50	4	122	126	143,76	17,02	1,891		
17:00	3,65	97	100,65	114,00	16,89	1,208	36,66	502

Table E- 16: Measured data on 24 June 2014

Local Time	Meteorological factors							
	Solar radiation (beam) I_b [W/m^2]	Solar radiation (diffuse) I_d [W/m^2]	Solar radiation (total horizontal) I_h [W/m^2]	Solar radiation (total inclined) I_T [W/m^2]	Air temp [°C]	Wind speed [m/s]	Basin temp [°C]	Distillate output [ml]
9:00	50,42	40,28	68,84	220,93	13,04	1,611	15,32	0
9:10	63,655	56,94	85,845	244,95	13,93	1,762		
9:20	84,08	72,67	110,9	293,12	14,29	1,546		
9:30	93,91	78,33	123,4	305,79	14,68	1,371		
9:40	111,57	102,9	143,7	338,05	14,82	1,402		
9:50	152,74	118,7	186,15	433,58	15,57	1,215		
10:00	181,01	135	217,8	493,73	16,74	1,018	32,86	11
10:10	163,1	137,6	196,85	434,97	18,62	0,168		
10:20	137,1	146,5	164,95	357,47	18,32	0,574		
10:30	186,32	176,7	217,9	469,17	19,52	0,048		
10:40	301,32	196,2	333,15	714,44	21,77	0,424		
10:50	343,14	201,8	373,55	788,42	22,38	1,715		
11:00	357,16	313,8	387,25	805,12	22,87	2,105	36,04	45
11:10	367,47	260,6	397,7	814,91	23,27	2,109		
11:20	388,31	179,9	420	848,59	23,88	2,44		
11:30	396,47	187	428,25	849,90	24,51	2,102		
11:40	408,12	239,1	440,3	863,87	24,3	2,066		
11:50	419,83	328,2	452,85	879,14	24,09	2,847		
12:00	426,48	282,6	460,15	884,85	23,93	3,194	47,7	95
12:10	430,29	401,5	464,55	885,82	24,32	2,573		
12:20	438,35	350	473,6	896,44	24,56	3,124		
12:30	444,78	172,7	480,85	904,56	24,51	4,084		
12:40	445,16	411,7	481,85	901,82	25,07	3,27		
12:50	445,16	549,1	482,45	899,37	25,17	4,331		
13:00	446,21	601,2	484,45	900,44	25,4	4,567	55,12	162
13:10	442,47	534,4	481,6	893,42	25,41	4,519		
13:20	376,73	552,6	412,95	771,62	25,69	4,285		
13:30	408	555	457,5	849,44	25,97	4,002		
13:40	355,28	487,3	410,95	762,41	26,05	4,571		
13:50	331,33	523,7	386,55	718,56	26,3	3,373		
14:00	339,34	523,2	394	735,99	25,98	3,895	48,76	200
14:10	388,73	478,4	445,15	836,92	26,83	3,949		
14:20	352,85	434,5	404,65	766,52	26,72	3,314		
14:30	481,02	410,2	546	1038,42	26,92	3,95		
14:40	392,69	420,8	440,55	848,46	26,9	4,306		
14:50	380,65	279,3	422,85	825,61	27,06	3,62		
15:00	367,98	170,1	422,05	826,20	27,18	4,197	41,52	305
15:10	330,25	147,1	380	753,00	28,09	3,872		
15:20	301,4	175	335	679,93	27,68	3,765		
15:30	278,22	334,2	309,9	640,04	27,25	3,655		
15:40	254,69	307,9	285,35	598,16	26,48	1,616		
15:50	230,8	279,9	260,55	554,84	25,42	2,476		
16:00	210,72	252,2	239,8	519,32	25,67	4,3	39,42	455
16:10	170,62	219,1	216,65	454,76	25,84	4,496		
16:20	63,6	210,3	192,7	376,52	25,82	4,88		
16:30	16,25	187,5	167,05	332,89	25,74	4,705		
16:40	15,05	155,5	141,95	294,40	25,23	4,722		
16:50	14,5	111,5	118	256,01	24,35	5,33		
17:00	13,2	75,74	93,5	211,84	23,21	4,79	35,12	530

Table E- 17: Measured data on 25 June 2014

Local Time	Meteorological factors							
	Solar radiation (beam) I_b [W/m^2]	Solar radiation (diffuse) I_d [W/m^2]	Solar radiation (total horizontal) I_h [W/m^2]	Solar radiation (total inclined) I_T [W/m^2]	Air temp [°C]	Wind speed [m/s]	Basin temp [°C]	Distillate output [ml]
9:00	1,455	40,28	41,735	170,72	14,96	2,313	18,33	0
9:10	1,71	56,94	58,65	197,10	15,09	2,153		
9:20	2,6	72,67	75,27	213,04	15,22	2,649		
9:30	3,185	78,33	81,515	184,72	15,26	2,254		
9:40	4,15	102,9	107,05	235,18	15,39	2,45		
9:50	5,6	118,7	124,3	250,76	15,62	2,416		
10:00	8,8	135	143,8	272,16	15,87	1,646	20,65	50
10:10	13,6	137,6	151,2	259,22	16,22	1,712		
10:20	13,8	146,5	160,3	257,08	16,19	2,255		
10:30	14,95	176,7	191,65	309,53	16,6	1,929		
10:40	6,55	196,2	202,75	313,87	16,76	1,991		
10:50	6,25	201,8	208,05	304,74	17,19	1,72		
11:00	1,55	312,25	313,8	544,97	17,85	2,146	26,33	90
11:10	5,05	260,6	265,65	393,74	18,19	2,289		
11:20	9,35	179,9	189,25	230,86	18,58	2,372		
11:30	10,5	187	197,5	237,39	18,79	2,655		
11:40	5,9	239,1	245	309,33	18,85	2,453		
11:50	4,25	328,2	332,45	468,75	19,06	3,068		
12:00	5,75	282,6	288,35	369,93	19,17	2,994	31,81	140
12:10	3,1	398,4	401,5	589,64	19,67	2,528		
12:20	0,05	350	350,05	470,11	19,85	3,58		
12:30	6,95	172,7	179,65	186,92	19,05	2,375		
12:40	3,1	411,7	414,8	586,02	19,52	2,973		
12:50	0,75	548,35	549,1	891,88	20,22	2,597		
13:00	2,75	598,45	601,2	1018,52	20,51	2,96	33,88	220
13:10	3,15	531,25	534,4	842,68	20,08	3,048		
13:20	3,05	549,55	552,6	887,45	20,93	2,535		
13:30	2,1	552,9	555	897,23	21,65	3,318		
13:40	1,8	487,3	489,1	743,08	21,52	2,736		
13:50	0,05	523,7	523,75	836,45	21,65	3,014		
14:00	0,3	522,9	523,2	848,03	21,33	3,144	35,00	290
14:10	1,15	478,4	479,55	754,30	21,27	3,227		
14:20	2,75	434,5	437,25	668,35	21,46	2,664		
14:30	2,9	410,2	413,1	628,90	21,06	3,239		
14:40	1,65	420,8	422,45	672,71	21,06	3,119		
14:50	4,35	279,3	283,65	379,58	20,62	3,053		
15:00	2,5	170,1	172,6	193,19	19,88	2,793	33,17	350
15:10	4,05	147,1	151,15	166,95	19,47	2,826		
15:20	2,4	175	177,4	214,68	19,31	2,701		
15:30	2,85	331,35	334,2	593,20	19,78	3,059		
15:40	1,9	306	307,9	558,68	20,09	2,256		
15:50	2,1	277,8	279,9	518,34	19,85	2,082		
16:00	2	250,2	252,2	478,75	19,88	2,321	30,86	400
16:10	2,55	216,55	219,1	420,32	19,48	2,5		
16:20	3,9	206,4	210,3	440,73	19,35	2,317		
16:30	4,05	183,45	187,5	416,63	19,3	1,882		
16:40	3,6	151,9	155,5	355,71	19,2	2,328		
16:50	2,45	109,05	111,5	242,97	18,8	2,431		
17:00	0,105	75,635	75,74	156,97	18,36	2,228	25,49	420

Table E- 18: Measured data on 26 June 2014

Local Time	Meteorological factors							
	Solar radiation (beam) I_b [W/m^2]	Solar radiation (diffuse) I_d [W/m^2]	Solar radiation (total horizontal) I_h [W/m^2]	Solar radiation (total inclined) I_T [W/m^2]	Air temp [°C]	Wind speed [m/s]	Basin temp [°C]	Distillate output [ml]
9:00	57,99	23,61	81,6	261,46	14,26	0,349	0,36	0
9:10	114,76	32,29	147,05	433,67	15,57	0,592		
9:20	104,32	37,33	141,65	372,34	14,71	1,119		
9:30	99,47	38,33	137,8	335,25	14,7	0,79		
9:40	103,31	28,74	132,05	313,05	14,58	1,2		
9:50	60,125	16,58	76,705	178,29	14,23	1,556		
10:00	140,75	35,5	176,25	393,39	14,59	1,18	10,36	10
10:10	148,22	35,68	183,9	401,61	15,17	1,117		
10:20	134,82	36,73	171,55	363,02	15,21	0,669		
10:30	140,97	36,28	177,25	369,30	15,7	0,252		
10:40	141,55	36,65	178,2	364,51	15,18	1,051		
10:50	182,24	46,71	228,95	459,12	16,05	0,904		
11:00	260,76	39,39	300,15	614,36	17,12	0,593	25,36	25
11:10	436,77	37,93	474,7	967,88	17,56	0,964		
11:20	371,47	32,83	404,3	814,90	18,53	0,093		
11:30	456,16	40,64	496,8	986,04	18,49	1,533		
11:40	206,01	51,24	257,25	485,44	17,83	2,308		
11:50	189,15	49,75	238,9	445,78	17,59	1,412		
12:00	134,12	53,63	187,75	339,81	17,16	2,901	40,36	40
12:10	538,14	70,91	609,05	1141,80	18,06	3,54		
12:20	495,2	46,95	542,15	1026,45	18,21	4,151		
12:30	498,4	47,9	546,3	1028,02	18,21	3,812		
12:40	440,82	48,48	489,3	914,63	18,37	3,311		
12:50	327,41	43,14	370,55	689,78	17,66	4,542		
13:00	491,14	42,91	534,05	990,44	18,17	4,536	60,36	60
13:10	488,51	37,59	526,1	977,09	18,16	4,547		
13:20	490,42	38,58	529	981,87	18,23	4,62		
13:30	511,08	47,27	558,35	1033,27	18,37	4,579		
13:40	427,51	49,34	476,85	886,78	18,5	4,362		
13:50	189,3	51,3	240,6	434,29	17,58	3,707		
14:00	186,57	54,93	241,5	435,66	17,03	4,46	80,36	80
14:10	206,17	52,63	258,8	480,31	16,86	4,191		
14:20	311,96	48,79	360,75	682,30	17,06	3,329		
14:30	142,51	37,09	179,6	333,00	16,15	3,695		
14:40	120,38	42,42	162,8	299,47	16,01	2,737		
14:50	194,02	47,03	241,05	461,75	16,44	3,54		
15:00	329,68	45,47	375,15	737,12	17,16	3,809	95,36	95
15:10	140,57	41,63	182,2	348,05	15,88	5,179		
15:20	85,14	36,86	122	222,37	15,55	4,425		
15:30	269,58	48,22	317,8	640,89	15,91	4,437		
15:40	178,31	33,89	212,2	437,42	15,6	4,026		
15:50	122,87	26,53	149,4	308,52	15,65	3,807		
16:00	255,08	45,52	300,6	633,98	16,12	3,943	110,36	110
16:10	176,47	40,18	216,65	460,57	15,98	4,537		
16:20	86,24	23,01	109,25	237,44	15,52	3,483		
16:30	40,3	9,73	50,03	113,41	14,68	3,511		
16:40	44,41	33,19	77,6	151,46	12,72	2,955		
16:50	31,745	16,03	47,775	104,38	12,82	2,832		
17:00	46,99	10,87	57,86	147,29	12,6	3,363	120,36	120

Table E- 19: Measured data on 27 June 2014

Local Time	Meteorological factors							
	Solar radiation (beam) I_b [W/m^2]	Solar radiation (diffuse) I_d [W/m^2]	Solar radiation (total horizontal) I_h [W/m^2]	Solar radiation (total inclined) I_T [W/m^2]	Air temp [°C]	Wind speed [m/s]	Basin temp [°C]	Distillate output [ml]
9:00	39,63	17,04	56,67	177,94	11,9	1,567	17,77	0
9:10	47,52	17,5	65,02	183,50	12,02	1,394		
9:20	60,67	21,43	82,1	213,75	12,1	1,767		
9:30	81,96	25,59	107,55	266,11	12,29	1,612		
9:40	95,38	29,97	125,35	294,54	12,59	0,949		
9:50	143,53	33,42	176,95	409,68	12,93	1,307		
10:00	181	30,15	211,15	485,12	13,55	1,337	19,56	10
10:10	129,3	29,5	158,8	349,22	13,42	1,49		
10:20	130,71	36,79	167,5	353,40	13,29	1,281		
10:30	152,69	41,36	194,05	401,61	13,51	1,346		
10:40	208,65	48,8	257,45	526,65	13,85	1,403		
10:50	213,66	47,24	260,9	527,16	14,2	1,754		
11:00	341,26	52,64	393,9	798,70	15,14	1,529	25,64	25
11:10	467,75	67,35	535,1	1065,31	15,58	2,131		
11:20	285,59	54,31	339,9	667,22	15,53	1,858		
11:30	270,14	49,26	319,4	623,23	15,26	2,085		
11:40	331,31	59,19	390,5	751,16	15,4	1,922		
11:50	242,91	58,04	300,95	569,00	15,73	0,828		
12:00	216,84	55,66	272,5	503,84	16,14	0,823	28,81	40
12:10	179,9	44,05	223,95	420,82	15,77	0,605		
12:20	317,87	52,88	370,75	695,60	16,18	0,577		
12:30	428,17	50,18	478,35	895,97	16,55	1,102		
12:40	588,42	57,13	645,55	1204,74	16,94	1,272		
12:50	565,71	52,04	617,75	1144,84	17,26	1,093		
13:00	505,46	42,44	547,9	1016,01	16,99	1,463	32,947	55
13:10	295,96	29,44	325,4	607,89	16,6	1,385		
13:20	528,54	42,41	570,95	1057,91	17,17	1,285		
13:30	487,74	40,66	528,4	979,70	18,33	1,057		
13:40	308,57	33,88	342,45	640,09	18,3	1,441		
13:50	223,44	41,41	264,85	493,00	17,99	0,792		
14:00	179,49	36,91	216,4	404,51	16,53	0,866	31,49	70
14:10	258,48	46,87	305,35	572,36	16,86	1,186		
14:20	466,3	57,5	523,8	986,79	18,67	1,275		
14:30	431,96	50,59	482,55	919,14	19,38	1,283		
14:40	255,2	36	291,2	562,48	19,76	0,678		
14:50	214,99	35,96	250,95	487,75	18,42	1,327		
15:00	350,54	50,96	401,5	785,17	19,06	1,664	26,5	90
15:10	216,61	51,54	268,15	515,76	18,61	1,224		
15:20	384,09	64,16	448,25	885,65	19,26	1,283		
15:30	378,74	64,66	443,4	885,04	18,9	1,665		
15:40	282,54	58,01	340,55	685,04	17,21	1,94		
15:50	255,95	45,35	301,3	625,34	16,79	1,866		
16:00	265,34	42,26	307,6	653,35	16,85	1,866	25,83	100
16:10	102,07	32,33	134,4	280,26	16,51	1,624		
16:20	98,77	64,33	163,1	316,83	16,15	1,253		
16:30	69,75	80,1	149,85	283,56	16,07	2,265		
16:40	45,98	57,12	103,1	194,24	15,89	2,417		
16:50	35,7	78,4	114,1	244,99	15,83	1,749		
17:00	39,58	56,57	96,15	216,44	15,76	1,708	21,81	110

Table E- 20: Measured data on 30 June 2014

Local Time	Meteorological factors							
	Solar radiation (beam) I_b [W/m^2]	Solar radiation (diffuse) I_d [W/m^2]	Solar radiation (total horizontal) I_h [W/m^2]	Solar radiation (total inclined) I_T [W/m^2]	Air temp [°C]	Wind speed [m/s]	Basin temp [°C]	Distillate output [ml]
9:00	62,52	13,94	76,46	246,88	12,91	1,147	18,8	0
9:10	80,975	14,97	95,945	285,30	12,35	1,534		
9:20	109,79	15,77	125,56	347,79	12,09	1,75		
9:30	134,87	16,73	151,6	401,08	12,63	1,504		
9:40	149,67	18,43	168,1	424,33	13,93	0,523		
9:50	199,41	21,64	221,05	538,15	13,68	1,386		
10:00	183,97	21,38	205,35	483,29	13,26	2,828	21,18	50
10:10	174,65	21,11	195,76	447,78	13,72	3,173		
10:20	188,575	22,83	211,405	471,30	15,16	1,868		
10:30	249,13	24,87	274	599,68	15,25	2,595		
10:40	392,44	26,71	419,15	899,98	16,01	2,253		
10:50	438,29	34,16	472,45	993,47	16,6	2,59		
11:00	236,3	28,95	265,25	546,87	16,97	1,707	27,01	90
11:10	377,47	29,53	407	831,12	17,88	1,874		
11:20	424,04	32,91	456,95	914,82	18,61	1,644		
11:30	455,41	38,84	494,25	978,72	19,33	1,526		
11:40	434,59	35,16	469,75	916,49	19,31	1,595		
11:50	468,99	32,96	501,95	971,57	20,39	1,142		
12:00	466,17	32,33	498,5	956,03	20,82	1,243	32,63	140
12:10	470,86	33,49	504,35	958,69	20,25	2,034		
12:20	475,63	35,27	510,9	963,35	21,14	1,568		
12:30	455,35	39,3	494,65	924,34	21,79	1,199		
12:40	470,57	44,43	515	962,02	22,08	1,688		
12:50	479,05	47,75	526,8	978,92	22,36	1,877		
13:00	420,27	42,68	462,95	859,32	22,22	2,09	34,75	220
13:10	480,75	41,4	522,15	963,25	22,37	2,229		
13:20	452	38,95	490,95	905,79	22,39	2,037		
13:30	482,85	40,75	523,6	966,98	22,61	2,345		
13:40	469,91	40,44	510,35	944,23	23	2,154		
13:50	436,28	37,67	473,95	880,05	23,31	1,747		
14:00	442,78	37,17	479,95	895,59	22,52	2,39	35,9	290
14:10	454,88	37,67	492,55	924,35	22,5	2,358		
14:20	438,7	36,65	475,35	898,06	22,44	2,173		
14:30	396,63	33,97	430,6	819,90	21,85	2,322		
14:40	404,83	35,12	439,95	850,40	21,95	2,098		
14:50	393,01	34,79	427,8	834,83	21,38	3,106		
15:00	366,73	33,42	400,15	789,37	21,28	3,077	34,02	350
15:10	346,24	32,81	379,05	756,35	22,44	1,989		
15:20	318,85	33,35	352,2	710,44	21,57	2,566		
15:30	291,78	35,37	327,15	668,36	21,97	2,536		
15:40	271,77	36,23	308	636,90	21,94	2,468		
15:50	267,37	39,38	306,75	641,14	21,67	2,263		
16:00	252,15	40,3	292,45	619,06	21,52	2,62	31,65	400
16:10	195,11	44,24	239,35	504,47	21,04	2,763		
16:20	111	108	219	416,99	20,56	2,806		
16:30	34,35	85	119,35	210,05	20,13	2,293		
16:40	40,9	68,5	109,4	204,64	19,38	2,823		
16:50	43,6	70,65	114,25	237,89	19,02	2,71		
17:00	33,5	83,7	117,2	293,14	19,08	2,067	26,14	430

Table E- 21: Measurement and derived data for 18 November 2014

Local Time	Meteorological factors						Solar still temperatures						Hourly distillate output			Efficiency
	Solar radiation (beam) I_b [W/m²]	Solar radiation (diffuse) I_d [W/m²]	Solar radiation (total horizontal) I_h [W/m²]	Solar radiation (total inclined) I_T [W/m²]	Air temp [°C]	Wind speed [m/s]	Outer cover temp [°C]	Inner cover temp [°C]	Vapour temp [°C]	Basin temp [°C]	Water temp [°C]	Condenser temp [°C]	Inner cover [ml]	External condenser [ml]	Total [ml]	Instantaneous [%]
7:00	191	29,5	220,5	199,76	16,62	0,911	20,93	17,32	17,62	17,36	17,62	7,747	0	0	0	0
7:15	238,315	34,685	273	251,78	16,3	1,478	20,46	17,4	18,05	18,1	18,42	9,2	-	-	-	-
7:30	287	40,2	327,2	305,64	17,43	0,948	20,94	17,53	19,03	18,86	19,24	11,26	-	-	-	-
7:45	330	51,7	381,7	360,08	17,51	1,321	21,37	17,54	21,53	19,68	20,07	12,81	-	-	-	-
8:00	376	57,3	433,3	412,04	17,97	2,406	21,56	17,55	21,62	20,51	20,9	15,69	0	0	0	0
8:15	428	63,7	491,7	470,56	18,64	2,268	22,05	17,63	21,73	21,66	21,85	16,63	-	-	-	-
8:30	471	74,6	545,6	525,04	18,92	2,448	22,44	18,61	21,76	23,08	23,02	18,73	-	-	-	-
8:45	518	80,5	598,5	578,69	19,35	2,821	23,08	19,62	23,15	25,03	24,47	20,77	-	-	-	-
9:00	568,2	86,2	654,4	635,40	19,99	3,448	23,22	20,87	24,85	27,63	26,31	22,93	0	20	20	2,01
9:15	603,1	92,8	695,9	677,96	20,63	2,337	23,64	22,69	27,36	31,03	28,93	22,04	-	-	-	-
9:30	639,3	98,6	737,9	728,89	21,23	2,241	23,75	25,74	30,16	33,07	31,29	23,32	-	-	-	-
9:45	675,6	104,2	779,8	784,68	21,96	2,193	24,34	29,12	32,69	36,04	33,4	24,56	-	-	-	-
10:00	708,13	110,87	819	823,56	22,36	1,849	25,1	32,39	35,85	40,06	36,33	25,06	20	100	120	7,69
10:15	735,54	116,46	852	860,28	22,67	3,392	26,19	35,65	38,97	44,22	39,95	27,37	-	-	-	-
10:30	781,83	122,17	904	916,63	22,97	2,808	26,37	38,57	41,92	48,29	44,42	27,36	-	-	-	-
10:45	737,85	133,15	871	886,47	23,56	2,479	26,46	41,58	45,36	52,5	48,87	27,49	-	-	-	-
11:00	790,7	134,3	925	944,45	23,91	2,704	26,89	44,43	48,61	55,92	52,38	28,04	75	300	375	16,89
11:15	827,25	135,75	963	985,60	23,96	3,533	27,96	47,65	51,55	59,13	55,79	29,56	-	-	-	-
11:30	852,99	136,01	989	1014,35	24,25	2,908	28,02	50,51	54,52	61,41	58,49	29,32	-	-	-	-
11:45	794,81	142,19	937	962,93	24,59	3,425	28,25	51,4	56,47	62,43	60,25	30,56	-	-	-	-

12:00	771,23	148,77	920	946,67	24,88	4,025	28,49	52,59	58,08	64,05	62	30,95	200	500	700	21,27
12:15	857,13	159,87	1017	1047,21	24,99	3,454	28,57	53,93	59,53	65,39	63,79	30,13	-	-	-	-
12:30	805,4	160,6	966	995,25	25,33	2,862	28,78	55,93	61,6	67,01	65,92	29,73	-	-	-	-
12:45	862,04	168,96	1031	1062,13	25,47	3,683	28,83	57,8	63,38	69,03	67,94	30,13	-	-	-	-
13:00	726,98	153,02	880	906,66	25,68	3,967	27,81	57,87	63,12	68,61	68,22	31,07	300	800	1100	27,19
13:15	827,69	147,31	975	1003,73	25,54	4,042	27,8	58,64	64,02	67,82	67,11	31,15	-	-	-	-
13:30	886,48	136,52	1023	1052,16	25,14	4,25	27,53	59,29	63,07	68,15	66,65	31,67	-	-	-	-
13:45	766,44	135,56	902	926,61	24,78	4,842	27,35	58,86	64,19	67,84	67,35	32,62	-	-	-	-
14:00	861,69	134,31	996	1021,76	24,45	3,667	26,95	58,88	64,01	67,36	67,06	32,58	400	1200	1600	30,13
14:15	846,93	123,07	970	992,79	24,26	5,083	26,47	59,36	63,62	67,48	66,93	32,15	-	-	-	-
14:30	825,83	117,17	943	962,56	23,94	4,175	26,3	58,83	62,15	66,55	65,56	31,72	-	-	-	-
14:45	784,76	111,24	896	911,81	23,83	4,733	26,07	58,5	61,54	65,26	64,65	31,63	-	-	-	-
15:00	725,36	105,64	831	842,43	23,71	3,867	25,93	57,55	59,8	63,86	62,98	31,13	500	1400	1900	22.02
15:15	689,84	99,26	789,1	796,62	23,46	3,767	25,79	56,01	58,36	62,3	61,53	30,93	-	-	-	-
15:30	494,42	93,18	587,6	690,79	23,33	4,383	25,65	54,1	56,31	60,22	59,46	30,73	-	-	-	-
15:45	542,18	86,92	629,1	635,18	22,94	3,875	25,54	50,96	53,01	57,75	56,08	30,27	-	-	-	-
16:00	508,37	80,33	588,7	591,96	22,72	4,183	24,47	47,2	50,12	54,32	53,87	29,49	550	1500	2050	15,82
16:15	491,39	74,91	566,3	568,39	22,44	3,642	24,24	42,41	45,27	50,89	49,45	29,41	-	-	-	-
16:30	408,17	68,63	476,8	478,32	22,15	3,296	24,04	41,27	44,11	49,01	48,33	29,18	-	-	-	-
16:45	376,48	52,92	429,4	431,89	22,02	3,531	23,96	39,88	42,56	46,88	46,01	28,84	-	-	-	-
17:00	320,01	41,99	362	364,29	21,94	3,433	23,75	37,45	40,07	44,74	43,46	28,22	560	1580	2140	15,59
17:15	256,41	40,59	297	299,87	21,35	3,198	23,46	35,94	38,07	42,89	41,26	27,62	-	-	-	-
17:30	162,52	34,04	196,56	198,45	20,84	2,664	23,04	33,19	36,25	41,45	40,18	27,44	-	-	-	-
18:00	130,4	27,9	158,3	160,65	20,45	2,785	22,56	31,87	34,97	39,15	38,45	27,31	580	1600	2180	15,78

Table E- 22: Measurement and derived data for 19 November 2014

Local Time	Meteorological factors						Solar still temperatures						Hourly distillate output			Efficiency
	Solar radiation (beam) I_b [W/m^2]	Solar radiation (diffuse) I_d [W/m^2]	Solar radiation (total horizontal) I_h [W/m^2]	Solar radiation (total inclined) I_T [W/m^2]	Air temp [°C]	Wind speed [m/s]	Outer cover temp [°C]	Inner cover temp [°C]	Vapour temp [°C]	Basin temp [°C]	Water temp [°C]	Condenser temp [°C]	Inner cover [ml]	External condenser [ml]	Total [ml]	Instantaneous [%]
7:00	200	28	228	212,06	16,26	0,789	18,77	11,44	13,4	16,67	16,86	8,19	0	0	0	0
7:15	247	34,8	281,8	264,61	16,32	1,764	19,66	11,92	14,49	17,31	17,57	9,66	-	-	-	-
7:30	295	40,2	335,2	317,23	17,43	1,209	20,66	12,28	15,49	18,02	18,34	10,22	-	-	-	-
7:45	332	51,7	383,7	365,58	17,63	1,023	21,43	12,44	15,34	18,8	19,15	11,23	-	-	-	-
8:00	385	57,1	442,1	423,49	18,43	0,844	22,94	13,19	16,36	19,62	19,57	13,36	0	0	0	0
8:15	432	63,2	495,2	476,65	19,06	1,268	23,17	14,42	17,35	20,56	20,43	16,2	-	-	-	-
8:30	471	74,2	545,2	527,01	20,41	1,237	24,14	14,71	18,54	21,83	21,74	17,9	-	-	-	-
8:45	522,55	80,45	603	585,10	20,68	1,352	25,22	15,13	20,22	23,69	23,32	19,48	-	-	-	-
9:00	574,7	86,1	660,8	643,46	20,88	1,512	25,98	17,81	22,16	26,26	25,28	20,43	0	30	30	2.99
9:15	612,1	92,6	704,7	688,23	21,25	1,356	26,15	18,62	23,7	29,57	27,95	21,29	-	-	-	-
9:30	645,4	98,6	744	737,95	21,51	0,918	26,34	21,1	26,57	33,61	31,22	22,25	-	-	-	-
9:45	684,2	104,3	788,5	797,90	22,36	1,657	26,36	22,11	30,62	37,99	35,01	24,26	-	-	-	-
10:00	716,47	110,53	827	835,16	22,87	1,503	27,19	28,45	34,08	42,43	38,97	25,53	20	150	170	10,64
10:15	745,1	116,9	862	873,34	23,96	1,075	27,37	33,2	37,31	47,1	43,44	25,82	-	-	-	-
10:30	778,76	122,24	901	916,13	24,56	1,362	27,42	38,62	42,51	51,54	48,66	28,02	-	-	-	-
10:45	792,56	133,44	926	944,44	25,08	1,529	29,31	41,67	47,58	57,28	53,26	29,63	-	-	-	-
11:00	807,06	134,94	942	963,23	25,76	1,677	29,7	46,79	51,03	60,05	57,03	30,73	100	350	450	18,14
11:15	823,97	135,03	959	982,64	26,26	1,997	30,2	48,3	54,67	62,86	60,29	32,38	-	-	-	-
11:30	836,06	136,94	973	998,61	26,85	2,621	30,53	50,99	57,02	65,22	62,95	33,94	-	-	-	-
11:45	851,55	142,45	994	1021,39	27,79	3,731	31,13	53,8	59,83	66,56	64,63	34,92	-	-	-	-

12:00	854,13	148,87	1003	1031,50	28,49	4,017	31,96	56,48	60,05	67,8	65,96	35,02	200	550	750	17,98
12:15	849,23	159,77	1009	1038,18	29,08	4,308	33,63	57,53	63,19	68,78	67,17	35,39	-	-	-	-
12:30	852,99	160,01	1013	1042,46	30,68	3,733	34,91	58,72	64,57	69,9	68,34	35,55	-	-	-	-
12:45	841,48	169,52	1011	1040,21	30,27	4,017	34,39	61,31	66,15	71,26	70,03	35,72	-	-	-	-
13:00	852,05	153,95	1006	1034,52	29,83	3,975	33,81	63,24	67,08	71,5	70,72	34,57	300	850	1150	23,73
13:15	850,27	148,73	999	1026,40	29,6	3,775	33,53	63,48	67,27	71,44	70,98	33,19	-	-	-	-
13:30	850,62	138,38	989	1014,83	28,83	4,008	33,09	63,79	67,17	71,36	70,85	32,33	-	-	-	-
13:45	838,15	137,85	976	999,78	28,33	4,483	32,86	62,62	66,42	71,23	70,69	32,25	-	-	-	-
14:00	821,45	137,55	959	980,27	27,87	4,042	32,51	62,23	66,35	71,13	70,41	31,83	400	1250	1650	31,32
14:15	809,67	127,33	937	955,26	27,71	3,998	32,04	61,87	66,23	71,04	70,32	31,69	-	-	-	-
14:30	789,04	121,96	911	925,81	26,18	3,817	31,83	61,76	66,08	70,31	70,29	31,58	-	-	-	-
14:45	765,23	116,77	882	892,96	25,54	3,873	31,5	60,78	65,63	69,87	69,23	30,73	-	-	-	-
15:00	740,35	110,65	851	857,67	25,22	4,625	30,73	60,28	63,92	67,74	67,06	30,65	500	1450	1950	21,54
15:15	709,2	104,8	814	816,01	24,98	4,392	29,62	58,11	61,61	66,03	65,96	29,67	-	-	-	-
15:30	650,84	98,86	749,7	751,63	24,56	4,658	28,08	55,19	58,73	64,69	63,8	28,56	-	-	-	-
15:45	586,42	92,78	679,2	680,50	24,26	4,925	27,22	54,94	57,05	62,58	61,96	27,86	-	-	-	-
16:00	548,95	86,35	635,3	637,25	24,13	5,117	26,35	52,28	55,58	60,13	59,76	27	550	1600	2150	19,49
16:15	360,9	79,96	440,86	442,93	23,48	4,925	25,11	49,41	52,05	57,82	56,41	26,85	-	-	-	-
16:30	329,43	73,73	403,16	406,06	22,66	4,1	24,15	47,27	50,41	55,29	54,15	26,66	-	-	-	-
16:45	318,97	57,57	376,54	378,53	22,02	3,767	23,28	45,34	48,99	53,42	52,33	26,14	-	-	-	-
17:00	276,29	45,57	321,86	324,26	21,14	3,367	22,21	43,35	46,81	51,46	50,64	25,78	600	1650	2250	19,33
17:15	237,67	45,49	283,16	285,69	20,27	3,975	21,46	41,32	44,44	49,55	48,95	24,75	-	-	-	-
17:30	223,52	38,8	262,32	264,92	20,17	3,858	20,65	39,77	42,49	47,43	46,16	23,62	-	-	-	-
18:00	199,92	31,88	231,8	233,94	20,05	3,742	20,62	37,03	40,2	45,22	44,6	22,84	620	1700	2320	18.88

Table E- 23: Measurement and derived data for 20 November 2014

Local Time	Meteorological factors						Solar still temperatures						Hourly distillate output			Efficiency
	Solar radiation (beam) I_b [W/m^2]	Solar radiation (diffuse) I_d [W/m^2]	Solar radiation (total horizontal) I_h [W/m^2]	Solar radiation (total inclined) I_T [W/m^2]	Air temp [°C]	Wind speed [m/s]	Outer cover temp [°C]	Inner cover temp [°C]	Vapour temp [°C]	Basin temp [°C]	Water temp [°C]	Condenser temp [°C]	Inner cover [ml]	External condenser [ml]	Total [ml]	Instantaneous [%]
7:00	194	27,4	221,4	200,33	15,46	1,916	19,42	12,44	14,41	15,5	15,67	9,55	0	0	0	0
7:15	241,5	33,5	275	253,47	15,77	2,362	19,54	13,11	15,43	16,21	16,44	10,71	-	-	-	-
7:30	292	38,6	330,6	308,74	16,32	2,191	19,98	13,9	16,42	17,04	17,29	9,38	-	-	-	-
7:45	335,85	49,15	385	363,24	17,17	2,493	20,47	15,03	17,66	18,03	18,29	9,98	-	-	-	-
8:00	386	54,4	440,4	418,89	18,35	2,825	21,08	15,98	18,97	19,23	19,43	13,62	0	0	0	0
8:15	435	60,2	495,2	474,17	18,46	2,742	21,29	16,77	20,04	20,5	20,55	17,21	-	-	-	-
8:30	478	71,8	549,8	529,42	19,92	2,883	21,94	17,51	21,02	21,91	21,73	18,77	-	-	-	-
8:45	524	77,1	601,1	581,62	19,24	3,242	22,37	18,63	22,61	23,88	23,27	19,53	-	-	-	-
9:00	572,6	83,7	656,3	637,74	19,75	3,058	22,71	20,11	24,41	26,46	25,33	20,14	0	30	30	0,.30
9:15	611,8	89,4	701,2	688,49	20,38	3,4	23,73	22,22	26,73	29,61	27,92	20,44	-	-	-	-
9:30	644,9	95,9	740,8	739,52	21,04	3,5	24,24	24,76	29,43	33,25	30,98	20,87	-	-	-	-
9:45	679,6	101,9	781,5	786,91	21,41	3,383	24,1	27,98	32,71	37,35	34,56	20,53	-	-	-	-
10:00	713,08	107,92	821	826,99	21,87	2,464	24,41	31,88	36,72	41,85	38,71	21,53	40	140	180	11,48
10:15	746,89	113,11	860	869,87	22,03	2,625	24,62	35,2	40,59	45,86	42,93	22,89	-	-	-	-
10:30	780,87	119,13	900	914,19	22,94	2,199	25,34	37,09	42,41	48,14	45,58	25,53	-	-	-	-
10:45	786,06	130,94	917	934,88	23,1	2,599	25,73	41,72	47,43	53,88	50,93	24,85	-	-	-	-
11:00	806,57	131,43	938	959,17	23,46	2,592	26,11	45,16	51,8	57,9	55,01	25,56	120	400	520	22,10
11:15	825,12	132,88	958	982,09	23,73	2,599	26,38	45,29	51,57	56,02	54,22	29,84	-	-	-	-
11:30	843,35	133,65	977	1003,60	24,98	2,692	26,67	44,23	50,64	54,48	53,02	31,31	-	-	-	-
11:45	850,49	139,51	990	1018,59	24,17	2,721	26,96	43,41	49,54	53,8	52,1	31,9	-	-	-	-

12:00	855,9	145,1	1001	1031,17	24,63	3,108	27,05	46,06	52,42	57,58	55,46	30,46	300	700	1000	29,00
12:15	852,48	156,52	1009	1040,28	24,95	3,792	27,61	45,15	51,52	55,5	53,86	30,29	-	-	-	-
12:30	856,05	156,95	1013	1044,92	25	3,733	27,87	46,62	53,71	58,88	57,08	30,51	-	-	-	-
12:45	848,24	165,76	1014	1046,12	25,08	3,592	27,98	47,65	54,84	59,75	58,18	29,73	-	-	-	-
13:00	858,75	150,25	1009	1040,78	25,13	3,333	27,87	52,93	59,32	66,07	65,63	29,28	500	1000	1500	29,72
13:15	861,88	144,12	1006	1037,15	25,08	2,802	28,28	55,06	61,35	68,04	67,94	31,28	-	-	-	-
13:30	862,76	133,24	996	1025,96	25,05	3,023	27,91	57,18	63,45	70,82	69,89	31,56	-	-	-	-
13:45	854,8	132,2	987	1015,42	25,02	2,842	27,73	45,56	50,24	54,66	53,73	31,55	-	-	-	-
14:00	752,51	131,49	884	908,02	24,96	3,296	27,32	44,43	50,37	54,16	53,54	30,45	600	1300	1900	27,51
14:15	815,08	120,92	936	959,43	24,74	3,231	27,05	43,47	49,4	53,05	52,41	30,41	-	-	-	-
14:30	811,9	114,1	926	946,70	24,12	3,356	26,69	42,09	48,72	52,76	52,15	29,86	-	-	-	-
14:45	787,08	108,92	896	913,17	23,75	3,417	26,01	41,43	48,91	52,39	51,58	29,64	-	-	-	-
15:00	761,91	102,09	864	877,24	22,84	3,742	25,78	40,93	47,1	51,49	50,56	28,97	750	1550	2300	28,57
15:15	731,92	96,08	828	836,98	22,76	3,6	25,52	39,42	46,86	51,28	50,31	27,75	-	-	-	-
15:30	589,02	90,98	680	684,10	22,53	3,85	24,97	38,87	45,31	49,98	49,47	27,05	-	-	-	-
15:45	550,25	84,21	634,46	638,52	22,34	4,075	24,76	37,59	43,45	48,53	47,32	26,8	-	-	-	-
16:00	526,51	78,59	605,1	610,99	22,16	3,892	24,43	36,73	42,41	47,74	46,98	26,28	800	1650	2450	15,45
16:15	494,45	72,64	567,09	572,87	22,09	3,408	24,36	35,98	42,71	46,28	46,06	26,03	-	-	-	-
16:30	462,31	66,47	528,78	532,69	21,82	3,525	24,23	34,88	41,87	46,15	45,73	25,41	-	-	-	-
16:45	442,38	50,72	493,1	499,19	21,23	3,758	23,89	33,45	39,72	44,66	43,01	25,08	-	-	-	-
17:00	389,81	39,95	429,76	433,75	20,73	4,108	23,43	32	37,64	42,12	41,73	24,8	820	1700	2520	10,21
17:15	342,26	38,76	381,02	385,79	20,53	3,717	22,88	31,29	35,12	39,72	39,17	24,39	-	-	-	-
17:30	304,78	32,22	337	342,42	20,19	4,192	23	29,93	32,75	37,19	36,49	24	-	-	-	-
18:00	274,81	26,59	301,4	307,13	20,03	4,042	22,31	28,84	30,87	35,53	34,12	23,62	840	1750	2590	14,51

Table E- 24: Measurement and derived data for 21 November 2014

Local Time	Meteorological factors						Solar still temperatures						Hourly distillate output			Efficiency
	Solar radiation (beam) I_b [W/m^2]	Solar radiation (diffuse) I_d [W/m^2]	Solar radiation (total horizontal) I_h [W/m^2]	Solar radiation (total inclined) I_T [W/m^2]	Air temp [°€]	Wind speed [m/s]	Outer cover temp [°C]	Inner cover temp [°C]	Vapour temp [°C]	Basin temp [°C]	Water temp [°C]	Condenser temp [°C]	Inner cover [ml]	External condenser [ml]	Total [ml]	Instantaneous [%]
7:00	175,85	33,45	209,3	155,96	9,97	0,974	14,71	7,35	10,28	12,86	15,61	9,78	0	0	0	0
7:15	217,7	40,2	257,9	214,91	10,45	1,276	14,79	7,54	10,67	13,96	16,02	10,27	-	-	-	-
7:30	263	47,3	310,3	272,33	10,87	0,579	15,24	8,35	11,54	14,42	16,21	10,44	-	-	-	-
7:45	303,9	58,1	362	327,28	11,87	0,915	16,15	8,76	11,74	15,13	18,63	11,23	-	-	-	-
8:00	369,2	66,9	436,1	401,31	12,12	1,558	17,07	9,78	12,71	15,85	18,85	11,83	0	0	0	0
8:15	401,4	72,1	473,5	443,31	12,64	2,352	17,85	10,54	13,14	16,37	18,97	12,69	-	-	-	-
8:30	444,5	83,8	528,3	500,17	13,02	2,296	17,98	10,86	13,26	17,61	19,27	13,16	-	-	-	-
8:45	488,8	89,9	578,7	552,57	13,85	2,066	18,1	11,76	13,64	19,76	19,73	13,79	-	-	-	-
9:00	538	96,7	634,7	610,08	14,15	2,325	18,71	12,09	15,58	21,03	21,54	14,2	0	0	0	0,00
9:15	577,2	102,9	680,1	659,62	14,68	2,423	18,89	13,94	16,92	22,87	23,67	14,68	-	-	-	-
9:30	614,4	109,2	723,6	707,77	15,29	2,174	19,79	16,19	19,85	25,03	24,99	15,66	-	-	-	-
9:45	652,8	115,2	768	761,71	15,41	1,397	18,34	16,85	20,09	26,69	25,74	16,29	-	-	-	-
10:00	728,4	121,6	850	845,85	15,93	1,19	19,14	17,41	21,36	26,99	27,19	17,83	0	30	30	0.28
10:15	634,1	127,4	761,5	862,84	16,29	1,351	19,78	19,39	23,4	28,62	29,23	18,47	-	-	-	-
10:30	630,1	133,1	763,2	868,87	16,41	1,319	20,27	21,7	27,18	32,73	32,86	19,36	-	-	-	-
10:45	804,215	144,785	949	875,14	18,17	0,836	21,04	24,54	29,01	35,19	34,94	20,22	-	-	-	-
11:00	791,6	145,4	937	876,44	17,91	0,653	21,22	28,28	32,54	38,02	37,07	21,92	20	150	170	10,15
11:15	331,4	146,6	478	876,94	16,14	1,628	21,23	32,12	38,65	44,23	43	22,54	-	-	-	-
11:30	347,6	147,7	495,3	879,24	16,93	2,42	21,25	38,01	43,37	48,97	47,76	23,16	-	-	-	-
11:45	578	153,9	731,9	884,64	17,71	3,027	21,54	40,83	45,14	51,13	50,02	24,34	-	-	-	-

12:00	523,1	159,6	682,7	887,24	18,91	2,842	22,22	43,66	47,23	53,06	52,15	25,41	100	350	450	19,77
12:15	472,28	170,42	642,7	897,97	18,87	2,717	22,54	45,27	48,4	54,97	53,24	26,09	-	-	-	-
12:30	597,274	171,526	768,8	892,14	19,21	3,317	23,01	47,89	50,87	55,05	54,74	26,54	-	-	-	-
12:45	601,5	179,7	781,2	905,47	19,96	2,458	23,63	48,81	51,12	55,78	55,12	27,01	-	-	-	-
13:00	742,82	163,18	906	934,25	20,27	2,435	24,95	49,15	51,24	55,45	55,14	27,31	270	650	920	31,38
13:15	759,99	157,01	917	945,71	21,01	2,756	25,34	49,17	51,23	55,26	55,15	27,76	-	-	-	-
13:30	732,93	145,07	878	905,36	20,84	2,522	25,69	47,15	50,2	55,11	55,11	27,95	-	-	-	-
13:45	678,83	144,17	823	848,53	20,31	3	26,09	46,74	49,53	54,43	53,52	28,06	-	-	-	-
14:00	424,3	143,5	567,8	788,83	20,29	3,425	26	46,32	49,25	54,02	52,43	28,63	400	950	1350	34.08
14:15	780,64	132,36	913	739,21	20,17	3,614	25,82	45,57	48,35	52,87	51,3	28,39	-	-	-	-
14:30	572,51	125,59	698,1	717,42	20,01	3,696	25,56	44,78	47,61	52,52	51,05	27,97	-	-	-	-
14:45	603,39	119,91	723,3	711,94	20,36	4,383	25,21	43,27	46,8	52,21	50,47	27,15	-	-	-	-
15:00	471,9	113,8	585,7	600,17	20,34	5,383	25,02	42,12	45,89	51,34	49,45	26,73	500	1100	1600	26,13
15:15	445,28	106,92	552,2	564,19	20,26	4,775	24,92	42	45,75	51,07	49,2	26,61	-	-	-	-
15:30	436,67	99,93	536,6	546,50	19,94	5,25	24,34	41,18	44,2	49,75	48,36	25,45	-	-	-	-
15:45	418,8	93,8	512,6	516,42	19,81	5,208	24,11	40,64	43,72	48,34	46,21	25,09	-	-	-	-
16:00	410,71	87,79	498,5	500,45	19,65	5,583	23,82	38,2	41,3	47,53	45,71	24,71	600	1200	1800	25,18
16:15	401,58	81,72	483,3	486,45	19,34	4,908	23,31	37,26	40,53	46,07	44,95	24,13	-	-	-	-
16:30	348,88	75,12	424	426,75	19,08	5,642	23,09	35,89	39,04	45,77	45,62	23,52	-	-	-	-
16:45	318,73	59,87	378,6	381,26	18,83	5,133	22,77	35,04	38,36	44,24	42,9	23,04	-	-	-	-
17:00	270,46	48,94	319,4	324,12	18,31	5,917	22,43	33,69	36,74	42	40,62	22,91	650	1250	1900	19,53
17:15	232,77	47,33	280,1	284,23	18,17	6,067	22,23	31,41	34,93	39,38	38,06	22,88	-	-	-	-
17:30	184,87	41,43	226,3	231,11	18,02	6,058	22,02	28,01	30,13	36,89	35,38	21,89	-	-	-	-
18:00	168,11	34,69	202,8	210,85	17,94	6,242	21,94	27,45	29,56	35,33	33,01	21,77	660	1290	1950	15,12

Table E- 25: Measurement and derived data for 22 November 2014

Local Time	Meteorological factors						Solar still temperatures						Hourly distillate output			Efficiency
	Solar radiation (beam) I_b [W/m^2]	Solar radiation (diffuse) I_d [W/m^2]	Solar radiation (total horizontal) I_h [W/m^2]	Solar radiation (total inclined) I_T [W/m^2]	Air temp [°C]	Wind speed [m/s]	Outer cover temp [°C]	Inner cover temp [°C]	Vapour temp [°C]	Basin temp [°C]	Water temp [°C]	Condenser temp [°C]	Inner cover [ml]	External condenser [ml]	Total [ml]	Instantaneous [%]
7:00	192,87	30,13	223	207,52	15,87	4,35	19,56	14	15,39	16,52	16,53	14,34	0	0	0	0
7:15	241	36,6	277,6	260,86	16,29	3,11	19,64	14,96	16,39	17,23	17,24	14,28	-	-	-	-
7:30	291,6	42,4	334	316,32	17,71	2,964	19,82	15,81	17,36	17,99	18,02	14,38	-	-	-	-
7:45	336	53,4	389,4	371,26	18,22	4,023	20,32	16,53	18,25	18,78	18,8	16,86	-	-	-	-
8:00	386	59,6	445,6	427,27	18,62	3,692	20,93	17,26	19,12	19,6	19,56	18,34	0	0	0	0
8:15	435	65,1	500,1	481,93	18,79	4,183	21,09	17,78	19,95	20,6	20,43	20,03	-	-	-	-
8:30	478	76,3	554,3	536,50	19,11	4,075	21,76	18,55	20,97	21,99	21,48	20,31	-	-	-	-
8:45	524	82,5	606,5	589,32	19,53	4,373	21,91	19,97	22,58	23,9	22,87	20,5	-	-	-	-
9:00	574,5	88,9	663,4	646,91	20,15	5,117	22,59	21,57	24,6	26,35	24,64	21,63	0	40	40	3,96
9:15	611	94,8	705,8	696,08	20,96	5,033	23,11	22,97	26,41	27,3	25,88	22,93	-	-	-	-
9:30	647,1	100,2	747,3	752,37	21,74	4,958	24,39	25	28,23	28,67	27,02	24,47	-	-	-	-
9:45	681,58	106,52	788,1	798,83	21,85	4,623	24,04	27,54	30,39	32,83	29,02	24,98	-	-	-	-
10:00	716,56	112,44	829	839,93	22,12	4,775	24,73	30,31	33,8	37,5	31,74	25,53	30	100	130	6.80
10:15	751,73	118,27	870	884,60	22,44	4,275	24,99	33,18	36,9	42,2	35,67	26,33	-	-	-	-
10:30	784,6	124,4	909	927,55	23,06	4,667	25,47	36,11	39,3	46,71	40,85	26,61	-	-	-	-
10:45	795,06	135,94	931	952,88	23,37	5,158	25,86	38,97	42,12	50,97	45,26	27,34	-	-	-	-
11:00	814,47	136,53	951	975,80	23,72	4,558	25,98	41,59	45,12	54,74	48,89	27,92	100	250	350	14.15
11:15	833,69	137,31	971	998,34	23,99	4,75	26,43	43,79	47,57	57,49	52,46	28,3	-	-	-	-
11:30	850,48	137,52	988	1017,43	24,18	4,775	26,87	46,44	50,05	59,17	55,34	28,57	-	-	-	-
11:45	859,15	142,85	1002	1033,08	24,45	4,858	27,03	48,13	52,25	60,77	57,69	28,78	-	-	-	-
12:00	863,92	148,08	1012	1044,25	24,8	5	27,24	49,84	54,34	62,48	59,84	29,06	200	450	650	17.87

12:15	859,72	158,28	1018	1050,96	25,05	3,825	27,81	51,49	56,52	64,16	61,96	28,82	-	-	-	-
12:30	861,61	158,39	1020	1053,19	25,28	3,717	28	53,86	59,38	66,33	64,57	28,65	-	-	-	-
12:45	850,34	168,66	1019	1051,99	25,25	3,564	28,06	55,39	61,01	68,11	66,83	28,36	-	-	-	-
13:00	862,2	152,8	1015	1047,31	25,22	4,217	28,13	56,66	62,68	69,76	68,78	28,26	350	800	1150	29.433
13:15	859,21	147,79	1007	1038,15	25,15	4,008	28,31	58,22	64,19	69,62	69,94	28,25	-	-	-	-
13:30	859,35	137,65	997	1026,56	25,14	4,292	28,02	58,85	64,67	69,28	70,3	28,15	-	-	-	-
13:45	844,87	137,13	982	1009,44	25,13	4,958	27,96	59	64,64	68,66	70,23	28	-	-	-	-
14:00	827,99	137,01	965	989,89	25,06	4,942	27,48	58,4	64,37	67,86	69,84	27,56	600	1200	1800	40.41
14:15	818,16	126,84	945	966,89	24,91	5,35	27,21	57,47	63,4	67,05	69,31	28,97	-	-	-	-
14:30	798,38	121,62	920	938,41	24,36	4,892	26,81	57,09	62,72	66,06	68,75	28,52	-	-	-	-
14:45	773,56	116,44	890	904,45	23,9	5,617	26,19	56,43	61,71	64,39	67,58	28,28	-	-	-	-
15:00	746,72	110,28	857	867,06	23,1	5,433	25,93	54,93	60,1	62,49	65,56	27,45	750	1500	2250	32.08
15:15	715,88	104,12	820	825,29	23,06	6,317	25,64	53,42	58,66	60,38	63,51	28,92	-	-	-	-
15:30	618,07	98,23	716,3	716,69	22,86	6,308	25,12	51,87	56,57	57,98	61,47	28,5	-	-	-	-
15:45	558,88	91,92	650,8	682,64	22,62	6,825	24,98	50,59	54,45	55,53	59,32	27,97	-	-	-	-
16:00	553,03	85,57	638,6	644,48	22,44	6,058	24,73	48,73	52,41	52,74	56,98	27,28	850	1500	2500	24.17
16:15	513,45	78,97	592,42	599,06	22,26	6,317	24,66	46,98	50,71	50,28	54,26	26,98	-	-	-	-
16:30	487,25	72,47	559,72	564,85	22,02	6,525	24,36	44,88	48,31	47,5	51,73	27,07	-	-	-	-
16:45	438,14	56,24	494,38	500,65	21,71	6,108	24,04	42,45	45,72	44,66	49,01	26,98	-	-	-	-
17:00	425,33	45,82	471,15	476,25	20,98	6,733	23,65	40	43,14	42,12	45,73	27,08	900	1650	2630	17.17
17:15	349,01	44,95	393,96	398,64	20,72	5,733	23,09	37,29	40,12	39,72	42,46	26,68	-	-	-	-
17:30	299,47	38,07	337,54	341,05	20,43	5,725	23,14	34,53	37	37,49	39,49	26,65	-	-	-	-
18:00	352,92	31,08	384	289,59	20,29	4,8	22,46	31,84	34,1	35,53	37,12	26,16	910	1740	2650	8.77

Table E- 26: Measurement and derived data for 23 November 2014

Local Time	Meteorological factors						Solar still temperatures						Hourly distillate output			Efficiency
	Solar radiation (beam) I_b [W/m²]	Solar radiation (diffuse) I_d [W/m²]	Solar radiation (total horizontal) I_h [W/m²]	Solar radiation (total inclined) I_T [W/m²]	Air temp [°C]	Wind speed [m/s]	Outer cover temp [°C]	Inner cover temp [°C]	Vapour temp [°C]	Basin temp [°C]	Water temp [°C]	Condenser temp [°C]	Inner cover [ml]	External condenser [ml]	Total [ml]	Instantaneous [%]
7:00	198,73	28,27	227	211,03	16,8	2,387	21,75	12,83	14,4	14,8	14,93	5,051	0	0	0	0
7:15	247	34,8	281,8	264,75	17,1	2,121	21,86	13,54	15,26	15,22	15,42	8,829	-	-	-	-
7:30	300	40,1	340,1	322,16	18,13	3,008	21,92	14,25	16	15,7	15,95	10,37	-	-	-	-
7:45	345	51,6	396,6	378,33	18,38	4,65	22,07	14,57	16,42	16,04	16,28	13,44	-	-	-	-
8:00	396	57,6	453,6	435,30	18,53	3,229	24,96	15,05	17,13	16,8	17,02	13,45	0	20	20	0
8:15	446	63,2	509,2	491,20	18,99	2,379	26,21	15,87	18,11	17,68	17,82	13,47	-	-	-	-
8:30	488	74,4	562,4	544,99	19,23	3,693	26,52	17,23	19,55	18,83	18,71	13,76	-	-	-	-
8:45	536	80,5	616,5	599,82	19,81	5,417	26,67	18,32	21,09	20,48	19,84	16,85	-	-	-	-
9:00	585,5	86,8	672,3	656,49	20,24	3,417	26,88	19,63	23,05	22,79	21,54	17,51	20	50	70	4,89
9:15	626,6	92,9	719,5	710,78	21,18	2,743	27,24	21,58	25,58	25,86	23,88	18,78	-	-	-	-
9:30	660,4	98,6	759	766,27	21,99	5,867	27,53	24,28	28,01	29,62	26,78	20,24	-	-	-	-
9:45	697,5	104,5	802	812,73	22	6,117	27,7	26,74	30,23	33,64	29,97	20,88	-	-	-	-
10:00	732,32	110,68	843	856,65	22,51	4,325	27,82	29,39	33,29	38,2	33,49	21,39	40	200	240	12,61
10:15	768,55	116,45	885	902,68	22,81	2,818	27,99	32,39	36,69	43,02	37,86	21,64	-	-	-	-
10:30	795,64	122,36	918	939,65	23,11	3,817	28,14	36,12	40,29	47,47	42,97	22,82	-	-	-	-
10:45	805,12	133,88	939	964,00	23,62	5,658	28,22	38,92	43,28	51,14	47,01	24,35	-	-	-	-
11:00	828,14	134,86	963	991,04	23,85	4,917	28,39	41,11	45,99	54,88	50,26	25	120	450	570	20,88
11:15	847,85	135,15	983	1013,64	24,18	3,764	28,4	43,98	48,91	57,84	53,6	25,36	-	-	-	-
11:30	862,81	136,19	999	1031,75	24,51	4,881	28,55	46,94	52,14	60,24	56,85	25,39	-	-	-	-
11:45	870,72	142,28	1013	1047,42	24,78	4,931	28,68	48,85	54,58	62,04	59,14	27,28	-	-	-	-
12:00	875,52	148,48	1024	1059,67	25,18	4,117	28,74	51,02	56,76	64,15	61,73	27,41	300	750	1050	28.10

12:15	870,26	159,74	1030	1066,39	25,23	4,992	28,84	52,38	58,46	65,71	63,57	27,74	-	-	-	-
12:30	872,51	160,49	1033	1069,66	25,46	4,792	28,96	54,23	60,69	67,22	65,37	28,11	-	-	-	-
12:45	862,63	170,37	1033	1069,48	25,78	4,758	28,82	55,62	62	68,39	66,71	28,89	-	-	-	-
13:00	872,72	155,28	1028	1063,78	25,96	4,617	28,66	57,36	63,33	69,65	69,07	28,97	500	1100	1600	31.85
13:15	871,77	150,23	1022	1056,68	26,07	4,45	28,53	58,6	64,49	68,48	70,37	29,46	-	-	-	-
13:30	868,88	140,12	1009	1041,97	25,78	4,225	28,44	59,33	65,5	69,21	70,95	29,86	-	-	-	-
13:45	854,91	140,09	995	1025,88	25,69	4,258	28,42	59,8	65,98	69,17	71,22	30,62	-	-	-	-
14:00	837,24	139,76	977	1005,27	25,63	4,425	28,31	59,83	66,7	69,14	71,54	30,93	600	1400	2000	24,43
14:15	825,86	129,14	955	980,17	25,17	4,383	28,28	59,78	66,62	69,05	71,52	31,15	-	-	-	-
14:30	806,58	123,42	930	951,61	24,86	4,281	28,05	59,07	66,13	68,02	70,7	31,65	-	-	-	-
14:45	781,33	118,67	900	917,61	24,07	4,65	27,85	58,3	65,57	66,43	69,82	32,02	-	-	-	-
15:00	755	111	866	879,06	23,5	5,533	27,45	56,98	63,76	63,71	67,36	32,08	700	1650	2350	24,52
15:15	725,11	105,89	831	839,27	23,28	5,367	27,13	55,47	61,67	60,95	65,19	31,93	-	-	-	-
15:30	691,36	99,74	791,1	794,16	23,15	5,464	26,67	53,81	59,38	58,47	63,03	31,44	-	-	-	-
15:45	536,82	94,28	631,1	634,12	22,98	4,925	26,57	52,45	57,38	56,41	61,09	30,32	-	-	-	-
16:00	505,32	87,48	592,8	596,46	22,73	5,342	26,15	50,67	55,54	53,94	58,72	30,07	750	1750	2500	15,62
16:15	435,61	81,16	516,77	521,43	22,56	4,967	23,99	48,43	53,29	51,08	55,78	29,44	-	-	-	-
16:30	406,03	74,82	480,85	487,26	22,43	5,258	23,65	46,34	51,17	48,3	53,19	28,9	-	-	-	-
16:45	388,04	58,38	446,42	456,19	21,86	5,617	23,38	43,86	48,4	45,31	50,33	28,67	-	-	-	-
17:00	347,05	47,31	394,36	402,32	21,15	5	23,1	41,2	45,23	42,71	46,78	28,78	800	1800	2600	15,60
17:15	281,87	47,43	329,3	368,41	21,01	5,408	24,56	38,37	41,88	40,14	43,31	29,29	-	-	-	-
17:30	261,56	40,64	302,2	357,20	20,72	5,517	24,1	35,07	38,05	37,39	39,75	28,82	-	-	-	-
18:00	240,53	33,97	274,5	296,26	20,32	4,55	23,72	32,01	34,55	35,09	36,97	28,01	810	1820	2630	6,42

Table E- 27: Measurement and derived data for 24 November 2014

Local Time	Meteorological factors						Solar still temperatures						Hourly distillate output			Efficiency
	Solar radiation (beam) I_b [W/m²]	Solar radiation (diffuse) I_d [W/m²]	Solar radiation (total horizontal) I_h [W/m²]	Solar radiation (total inclined) I_T [W/m²]	Air temp [°C]	Wind speed [m/s]	Outer cover temp [°C]	Inner cover temp [°C]	Vapour temp [°C]	Basin temp [°C]	Water temp [°C]	Condenser temp [°C]	Inner cover [ml]	External condenser [ml]	Total [ml]	Instantaneous [%]
7:00	198	29,8	227,8	211,76	17,87	6,008	20,75	13,35	15,17	16,41	16,47	10,75	0	0	0	0
7:15	248	35,9	283,9	266,63	18,62	4,975	20,82	14,14	15,98	16,98	17,05	10,82	-	-	-	-
7:30	299	41,7	340,7	322,65	18,96	5,425	21,01	14,88	16,75	17,59	17,69	11,34	-	-	-	-
7:45	346	52,2	398,2	379,72	19,11	6,375	21,44	15,39	17,39	18,21	18,31	11,56	-	-	-	-
8:00	401	58,3	459,3	440,57	19,26	5,917	22,01	15,85	18,04	18,89	18,94	12,77	0	10	10	0
8:15	447	64,8	511,8	493,51	19,78	5,675	22,54	16,46	18,82	19,82	19,75	13,34	-	-	-	-
8:30	490	75,3	565,3	547,58	19,91	5,483	22,56	17,48	20,05	21,15	20,77	14,1	-	-	-	-
8:45	537	81,5	618,5	601,52	20,05	5,558	23,24	18,65	21,53	21,39	21,04	14,23	-	-	-	-
9:00	587,8	87,9	675,7	659,56	20,27	4,325	23,96	19,75	23,27	23,12	22,01	15,55	20	40	60	4,86
9:15	566,6	93,3	659,9	650,98	21,31	5,304	24,34	21,44	25,2	25,56	23,65	15,32	-	-	-	-
9:30	624,9	99,4	724,3	730,66	22,12	5,725	24,66	23,59	27	28,73	25,71	15,28	-	-	-	-
9:45	693,15	105,15	798,3	810,33	22,92	4,867	25,23	26,56	29,43	32,86	28,34	16,01	-	-	-	-
10:00	721,96	111,04	833	845,59	23,09	4,858	26,25	29,45	32,92	37,25	31,58	17,09	40	150	190	9,77
10:15	756,16	117,84	874	890,45	23,09	6,258	26,84	32,52	36,28	41,6	35,8	17,59	-	-	-	-
10:30	785,65	123,35	909	929,40	22,67	5,158	26,93	34,99	38,19	45,85	40,44	17,6	-	-	-	-
10:45	794,28	134,72	929	952,69	22,74	4,014	27,08	37,37	41,33	50,27	44,76	18,17	-	-	-	-
11:00	812,35	135,65	948	974,60	21,08	4,625	27,16	40,27	44,65	54,04	48,81	19,87	120	450	570	24,49
11:15	833,48	136,52	970	999,21	21,15	4,883	27,24	42,09	46,59	56,64	51,9	19,94	-	-	-	-
11:30	850,78	137,22	988	1019,34	21,53	4,583	27,97	44,05	49,02	58,27	54,61	20,76	-	-	-	-
11:45	858,88	143,12	1002	1035,02	21,89	5,283	28,14	46,3	51,43	59,76	57,15	20,95	-	-	-	-
12:00	862,85	149,15	1012	1046,21	22,28	6,333	28,28	47,61	53,08	61,35	59,07	21,27	300	700	1000	25,59

12:15	854,36	160,64	1015	1049,83	22,26	6,108	28,33	48,91	54,28	62,68	60,34	22,54	-	-	-	-
12:30	856,4	161,6	1018	1053,10	21,95	7,308	28,37	50,04	55,54	63,75	61,43	23,15	-	-	-	-
12:45	846,95	171,05	1018	1052,94	21,38	8,45	28,39	49,89	55,8	64,28	61,97	24,01	-	-	-	-
13:00	862,19	155,81	1018	1052,44	21,14	8,12	28,23	50,32	56,08	64,42	61,98	25,49	500	1000	1500	29,49
13:15	854,44	150,56	1005	1038,12	21,39	7,767	28,14	51,34	57,38	65,01	62,43	25,23	-	-	-	-
13:30	855,59	138,41	994	1025,45	21,81	8,02	28,04	52,19	57,33	63,99	64,55	25,15	-	-	-	-
13:45	843,64	138,36	982	1011,43	22,35	7,125	27,76	52,38	57,46	62,95	64,32	25,08	-	-	-	-
14:00	818,84	137,16	956	982,61	22,88	7,233	27,61	52,38	57,63	62,68	64,26	24,78	600	1300	1900	25,23
14:15	815,16	126,84	942	965,76	22,98	7,258	27,45	52,26	57,67	62,43	64,22	24,43	-	-	-	-
14:30	794,2	121,8	916	936,24	22,96	7,892	27,35	51,74	57,01	61,48	63,81	23,87	-	-	-	-
14:45	769,24	116,76	886	902,30	22,81	8,63	27,18	51,11	55,99	59,96	62,59	23,2	-	-	-	-
15:00	746,97	111,03	858	869,98	22,73	8,47	26,91	50,35	55,38	58,16	61,86	23,08	700	1550	2250	24,99
15:15	721,28	105,72	827	834,26	22,83	8,5	26,75	49,24	54,79	56,52	60,36	22,95	-	-	-	-
15:30	684,33	100,57	784,9	787,05	22,63	7,458	26,56	48,49	53,95	54,91	59,08	22,76	-	-	-	-
15:45	633,16	94,94	728,1	733,56	22,55	6,833	26,37	47,54	52,8	53,42	57,56	22,42	-	-	-	-
16:00	616,11	89,39	705,5	711,65	22,43	8,21	26,16	47,14	51,33	51,21	55,47	21,87	800	1700	2500	21,91
16:15	556,33	84,17	640,5	645,89	22,16	8,74	24	45,23	49,27	48,5	52,6	21,67	-	-	-	-
16:30	408,65	77,79	486,44	596,45	22,03	8,37	23,87	43,09	47,14	45,78	50,08	21,38	-	-	-	-
16:45	457,12	62,29	519,41	528,55	21,83	8,31	24,12	39,86	43,81	43,05	47,21	20,84	-	-	-	-
17:00	401,95	52,14	454,09	478,52	21,75	8	24,87	34,4	40	40,36	43,58	20,02	810	1800	2610	14,50
17:15	343,44	51,36	394,8	402,35	21,61	8,67	23,9	31,36	36,72	37,71	40,11	19,03	-	-	-	-
17:30	313,85	45,25	359,1	367,99	21,32	8,47	22,88	28,4	32,63	34,87	36,71	18,78	-	-	-	-
18:00	171,19	39,51	210,7	215,83	20,94	8,57	22,52	26,02	29,81	32,63	34,11	18,04	830	1810	2640	8,86

Table E- 28: Measurement and derived data for 25 November 2014

Local Time	Meteorological factors						Solar still temperatures						Hourly distillate output			Efficiency
	Solar radiation (beam) I_b [W/m^2]	Solar radiation (diffuse) I_d [W/m^2]	Solar radiation (total horizontal) I_h [W/m^2]	Solar radiation (total inclined) I_T [W/m^2]	Air temp [°C]	Wind speed [m/s]	Outer cover temp [°C]	Inner cover temp [°C]	Vapour temp [°C]	Basin temp [°C]	Water temp [°C]	Condenser temp [°C]	Inner cover [ml]	External condenser [ml]	Total [ml]	Instantaneous [%]
7:00	147,9	29,2	177,1	159,73	16,51	3,858	20,8	13,49	15,98	18,44	18,47	15,35	0	0	0	0
7:15	298,9	35,2	334,1	307,49	16,62	4,3	20,36	15,42	17,66	19,38	19,38	13,3	-	-	-	-
7:30	262,3	41,4	303,7	284,34	17,32	4,525	20,83	16,71	19,06	20,43	20,37	16,17	-	-	-	-
7:45	242,8	52,5	295,3	280,52	17,49	4,592	21,28	17,24	19,86	21,49	21,34	18,09	-	-	-	-
8:00	205,8	58,1	263,9	253,42	17,86	4,525	21,48	17,85	20,77	22,59	22,39	18,57	0	0	0	0
8:15	463,2	64,1	527,3	509,09	18,42	5,05	21,95	18,19	21,38	23,38	23,06	18,22	-	-	-	-
8:30	427,8	75,3	503,1	489,83	18,81	4,117	22,03	19,76	22,88	24,83	24,44	18,44	-	-	-	-
8:45	496,7	81,8	578,5	564,85	19,24	5,658	22,97	21,67	24,93	26,75	26,11	19,75	-	-	-	-
9:00	481,4	87,7	569,1	561,06	19,95	5,65	23,11	22,66	26	28,35	27,51	21,39	0	30	30	3,42
9:15	565,5	93,3	658,8	649,41	20,51	5,625	23,52	24,2	27,78	30,08	28,99	21,31	-	-	-	-
9:30	552,8	99,6	652,4	658,64	21,05	5,592	23,64	24,95	28,62	32,22	30,3	22,51	-	-	-	-
9:45	691,7	105,7	797,4	809,05	21,88	5,308	24,21	27,66	31,2	35,86	32,25	22,56	-	-	-	-
10:00	716,41	111,59	828	840,09	22,24	6,258	25,04	30,09	34,15	39,46	34,54	22,72	40	140	180	11,33
10:15	749,54	117,46	867	882,78	22,56	5,767	26,08	32,47	36,21	42,82	37,65	22,85	-	-	-	-
10:30	784,75	123,25	908	927,67	22,89	5,5	26,21	34,91	38,3	45,9	41,39	23,35	-	-	-	-
10:45	795,63	134,37	930	952,94	23,49	5,433	26,29	36,97	40,83	49,14	44,91	23,6	-	-	-	-
11:00	814,67	135,33	950	975,82	23,76	5,633	26,78	39,21	43,7	52,55	48,3	23,84	120	400	520	21,90
11:15	831,01	136,99	968	996,29	23,98	5,164	27,91	41,34	46,17	55,22	51,37	24,24	-	-	-	-
11:30	849,1	137,9	987	1017,42	24,14	5,683	27,99	43,49	48,41	57,1	53,85	24,99	-	-	-	-
11:45	858,9	143,1	1002	1034,09	24,48	6,758	28,01	45,02	50,08	58,29	55,55	25,23	-	-	-	-

12:00	863,38	149,62	1013	1046,30	24,78	5,942	28,37	46,38	51,65	59,56	56,99	25,15	300	700	1000	28,61
12:15	860,44	160,56	1021	1055,07	24,97	7,017	28,48	48,21	53,06	61,05	58,75	25,29	-	-	-	-
12:30	865,29	161,71	1027	1061,42	25,25	7,483	28,66	48,76	54,3	62,09	59,62	25,39	-	-	-	-
12:45	855,68	170,32	1026	1060,20	25,36	6,633	28,35	49,82	55,44	62,99	61,08	24,8	-	-	-	-
13:00	868,36	154,64	1023	1056,55	25,49	6,975	27,82	51,17	56,89	63,92	61,96	25,2	500	1000	1500	29,35
13:15	864,44	148,56	1013	1045,32	25,43	8,58	27,77	51,11	57,28	64,13	61,66	25,96	-	-	-	-
13:30	863,8	138,2	1002	1032,69	25,02	7,925	27,49	51,04	57,13	64,3	61,73	25,77	-	-	-	-
13:45	847,25	137,75	985	1013,50	24,64	8,8	27,15	51,09	56,69	64,18	61,33	25,83	-	-	-	-
14:00	830,33	137,67	968	993,95	24,33	7,775	26,84	51,18	56,72	61,89	62,97	25,7	600	1300	1900	24,97
14:15	818,55	127,45	946	968,89	24,12	7,358	26,36	50,8	56,54	60,53	63,44	26,04	-	-	-	-
14:30	800,88	122,12	923	942,42	23,89	7,767	26,19	50,47	55,86	59,9	63,26	26,22	-	-	-	-
14:45	781,36	116,64	898	913,51	23,71	8,16	25,97	49,89	55,58	58,74	62,41	26,24	-	-	-	-
15:00	754,76	110,24	865	876,06	23,66	8,09	25,82	48,74	54,86	56,66	60,64	25,97	750	1550	2300	28,38
15:15	724,77	104,23	829	835,25	23,31	7,1	25,66	48,15	53,99	55	59,24	25,78	-	-	-	-
15:30	661,71	98,19	759,9	761,03	23,17	7,6	25,54	47,16	52,36	53,3	57,77	25,93	-	-	-	-
15:45	621,07	91,83	712,9	716,84	22,84	7,067	25,82	45,99	51,08	51,4	56,09	25,57	-	-	-	-
16:00	589,67	85,33	675	684,25	22,61	6,983	24,85	44,8	49,48	49,17	53,87	25,75	800	1650	2450	13,70
16:15	522,78	78,74	601,52	613,21	22,23	6,558	24,67	43,58	48,03	46,75	51,37	25,84	-	-	-	-
16:30	477,02	72,41	549,43	568,79	22,04	6,417	24,31	41,9	46,31	44,27	49,06	26	-	-	-	-
16:45	436,11	56,02	492,13	508,09	21,99	6,242	24,16	39,77	43,48	41,58	46,16	26,42	-	-	-	-
17:00	413,93	44,86	458,79	476,32	21,93	6,5	24,15	37,29	40,87	38,99	42,7	26,55	850	1700	2550	13,23
17:15	348,49	44,63	393,12	400,65	21,27	7,125	24,06	34,54	37,66	36,45	39,19	26,62	-	-	-	-
17:30	304,94	38,16	343,1	352,16	20,78	7,433	23,84	31,54	34,05	33,94	35,94	26,23	-	-	-	-
18:00	256,86	31,04	287,9	293,31	20,33	6,317	23,56	28,68	30,81	31,8	33,33	25,54	860	1750	2610	13.02

REPORT F-1: pH and TDS Analyses of water

Brief: **pH and TDS analyses**
Date of Request: 26 November 2014
Work Commenced: 27 November 2014
Date of Report: 8 December 2014
Technical Staff: K. Inise (BTech. Analytical Chemistry)
N. Mshicileli (M.Sc. Chemistry)
Certified by: L. Dolley (M.Sc., Pr. Sci. Nat.)

1. Sample Reception & Treatment

Two samples were received on the 27th of November 2014 and stored in a fridge prior to analysis.

2. Methodology

TDS was measure using a 32% hand held refractometer and pH measured using pH meter.

3. Results

The results presented in Table1 below are the average of duplicate measurements of the samples.

Table 1: pH and TDS of water samples

Sample Name/Number	TDS	pH
Before distillation	0	8.06
After Distillation	0	7.62

4. Discussion & Recommendations

The ideal pH level for drinking water should be between 6.5 -8.5. The results are therefore satisfactory before and after distillation.

5. Declaration

I declare that all analyses were performed with scientific protocols strictly adhered to and that the results are reliable (as qualified) within the scope of the methods used.

L. Dolley

M.Sc., Pr. Sci. Nat. (Biological Science; No. 400019/97)

References

1. GEA Niro Analytical Methods A, 19a.
2. AOAC 942.15(2005) 18th Edition, Chapter 37, Pg.10-11
3. AOAC 920.149

Notes

Herewith explanatory notes in terms of abbreviations and other terms needing clarification in this report:

TDS: Total Dissolved Solids

REPORT F-2: Microbiological analysis of water samples

Report Number: **140350**
Brief: **Heterotrophic plate counts and Total Coliforms determinations**
Date of Request: 26th November 2014
Work Commenced: 26th November 2014
Date of Report: 9th December 2014
Technical Staff: Z. Mthethwa (B. Tech Food Technology)
D. Ketso (B. Tech Food Technology)
L. Pehene (N.D. Food Technology)
S. Rabiu (3rd year Biotechnology)
R. Gwanpu (B.Tech Food Technology)
K. Woolward (M.Sc.)
Certified by: L. Dolley (M.Sc., Pr. Sci. Nat.)

1. Sample Reception & Treatment

The water samples were received on Wednesday the 24th of November 2014 and analyzed on the same day. All samples were stored cool in the fridge at the ATS building at CPUT (Bellville) prior to analysis.

2. Methodology

Standard methodology was used based on literature and local industry standards.

3. Results

Table 1 shows the results of microbial analyses done on water samples dated 26/11/2014.

Table 1: Results of microbial analysis done on the water samples as supplied for analysis on the 26th of November 2014

No.	Sample	Average number of colony forming units (CFU)	
		Heterotrophic plate counts per ml	Total Coliforms per 100 ml
1	Water sample Before Distillation	5 700	>250/ml
2	Water sample after Distillation	0	0

4. Discussion & Recommendations

H_2O Specification in South Africa

1	2	3	4
Determinants	**Risk**	**Unit**	**Standard limits**
E.coli [a] or Faecal coliform [b]	Acute health – 1	Count per 100 mL	Not detected
Cytopathogenic virus	Acute health – 2	Count per 10 L	Not detected
Protozoan parasites -Giardia species -Cryptosporidium species	Acute health – 2 Acute health – 2	Count per 10 L Count per 10 L	Not detected Not detected
Total coliforms	Operational	Count per 100 mL	≤ 10
Heterotrophic plate count	Operational	Count per mL	≤ 1 000
Somatic coliphages	Operational	Count per 10 mL	Not detected

Table 1: Water samples

Based on the above set of specifications the water sample before distillation, showed unsatisfactory results for both the heterotrophic plate counts and Total coliforms counts, while the water sample after distillation sample showed satisfactory results for both the heterotrophic plate counts total coliforms counts.

5. Declaration

I declare that all analyses were performed with scientific protocols strictly adhered to and that the results are reliable within the scope of the methods.

L. Dolley

M.Sc., Pr. Sci. Nat. (Biological Science; No. 400019/97)

References

1. H_2O Specification in South Africa (SABS)

Notes

Herewith explanatory notes in terms of abbreviations and other terms needing clarification in this report:

DoH: Department of Health

N/R: Not Requested

TVC: Total Viable Count (sometimes referred to as Total Count)

Y&M: Yeasts and Mould

>: Greater than

<: Less than

TBC: To be confirmed

TNTC: Too numerous to count